Investigating the role of strigolactones in root system architecture

by

Bethany Richmond

A thesis submitted in partial fulfilment of the requirements for the degree of

Doctor of Philosophy in Life Sciences

University of Warwick, School of Life Sciences

February 2023

List of abbreviations

4DO	4-deoxyorobanchol
5DS	5-deoxystrigol
ABA	Abscisic acid
BES1	BRI1-EMS-SUPPRESSOR 1
bp	Base pair
BR	Brassinosteroid
BZR1	BRASSINAZOLE RESISTANT 1
BZS1	BZR1–1D SUPPRESSOR 1
CCD	CAROTENOID CLEAVAGE DEOXYGENASE
CK	Cytokinin
Col-0	Columbia-0
COP1	CONSTITUTIVE PHOTOMORPHOGENIC 1
Ct	Cycle threshold
D14	DWARF14
DEG	Differentially expressed gene
DNA	Deoxyribose nucleic acid
DPBA	Diphenylboric acid 2-aminoethyl ester
ent-4DO	Enantiomeric 4-deoxyorobanchol
ent-5DS	Enantiomeric 5-deoxystrigol
GA	Gibberellin
GC content	Guanine-cytosine content
gDNA	Genomic DNA
GO	Gene ontology
HY5	ELONGATED HYPOCOTYL 5
HYH	HY5-HOMOLOG
IAA	Indole-3-acetic acid
JA	Jasmonate
KAI2	KARRIKIN-INSENSITIVE2
KEGG	Kyoto Encyclopedia of Genes and Genomes

KL	KAI2 ligand
MAX	MORE AXILLARY GROWTH
mRNA	Messenger RNA
MS	Murashige and Skoog
OD	Optical density
NPA	N-naphthylphthalamic acid
PCR	Polymerase chain reaction
rac-GR24	*Racemic* GR24
RNA	Ribose nucleic acid
ROS	Reactive oxygen species
RT-qPCR	Reverse transcription quantitative polymerase chain reaction
SA	Salicylic acid
SCF	Skp1, Cullin, F-box complex
SL	Strigolactone
SMAX	SUPPRESSOR OF MAX2
SMXL	SUPPRESSOR OF MAX2-LIKE
TF	Transcription factor
TUB	TUBULIN

List of figures

List of tables

Acknowledgements

I am incredibly lucky to have had the support of many people through my PhD. First and foremost, I would like to express my sincere gratitude to my supervisor Professor Miriam Gifford, whose expertise, guidance, and support have been invaluable throughout the course of my PhD. Despite facing obstacles, pandemics and personal dilemmas, her encouragement and faith in me has been continual, and for that I am immensely thankful.

Thank you to my Advisory Panel, Professor Isabelle Carré, and Professor Rosemary Collier, for their guidance and counsel, which strengthened my confidence as a scientist. I am also hugely grateful to the members of the Gifford team and C30/C46 colleagues for their assistance throughout the course of this research. From helping interpret results to extracting seed, I appreciate every input and contribution to this work. Thanks to Gary Grant for tending to my plants at PBF and sharing his knowledge, and to Dr Beatriz Lagunas for her advice in my initial years. I owe special thanks to my colleagues Helen Wilkinson, Alice Coppock, Megan Lewis, Lisa King, and Liam Walker; their friendship and practical support has been invaluable. To my mentor Mike, our conversations have been a comfort and a joy.

On a personal note, I thank my mum, Ginny, and my three sisters, Annabelle, Chloe, and Eleanor, for their unwavering love and understanding in this endeavour. My girls, I truly would and could not have done this without your motivation and reassurance. Your support means everything to me. Finally, I thank my partner Connor for his boundless love and encouragement from the beginning. Connor, you give me strength, resilience, and reason. You have sacrificed so much to support my PhD journey, and for that I will forever be grateful. Here's to the next chapter!

Declaration

This thesis is submitted to the University of Warwick in support of my application for the degree of Doctor of Philosophy. It has been composed by myself and has not been submitted in any previous application for any degree. The work presented (including data generated and data analysis) was carried out by the author except in the cases outlined below:

- The results contained in Chapter 3 ‘Effect of strigolactones on root system architecture and root transcriptome in *Arabidopsis thaliana*’ and Chapter 4 ‘The strigolactone signalling pathway influences flavonoid biosynthesis in *Arabidopsis thaliana*’ are part of a published work and as such contain small contributions from others as detailed in the Author Contributions of the publication (Richmond et al., 2022).

Publications resulting from this work:

- Richmond, B.L., Coelho, C.L., Wilkinson, H., McKenna, J., Ratchinski, P., Schwarze, M., Frost, M., Lagunas, B., Gifford, M.L., 2022. Elucidating connections between the strigolactone biosynthesis pathway, flavonoid production, and root system architecture in Arabidopsis thaliana*. Physiologia Plantarum. 174, e13681. https://doi.org/10.1111/ppl.13681*

Abstract

Regulation of root architecture impacts plant health and fitness, thus characterising these changes are of great importance to agriculture. More efficient crops with greater yields are needed to feed the ever-growing population, under the more variable environmental conditions brought by the climate crisis. Understanding the molecular processes regulating root system architecture environmental responsiveness could better inform agricultural practice. Strigolactones are small plant signalling molecules that are involved in symbiotic plant-microbe interaction signalling, such as in legume-rhizobial nodulation. Strigolactones are also endogenous plant cues that regulate many plant developmental processes, in concert with other plant hormones.

This work aimed to elucidate the role of strigolactones in root system architecture. Transgenic mutant lines with knockdown or reduced expression of key strigolactone biosynthesis and signalling genes (*max3-9, max4-1*, and *d14-1*) were found to exhibit altered root phenotypes including long, dense root hairs compared to wildtype. RNA sequencing was used to investigate root transcriptomic changes in (*max4-1* and *max2-1*). Of note was that flavonoid biosynthesis was significantly downregulated in the strigolactone signalling mutant *max2-1*. This downregulation was validated through reverse transcriptase quantitative polymerase chain reaction (RT-qPCR) of key flavonoid biosynthesis genes on whole plant tissue. Root tip accumulation of flavonoids was also found to be significantly decreased in the strigolactone signalling mutant, as shown through confocal microscopy of roots stained with diphenylboric ethyl ester (DPBA), a fluorescent flavonoid stain.

Wildtype plants treated with the synthetic strigolactone analogue $GR24^{4DO}$ were found to have significantly longer lateral roots and shorter root hairs compared to mock treated roots. Transcriptomic changes underlying these phenotypes were investigated through RNA-sequencing, finding a significant enrichment of photosynthesis-related genes with $GR24^{4DO}$ treatment compared to mock treatment.

Overall, this work posits strigolactone as an important regulator of nutrient and energy acquisition, through modulation of root system architecture and light-harvesting, according to environmental cues.

Chapter 1 Introduction

1.1 Plant root architecture and the environment

Plants are sessile organisms and must be able to adapt to their environment to survive. Root systems play a central role in plant development and survival, providing anchorage, water and nutrient uptake and interacting with beneficial, neutral, and detrimental microbes within the soil. Soils have inherent heterogeneity; they have largely variable water and nutrient levels, and microbiome composition across space and time. Many plants, including model organisms *Arabidopsis thaliana* and *Medicago truncatula* exhibit developmental plasticity within root systems that mean they respond rapidly to local changes as they arise. Their study can help understand plant-environment interactions.

Developmental decisions are based on the integration of many mutual and antagonistic environmental cues. On a molecular level, these signals can lead to the activation or repression of certain transcription factors (TFs), which causes differential expression (DE) of their target genes. It is these local and systemic changes in gene expression which play a major role in regulation of different developmental fates. Whilst the field of plant developmental biology is heavily researched, determining the precise molecular basis of developmental responses to environmental changes is complicated and questions are expansive. Many of these developmental decisions involve a multitude of hormones, signalling pathways and transcriptional programs, working across a range of cell types and over an extended period of time, based on our knowledge of crosstalk between responses (as reviewed in Vega et al., 2019).

The vast majority of nutrients for plant growth are obtained from the local environment, the majority of which are acquired from the soil via the root system. Thus, a crucial role of root system development is enabling and maximising nutrient uptake. To do so, plants can adjust the direction of root growth for more successful nutrient mining, according to the local nutrient

levels, as well as a large number of aspects of root development, collectively characterised as forming the root system architecture (RSA). By inducing branching, through the formation of lateral (secondary) roots from the embryonic primary root, plants increase the surface area for root nutrient foraging. The formation of these lateral roots is regulated through the integration of many signals (as reviewed in Torres-Martínez et al., 2019), including abiotic stressors and nutrient availability, particularly nitrogen (N), typically in the form of nitrate, a key limiting factor to plant growth (as reviewed in Liu et al., 2019). On a finer scale, root hair epidermal cells further increase root surface area for optimising nutrient mining. In legumes, interaction of plants with rhizobia at root hairs leads to development of nodules on root systems, housing beneficial N-fixing bacteria. All of these aspects of root system architecture are highly plastic and the result of a dynamic interplay between gene regulatory networks, and phytohormones, controlling gene expression and transcription levels, play a crucial role in the coordination of developmental and environmental cues.

1.2 Hormonal regulation of root morphogenesis

1.2.1 Regulation of primary root growth

The primary root is comprised of at least 15 different cell types and has both radial and longitudinal organisation. Primary root growth is controlled by proliferation of cells within the root apical meristematic region and lengthening of cells within the so-called elongation zone (Figure 1.1). The major phytohormone auxin (indole-3-acetic acid, IAA) is a known regulator of primary root growth (as reviewed in Petricka et al., 2012). Auxin forms a gradient along the primary root, with the highest auxin accumulation at the root apex, and a decrease towards the elongation zone.

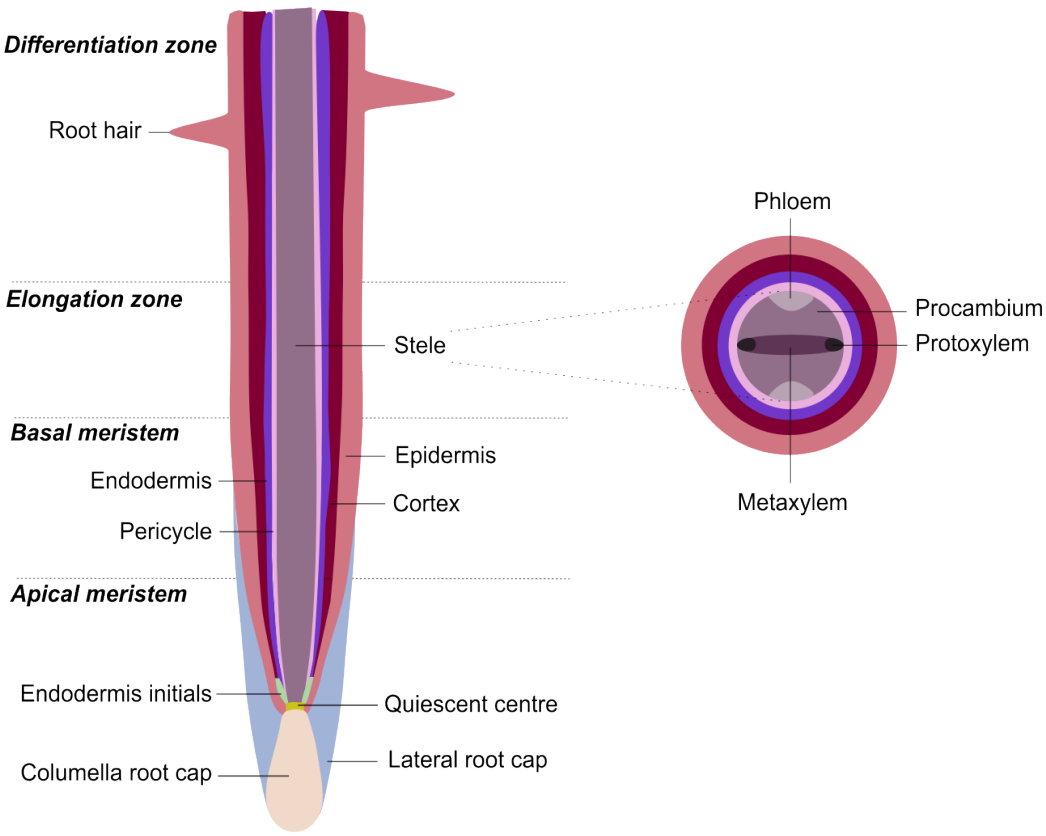

Figure 1.1 Cell organisation in *A. thaliana* root tip. Longitudinal *A. thaliana* root section depicting organisation of different cell types arranged into distinct zones. Cell division for primary root growth occurs within the meristematic region, and particularly rapidly within the root apical meristem. The rate of cell division declines with distance from the root tip, and cells begin to elongate within the elongation zone.

Graduated auxin accumulation is affected by the directional transport of auxin from shoot to root via auxin influx carriers – AUXIN1 (AUX1)/LIKE-AUXs (LAXs) – and auxin efflux transporters – PIN-FORMED (PIN) and MULTIDRUG RESISTANCE (MDR)/PHOSPHOGLYCOPROTEIN (PGP) protein families (as reviewed in Geisler, 2021). In addition to this, auxin is synthesised in the root, maintaining meristematic activity (Brumos et al., 2018; Chen et al., 2014). Uneven distribution of auxin along epidermal cells in the root elongation zone is the key driver of positive root gravitropism (Band et al., 2012), guiding the primary roots downwards, deeper into the water and nutrient-containing soil. Intriguingly, exogenously-applied auxin seems to have a dual impact on primary root growth, depending on its concentration; very low auxin concentrations promote primary root elongation, whereas higher concentrations inhibit it (as reviewed in Waidmann et al., 2020). Shorter and malformed primary roots compared to wildtype are demonstrated by loss-of-function auxin biosynthesis (Chen et al., 2014) , transport (Mravec et al., 2009; Vieten et al., 2005) and signalling mutants (Hamann et al., 1999), suggesting that auxin promotes primary root growth at native endogenous levels.

Auxin also promotes primary root elongation through facilitating the response of root cells to another phytohormone, gibberellin (GA) (Figure 1.2). GA promotes primary root elongation through degrading DELLA domain-containing proteins (DELLAs), relieving the growth-limiting repression on downstream targets that DELLAs have been characterised to have. The primary roots of gibberellin-deficient *Arabidopsis* mutant *ga1-3* were found to be significantly shorter than wildtype, but this phenotype was rescuable through application of GA (Fu and Harberd, 2003). This demonstrates that GA-mediated DELLA protein degradation allows primary root elongation. Expression of gain-of-function DELLA protein, GIBBERELLIC ACID-INSENSITIVE (GAI), in endodermal cells, causes significant inhibition of primary root length (Ubeda-Tomás et al., 2008). More recently, GA was found to accumulate within elongating endodermal cells, and treatment with GA-biosynthesis inhibitor paclobutrazol led to significantly reduced accumulation as well as root length in wildtype (Shani et al., 2013). Fu and Harberd (2003) found that application of auxin transport inhibitor 1-N-naphthylphthalamic acid

(NPA), prevented exogenously applied GA from restoring a wildtype primary root length to *ga1-3* roots, suggesting auxin promotion of GA signalling. GAs have therefore emerged as a key players, in conjunction with auxin, in promoting primary root elongation (as reviewed in Shtin et al., 2022).

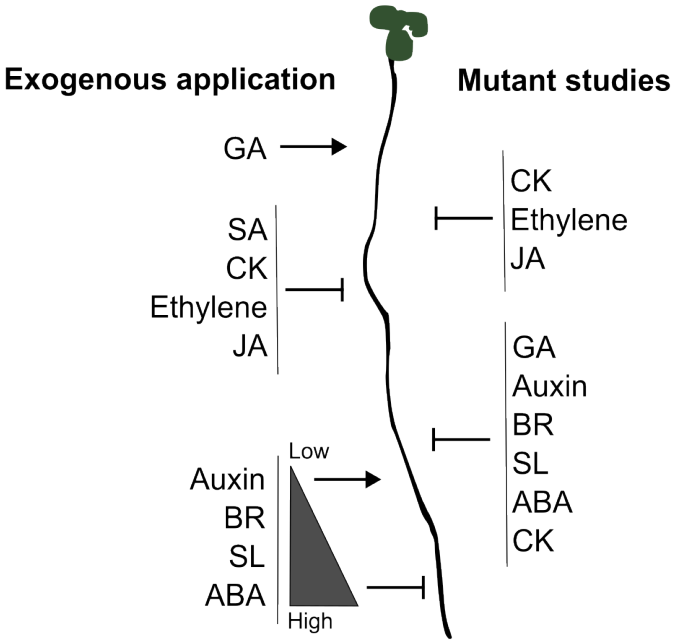

Figure 1.2 Phytohormone regulation of *A. thaliana* primary root elongation. Different phytohormone effects on primary root growth under controlled experimental conditions are depicted. Arrows represent primary root growth promotion; blunt arrows represent primary root growth inhibition. Adapted from Lopez-Ruiz et al. (2020).

Cytokinins (CK) inhibit primary root elongation by reducing cell division in the root apical meristem, thereby regulating overall meristem size. Increasing CK levels through exogenous application leads to shorter primary root lengths, and a smaller root apical meristem; CK biosynthesis mutants have longer primary roots compared to wildtype (Ioio et al., 2007). Conversely, overexpression of CK-degrading *CYTOKININ OXIDASE/ DEHYDROGENASE* (CKX) induces formation of longer root meristems (Werner et al., 2003). Ethylene, and its precursor 1-aminocyclopropane-1-carboxylic acid (ACC), also inhibit primary root growth. This mechanism is two-fold; ethylene inhibits cell division in the root apical meristem (Street et al., 2015) and inhibits cell elongation in the elongation zone through upregulating

auxin biosynthesis (Swarup et al., 2007). Accordingly, ethylene biosynthesis inhibitor pyrazinamide (PZA) leads to formation of significantly longer primary roots by relieving ethylene-mediated inhibition of cell elongation (Sun et al., 2017).

Jasmonate (JA) reduces primary root growth in an auxin-dependent manner, inhibiting both cell division and cell elongation (Chen et al., 2012). JAs promote degradation of JA ZIM domain family (JAZ) proteins, allowing the transcriptional regulation activity of *JASMONATE INSENSITIVE 1* (*MYC2/JAI1*). In turn, this represses expression of *PLETHORA1* and 2 (*PLT1/PLT2*) in the stem cell niche (Chen et al., 2011). A PLT protein gradient within the primary root regulates division and differentiation in a concentration-dependent manner; higher expression of *PLT1* and *PLT2* is associated with zones of cell differentiation and division (Mähönen et al., 2014). Exogenously-applied JA reduces expression of cell cycle–related genes and meristem cell number in Col-0, but not *myc2-2* mutants (Chen et al., 2011).

Exogenously-applied abscisic acid (ABA) also has a biphasic concentration-dependent effect on primary root growth: high ABA concentrations inhibit primary root growth, whereas low concentrations promote primary root growth (as reviewed in Sun et al., 2018). Low ABA levels maintain quiescent centre (QC) activity, suppressing stem cell differentiation (Zhang et al., 2010). This low ABA response is auxin-dependent, as the longer primary root length in response to low levels of ABA could be blocked through application of auxin efflux inhibitors NPA (Li et al., 2017b). Li et al. (2017b) also demonstrated that ABA-induced primary root elongation was diminished in mutants of auxin *PIN2* and an auxin-insensitive gene *INDOLE-3-ACETIC ACID 7* (*IAA7*). High ABA levels inhibit primary root elongation through an ethylene-dependent and auxin-dependent mechanism. The auxin influx inhibitor NPA, as well as ethylene perception inhibitor, silver thiosulfate (STS), and biosynthesis inhibitor, aminoethoxyvinylglycine (AVG), blocked high ABA inhibition of primary root length (Li et al., 2017b). Consistently, high concentrations of ABA decreases expression of *PLTs* and key auxin genes, *PINs*, within the root (Promchuea et al., 2017).

Brassinosteroids (BRs) are perceived by BR receptor BRASSINOSTEROID INSENSITIVE1 (BRI1) and promote downstream BR signalling through the transcription factors BRI1-EMS-SUPPRESSOR1 (BES1) and BRASSINOSTEROID RESISTANT1 (BZR1) (as reviewed in Planas-Riverola et al., 2019). Again, the role of BRs in primary root development is concentration-dependent: BR signalling mutants, gain-of-function *bes1-D* mutants and BR-treated plants exhibit shorter primary roots compared to wildtype (Chaiwanon and Wang, 2015; González-García et al., 2011). Thus, a correct concentration of BR appears crucial for normal primary root development. Moreover, BR signalling is highly spatially segregated with root tissues; BZR1 is less activated within the stem niche compared to high activation within the transition and elongation zones (Chaiwanon and Wang, 2015; Vukašinović et al., 2021). BR signalling also has tissue-specific responses: epidermal BR signalling induces cell proliferation, but stele BR signalling promotes cell differentiation (Vragović et al., 2015). There is interplay between BR and ABA signalling within the primary root in that activated BZR1 directly suppresses the major ABA signalling component ABA INSENSITIVE 5 (ABI5) (Yang et al., 2016). Yang et al. (2016) reported that primary root inhibition by ABA is partially suppressed in the *bzr1-1D* dominant mutant, reflecting antagonistic crosstalk between ABA and BR signalling. There is also evidence of BR and auxin antagonism in primary root growth. For example, expression of *PLT*s in the quiescent centre is repressed by BR signalling, but induced by auxin (Chaiwanon and Wang, 2015).

Salicylic acid (SA) functions to balance stress responses and morphogenesis (as reviewed in Bagautdinova et al., 2022). As with BRs, a precise balance of SA appears necessary for normal primary root growth as both SA-accumulating and SA-depleted mutant plants exhibit decreased primary root length compared to wildtype (Z. Meng et al., 2017; Xu et al., 2017). The effect of exogenously-applied SA is also concentration-dependent (as reviewed in Bagautdinova et al., 2022), with low SA concentrations typically increasing primary root growth, and higher concentrations inhibiting it. SA regulates primary root length through suppressing or promoting meristem cell divisions, and the effect of exogenous SA application largely

varies between species. In *A. thaliana*, 30 μM SA inhibits primary root growth through reducing meristem expression of the cell division marker *CYCLIN B1;1* (*CYCB1;1*), whereas 150 μM SA significantly reduces *CYCB1;1* expression (Pasternak et al., 2019). However, in *Oryza sativa*, a mutation in SA-biosynthesis *gene ABNORMAL INFLORESCENCE MERISTEM1* (*AIM1*) causes a decrease in *CYCLIN* gene expression, alongside a significant reduction in meristem size (Xu et al., 2017). Xu et al. (2017) also found that treatment with 0.5 mM exogenous SA can rescue primary root length in *aim1*. SA interplays with auxin signalling; SA has been shown to reduce levels of the auxin receptors TRANSPORT INHIBITOR RESPONSE 1 (TIR1) and AUXIN RECEPTOR F-BOX (AFB1), suppressing downstream auxin signalling (Wang et al., 2007). Within the primary root, SA has also been shown to affect root meristem patterning through modulating PIN positioning and therefore auxin accumulation (Ke et al., 2021; Pasternak et al., 2019).

The structurally similar phytohormones, strigolactones and karrikins, have also both been implicated in primary root elongation. Strigolactones (SLs) are carotenoid-derived small signalling molecules which were originally identified as germination stimulants for root-parasitic weeds, including their namesake *Striga* spp. (Cook et al., 1972). Their role as rhizospheric allelochemicals was later characterised, instigating symbiotic plant-microbe interactions with arbuscular mycorrhizae (Akiyama et al., 2005; Choi et al., 2020). In more recent years, the role of strigolactones as plant developmental cues has been uncovered (as reviewed in Bhoi et al., 2021). Aboveground, SLs regulate shoot branching (Gomez-Roldan et al., 2008), leaf senescence (Ueda and Kusaba, 2015) and reproductive organ development (Umehara et al., 2008), belowground, they coordinate root system architectures such as the inhibition of adventitious root formation (Rasmussen et al., 2012) and regulation of root hair density (Kapulnik et al., 2011a, 2011b). On a whole plant level, SLs also appear to confer resistance to external stressors, including nutrient-deficient growth conditions, salinity, and drought, through regulating leaf water loss rate and inducing stomatal closure (Ha et al., 2014). *Arabidopsis* strigolactone biosynthesis mutants appear to exhibit a short primary root phenotype under particular environments (Richmond et al., 2022;

Ruyter-Spira et al., 2011; Villaécija-Aguilar et al., 2019). Ruyter-Spira et al., (2011) found that application of *rac*-GR24 – a synthetic strigolactone, which also stimulates karrikin signalling to an extent – increases primary root length, enhancing both meristem and transition zone length. Ethylene biosynthesis gene ACC SYNTHASE 2 (*ACS2*) is upregulated upon exogenous GR24 treatment, suggesting that this response may be ethylene mediated. Furthermore, the divided components of GR24 that stimulate strigolactone signalling ($GR24^{5DS}$ and $GR24^{4DO}$) and both strigolactone and karrikin signalling ($GR24^{ent\text{-}5DS}$) were found to promote primary root elongation (Li et al., 2016b). Mutation of the karrikin signalling proteolytic target in *Lotus japonicus* results in formation of a shorter primary root compared to wildtype, as well as upregulation of ethylene signalling (Carbonnel et al., 2020), suggesting karrikin-mediated primary root elongation may also be ethylene-driven.

1.2.2 Regulation of lateral root initiation and growth

Lateral roots are formed from founder pericycle cells within the primary root (Figure 1.3). These founder cells undergo several rounds of periclinal cell division, leading to formation of a lateral root primordium which emerges through overlying endodermal, cortical, and epidermal layers. The lateral root primordium develops a meristematic zone with a quiescent centre (QC), similar to the root apical meristem. Cell division within this meristematic tissue then allows lateral root growth and elongation.

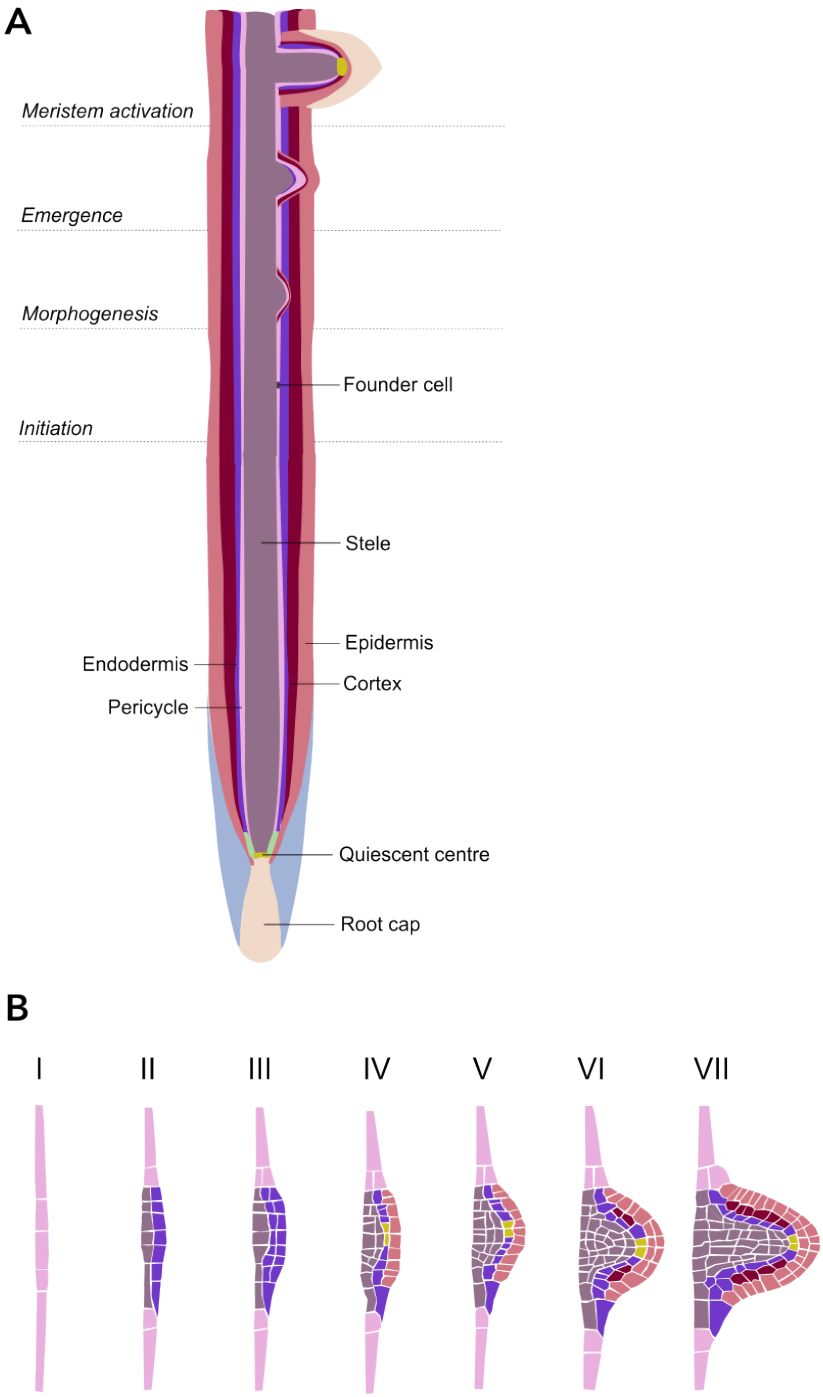

Figure 1.3 Lateral root formation from *A. thaliana* primary root. Lateral roots form within the differentiation zone of the primary root. In a process involving regulation of auxin levels, some pericycle cells are specified as lateral root founder cells. (B) Depending on other environmental factors or endogenous signalling, founder cells undergo anticlinal asymmetric cell division, creating a single-layered primordium (I). Next, the cells undergo periclinal divisions forming an inner and outer layer (II). A dome-shaped primordium is formed through further anticlinal and periclinal divisions (III-VII). As the primordia develops, a meristematic zone and quiescent centre forms, analogous to that of the root apex. This allows lateral root elongation through cell division. Adapted from Torres-Martínez et al. (2019).

Auxin is a key regulator of lateral root formation by specifying founder cells (Dubrovsky et al., 2008), and regulating primordia development (De Smet et al., 2008; Singh et al., 2020) (Figure 1.4). For example, *A. thaliana* loss-of-function mutants in auxin TRANSPORT INHIBITOR RESPONSE (TIRs), have reduced lateral root number owing to reduced polar auxin transport (Ruegger et al., 1997). Similarly, mutants in AUXIN TRANSPORTER PROTEIN 1 (AUX1), with perturbed auxin transport from source to sink tissues, exhibit reductions in lateral root number (Marchant et al., 2002) – a phenotype which is rescuable through the addition of a synthetic auxin, 1-naphthylacetic acid. In *Oryza sativa*, ectopic expression of *OsAUX1* increases lateral root initiation (Yu et al., 2015). However, lateral root length in *A. thaliana aux1* mutants is similar to wildtype, suggesting the elongation response to auxin is not entirely conserved between primary and lateral roots (Yu et al., 2015). There is interplay between auxin and ABA signalling during the development of lateral root primordia, through the key ABA signalling transcription factor ABSCISIC ACID INSENSITIVE 3 (ABI3) (Figure 1.4). Lateral root initiation promotion by exogenous auxin or auxin transport inhibitors is suppressed in the *abi3* mutant (Brady et al., 2003), thus implicating ABA in auxin-mediated lateral root initiation. Alternately, in lateral root emergence, ABA inhibits cell division and expansion. When the ABA biosynthesis gene NINE-CIS-EPOXYCAROTENOID DIOXYGENASE 3 (NCED3) is disrupted in *A. thaliana*, emerged lateral roots are significantly longer than wildtype (Guo et al., 2009).

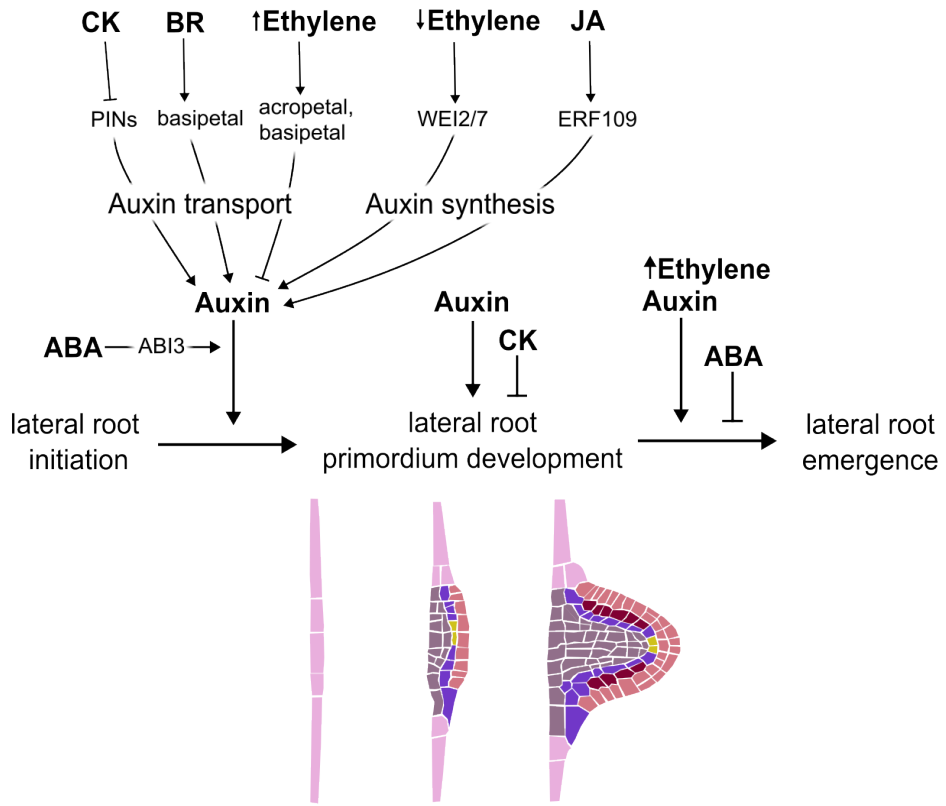

Figure 1.4 Hormonal control of lateral root formation in *A. thaliana*. Auxin is a key positive regulator of each stage of lateral root formation and a balanced auxin gradient is necessary for lateral root primordium patterning. Different phytohormone effects on lateral root formation are depicted. Arrows represent lateral root formation promotion; blunt arrows represent lateral root formation inhibition. Adapted from Jung and McCouch (2013).

Jasmonates (Jas) and brassinosteroids (BRs) also promote lateral root formation through interacting with auxin signalling. Overexpression of JA signalling leads to an increased number of lateral root primordia and increased lateral root density in *A. thaliana* seedlings, a phenotype also seen in plants treated with exogenous auxin (Cai et al., 2014). The JA-responsive ETHYLENE RESPONSE FACTOR 109 (ERF109) directly upregulates expression of key auxin biosynthetic genes, *ANTHRANILATE SYNTHASE α1* (*ASA1*) and *YUCCA2* (*YUC2*), thereby promoting auxin signalling (Cai et al., 2014) (Figure 1.4). In *O. sativa*, exogenous BR treatment increases lateral root number, and it was demonstrated that overexpression of BR signalling promoter BRASSINAZOLE RESISTANT 1 (BZR1) significantly increased lateral root formation and promoted auxin signalling (Hou et al., 2022).

Cytokinins inhibit lateral root primordia formation in *Arabidopsis* by disrupting *PIN-FORMED* (*PIN*) gene expression, and therefore auxin signalling (Laplaze et al., 2007) (Figure 1.4). This disrupts the necessary formation of an auxin gradient within the lateral root meristem, dysregulating cell division and therefore affecting lateral root primordia development. Through their ability to modulate auxin patterning, cytokinins also appear to play a role in the bending angle of emerged lateral roots, directing growth (Waidmann et al., 2019).

Strigolactone and karrikin signalling has also been associated with lateral root development. *Rac*-GR24 treatment has consistently been shown to lead to a reduction in lateral root emergence and overall density in wildtype plants (Kapulnik et al., 2011a; Ruyter-Spira et al., 2011). Accordingly, both karrikin and strigolactone signalling *Arabidopsis* mutants, and a strigolactone/karrikin double mutant, have increased lateral root density in comparison to wildtype (Villaécija-Aguilar et al., 2019). Though the precise mechanism by which strigolactones and karrikins regulate lateral root development is yet to be fully elucidated, it is already clear that they both have significant influence on lateral root development.

1.2.3 Regulation of root hair initiation and growth

Root hairs are produced as an elongation from epidermal cells, increasing in density with distance from the root tip. The development of root hairs depends on two steps: fate determination of hair or non-hair epidermal cells, and morphogenesis for root hair elongation (Figure 1.5). In *A. thaliana*, fate is determined dependent on whether an epidermal cell is located on top of the junction of two cortical cells (hair cell) or not (non-hair cell) (Lee and Schiefelbein, 2002).

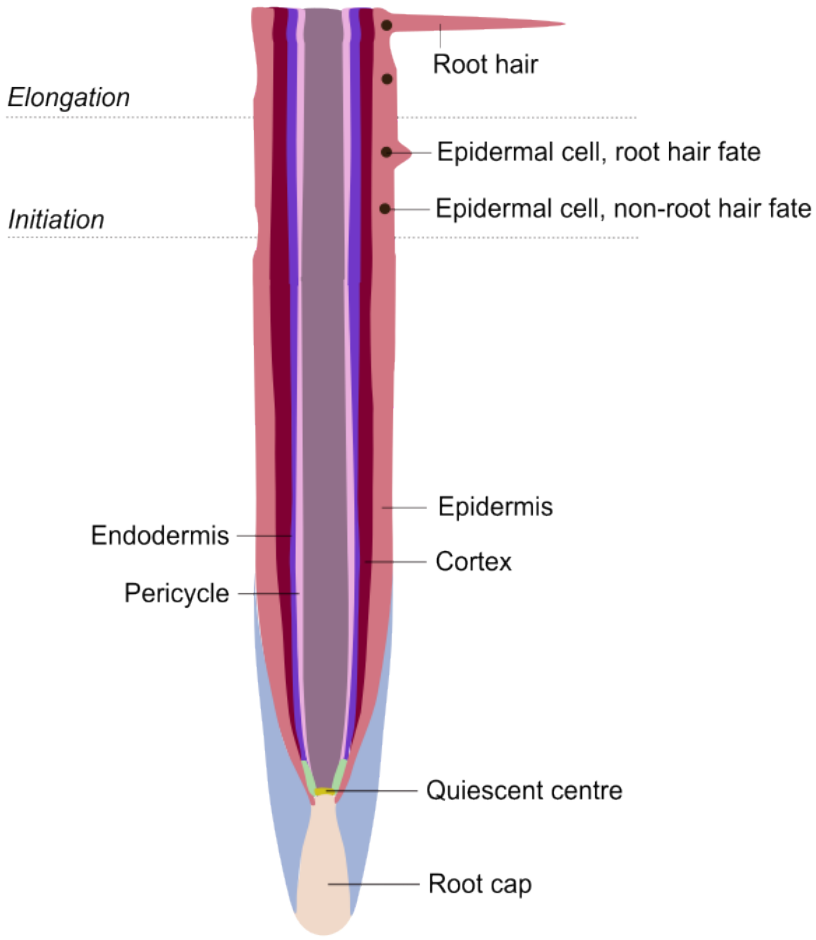

Figure 1.5 Root hair formation on *A. thaliana* primary root. Root hairs are tubular-shaped extensions from epidermal cells. Root hair cell fate is determined within the meristematic and elongation zones via means of positional information, morphogenesis occurs within the elongation zone. Elongation of root hairs occurs via a process of highly polarised cell expansion at the root hair apex, called tip growth.

Auxin largely controls the polarised tip growth of root hairs, through maintaining levels of reactive oxygen species (ROS), and calcium ions (Ca^{2+}). A careful balance between Ca^{2+} and ROS is necessary to drive controlled polar cell expansion and avoid cell wall rupture (as reviewed in Mangano et al., 2016). Exogenous application of peroxide (H_2O_2) – which induces ROS formation – was found to inhibit root hair expansion (Dunand et al., 2007), whereas ascorbic acid – a ROS scavenger – led to significantly reduced root hair length and density (Tyburski et al., 2012). Auxin has been shown to upregulate expression of the key root hair initiation gene *ROOT HAIR DEFECTIVE SIX-LIKE 4* (*RSL4*) (Yi et al., 2010), which enhances root hair

elongation by increasing local levels of reactive oxygen species (ROS) (Figure 1.6). Yi et al. (2010) demonstrated that loss-of-function *rsl4 Arabidopsis* seedlings have a retarded root hair elongation phenotype, whilst constitutive *RSL4* expression results in the formation of very long root hairs.

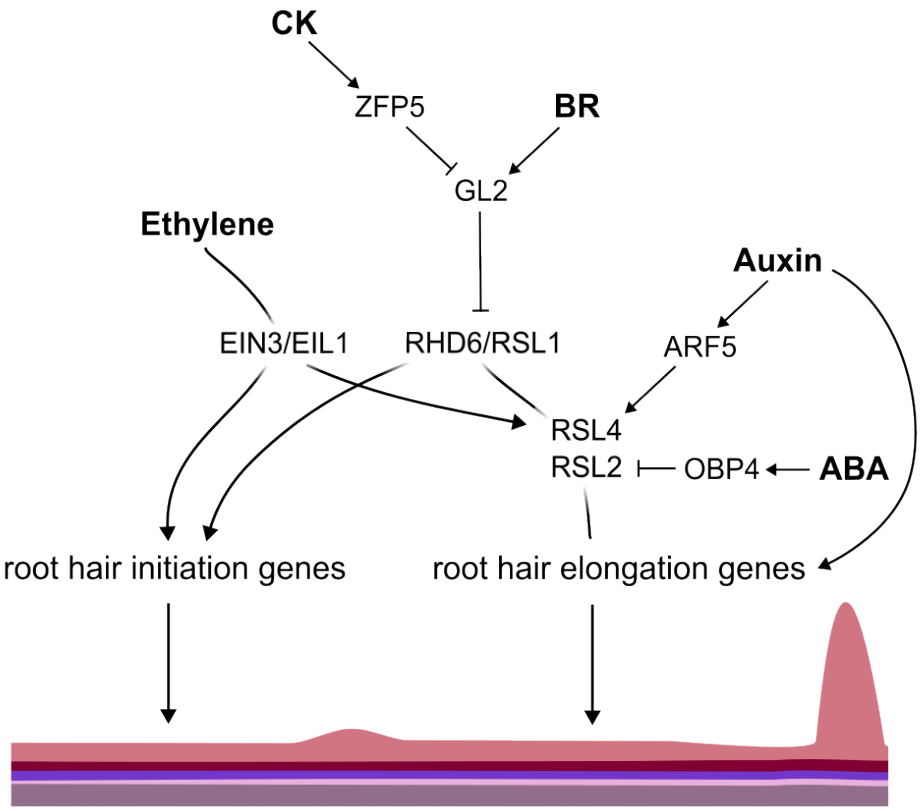

Figure 1.6 Hormonal regulation of root hair development in *A. thaliana*. Root hair development is tightly regulated through hormone-driven transcriptional cascades. Auxin, cytokinin and ethylene are key drivers of root hair development, whilst ABA and BR are repressors. Arrows represent promotion, blunt arrows represent inhibition. Adapted from Vissenberg et. al (2020).

Ethylene positively regulates root hair development. Ethylene treatment activates transcription factors ETHYLENE INSENSITIVE 3 (EIN3) and its homolog EIN3-LIKE1 (EIL1), which stimulating expression of key root hair initiation and elongation genes; *RSL1, RSL2, RSL4, and ROOT HAIR DEFECTIVE 6* (*RHD6*) (Feng et al., 2017; Zhang et al., 2016) (Figure 1.6). Similar to the regulation by auxin, ethylene-induced root hair formation is driven by the accumulation of ROS (Martin et al., 2022). Ethylene signalling

mutant *ethylene insensitive 2* (*ein2*) has shorter root hairs (Rahman et al., 2002), whilst *ethylene overproducing 1* (*eto1*) has longer root hairs compared to wildtype (Strader et al., 2010). Intriguingly, Strader et al. (2010) showed that the *aux1* mutation inhibits the long root hair phenotype of *eto1* seedlings, indicating that auxin transport is required for ethylene-mediated root hair development. There is a large overlap between the roles of auxin and ethylene across plant development (as reviewed in Muday et al., 2012). This ethylene-auxin crosstalk is evident in root hair morphogenesis, as illustrated by the finding that auxin biosynthetic genes are upregulated by ethylene during initiation of polar root hair expansion (Swarup et al., 2007). Similarly, transcriptomic analyses demonstrated that a large subset of core root hair genes are upregulated by both auxin and ethylene treatment (Zhang et al., 2016). Ethylene-auxin interplay can be explained on a molecular level. For example, the *AUX1* promotor has a binding site for an ethylene signalling transcription factor, ETHYLENE INSENSITIVE 3 (EIN3) (Chang et al., 2013). Vice versa, transport of ethylene precursor ACC is promoted by LYSINE HISTIDINE TRANSPORTER 1 (LHT1), the expression of which is regulated by auxin (Lewis et al., 2013). These are just two examples of molecular locations for crosstalk.

Cytokinin (CK) also regulates root hair development. Application of exogenous CK results in root hair elongation, whereas cytokinin oxidase (CKX) overexpressing lines have a short root hair phenotype (An et al., 2012). Alongside ethylene and auxin, CK treatment upregulates a shared subset of core root hair genes (Zhang et al., 2016), indicating substantial interplay between ethylene, auxin and CK signalling in root hair development. CK has also been shown to regulate aspects of both auxin and ethylene signalling in plant development (as reviewed in Liu et al., 2017), but in root hair development, CK signalling appears to be somewhat independent of auxin-ethylene signalling. CK can restore root hair elongation in both ethylene and auxin signalling mutants (Zhang et al., 2016). The mechanism for CK promotion of root hair development involves the transcription factor ZINC FINGER PROTEIN5 (ZFP5) (Figure 1.6). Loss-of-function *zfp5* mutants have shorter root hairs compared to wildtype, and this phenotype is not rescuable

by exogenous CK treatment (An et al., 2012). An et al., (2012) found that cytokinin induces *ZFP5* expression which directly upregulates expression of *CAPRICE* (*CPC*), a key promotor of root hair development. In *A. thaliana*, three genes regulate root hair formation: GLABRA2 (GL2), TRANSPARENT TESTA GLABRA (TTG), and WEREWOLF (WER). In mutant *gl2*, *ttg* and *wer* plants, root hair cell fate is dysregulated, and more root epidermal cells differentiate into root hair cells than in wildtype plants (Galway et al., 1994; Lee and Schiefelbein, 1999; Masucci et al., 1996). CPC negatively regulates *GL2* expression (Lee and Schiefelbein, 2002), thereby promoting root hair initiation.

Brassinosteroids (BRs) negatively regulate root hair development through promoting *GL2* expression (Cheng et al., 2014). GL2 directly represses transcription of *RHD6* and *RSL1*, thereby suppressing root hair initiation (Lin et al., 2015) (Figure 1.6). Consistently, in *A. thaliana* exogenous application of BR leads to the formation of fewer root hairs, while application of a BR-biosynthesis inhibitor produces more root hairs (Cheng et al., 2014). Abscisic acid (ABA) also negatively regulates root hair formation through suppressing *RSL2* expression, preventing root hair elongation. ABA activates the transcription factor OCS ELEMENT BINDING FACTOR 4 (OBP4), which directly repressed *RSL2* expression (Rymen et al., 2017).

Strigolactones and karrikins have also both been implicated in root hair development, as *rac*-GR24 treatment increases root hair length and density in *Arabidopsis* (Kapulnik et al., 2011b, 2011a; Richmond et al., 2022). Karrikin receptor mutants have shorter and less dense root hairs compared to wildtype, a phenotype not rescuable through exogenous KAR addition (Villaécija-Aguilar et al., 2019). Mutation of the karrikin signalling proteolytic target in *Lotus japonicus* results in a long root hair phenotype, alongside ethylene biosynthesis upregulation (Carbonnel et al., 2020). This is indicative of karrikin modulation of ethylene signalling to regulate root hair development. There is also substantial evidence for strigolactone-mediated root hair development. Exogenous treatment with synthetic SL-specific mimics $GR24^{4DO}$ and

GR24^{5DS} lead to significantly increased root hair lengths compared to wildtype (Li et al., 2016b).

1.2.4 Phytohormone responses to nitrogen availability

N-availability is a key limiting factor to plant growth since its many forms (inorganic and organic) are required for formation of nucleic acids and proteins. Since N-availability varies spatially and temporally, plants must adapt their three-dimensional root system architecture accordingly. The overall N content of the plant is communicated via modulation of peptide and phytohormone transport which, in turn, drives optimal root development (as reviewed in Jia et al., 2022). A mild N deficiency drives a foraging response, promoting development of primary roots, lateral roots, and root hairs, to enhance exploration of the soil, whereas growth is suppressed in severe N starvation, in order to survive (Figure 1.7).

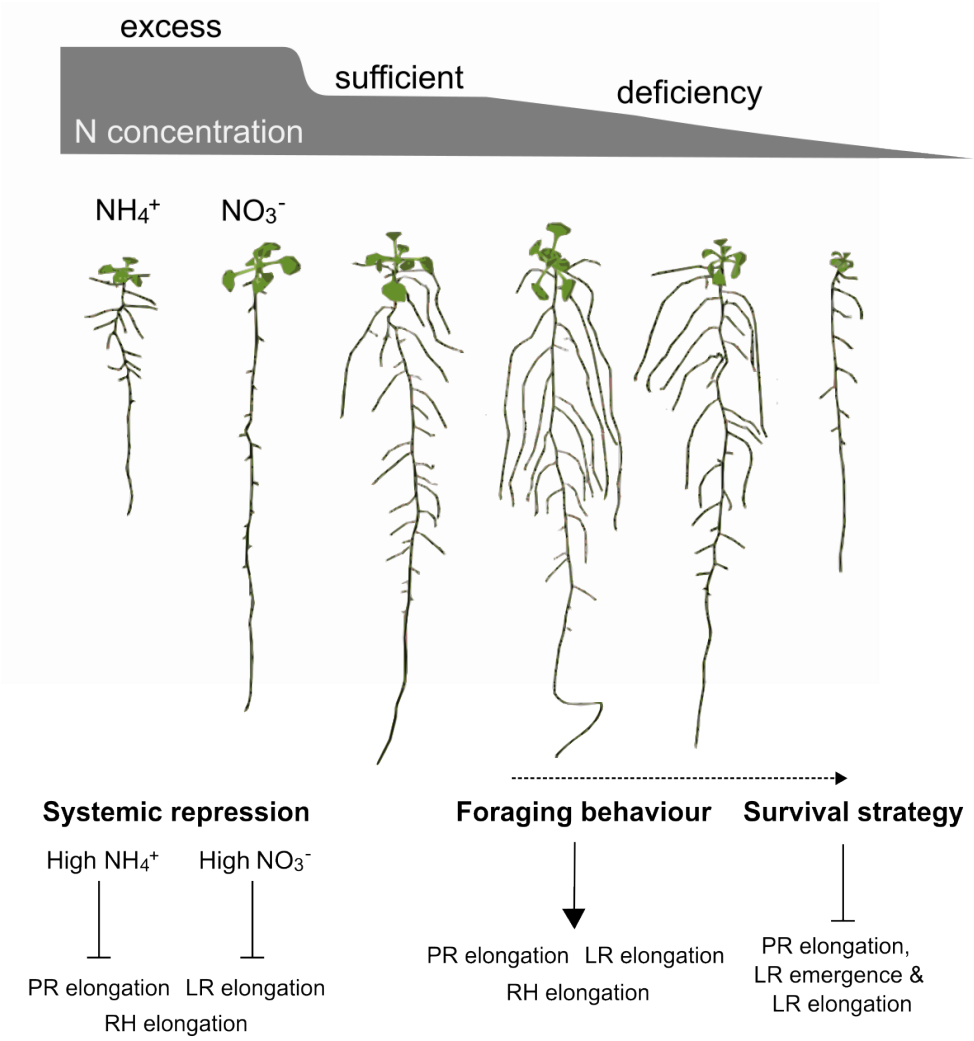

Figure 1.7 Root system architectural responses to nitrogen availability. With excess nitrogen (N), root growth is systemically repressed: excess ammonium (NH_4^+) causes primary root (PR) growth inhibition, whereas excess nitrate (NO_3^-) causes lateral root growth (LR) inhibition. Mild N deficiency induces N foraging responses, including promotion of primary and lateral root lengths, and root hair (RH) elongation. Severe N deficiency induces a systemic survival strategy, inhibiting primary root growth and lateral root emergence and elongation to conserve N supply. Adapted from Giehl and von Wirén (2014).

N-availability drives root development largely through modulating auxin signalling. In *A. thaliana*, NITRATE TRANSPORTER 1.1 (NRT1.1) plays a key role in nitrate signalling and acquisition. NRT1.1 regulates nitrate sensing through regulating expression of other nitrate transporters, and auxin translocation (Krouk et al., 2010). Under very low N, NRT1.1 suppresses lateral root formation through upregulating basipetal auxin transport,

preventing auxin accumulation in the lateral root primordia (Bouguyon et al., 2016; Krouk et al., 2010). This mechanism preserves N stores for plant survival. Mild N-deficiency drives upregulation of the expression of key auxin biosynthetic genes, such as YUCCAs (YUCs), within the root apical meristem and lateral root tips, thereby promoting primary root and lateral root elongation (Jia et al., 2021). Furthermore, auxin-responsive AUXIN RESPONSE FACTOR 8 (ARF8) stimulates pericycle lateral root initiation in response to moderate levels of N (Gifford et al., 2008), promoting root growth towards N sources. The root foraging response to low N is also driven through brassinosteroid signalling (BR); low N induces expression of key BR biosynthetic genes – such as *DWARF1*, as well as root growth promotion (Jia et al., 2020).

Biosynthesis of cytokinin (CK) is also tightly regulated by plant N levels; in *A. thaliana*, CK biosynthesis is upregulated after nitrate treatment (Takei et al., 2004). Given that CKs generally suppress primary and lateral root growth, this suggests a role for CK in reducing the foraging response when there is sufficient N-availability. Consistent with this, CK biosynthesis and perception mutants respond differently to N levels, having shorter primary roots after nitrate treatment compared to wildtype (Naulin et al., 2020). This further supports that CK also acts as a central regulator of root development in response to N-availability.

1.2.5 Phytohormone roles during nodulation in leguminous plants

In order to deal with limited environmental N, leguminous plants have entered a symbiotic relationship whereby they house beneficial N-fixing bacteria in root nodules (Figure 1.8). On stimulation by rhizobial Nod factors, two plant developmental programs are initiated: ‘controlled' rhizobial infection of the epidermis and nodule organogenesis. The process of nodulation is highly host-specific, only occurring when compatible rhizobia interact with root hairs in the competent developmental root hair elongation zone (as reviewed in Roy et al., 2020). Nodulation is also a costly procedure for the plant (involving much carbon investment), and so it is tightly controlled by phytohormone signalling.

There is extensive overlap between the developmental programs of lateral root and nodule organogenesis. Both processes are induced under low N conditions, involve the reactivation of cell division in differentiated cells, and share key regulatory genes, such as *NODULE INCEPTION* (*NIN*) and *CYTOKININ RESPONSE 1* (*CRE1*) (Gonzalez-Rizzo et al., 2006; Schiessl et al., 2019) which both regulate nodulation and lateral root development.

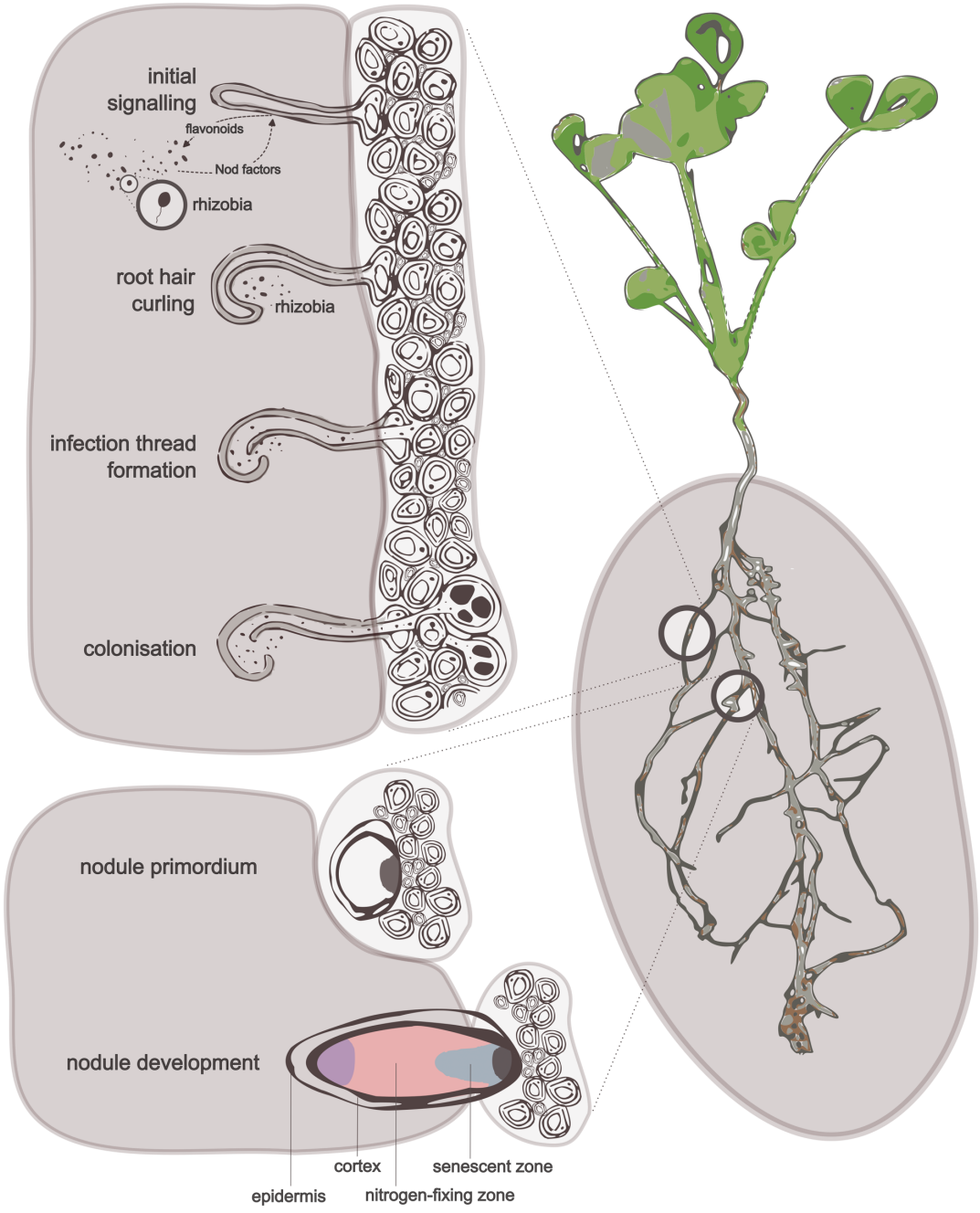

Figure 1.8 Process of indeterminate nodule initiation and development in *Medicago truncatula*. Legumes release flavonoids in their root exudates which attract compatible rhizobia from the local vicinity. Sensing of flavonoids induces rhizobia to express *nod* genes and excrete the resultant nod factors into the soil. Appropriate nod factors are sensed by the plant and initiate root hair curling, whereby the root hair curls around a rhizobium. A tubular infection thread forms, allowing the rhizobium to travel down the root hair and into the root cortex, colonising the root. Cortical cells divide rapidly to form the nodule primordium. Symbiosome membranes form around the rhizobia, and they differentiate into bacteroids within the pink nitrogen-fixing zone. An active meristem is maintained throughout the nodule lifespan. Adapted from Wilkinson et al. (2023).

Cytokinin plays an opposite role on lateral root compared to nodule organogenesis. Knockdown via RNAi of *Medicago truncatula* cytokinin receptor CRE1 led to cytokinin-insensitive plants with an increased number of lateral roots and strongly reduced nodule number (Gonzalez-Rizzo et al., 2006). In *L. japonicus,* exogenously applied synthetic cytokinin induced the formation of empty nodule primordia, in the absence of rhizobia (Heckmann et al., 2006). However, this did not occur in mutants of key nodulation genes, such as *NIN* and *Nodulation Signalling Pathway 1* and *2* (*NSP1*/*NSP2*). NSP1 and NSP2 are transcription factors essential to nodulation which activate cortical cell division (Hirsch et al., 2009; Kaló et al., 2005), indicating that cytokinin-mediated primordia formation relies on this activation of cortical cell division. Heckmann et al. (2011) demonstrated that cytokinin treatment regulated expression of proteins specifically associated with nodule organogenesis – including *NIN*, *NSP1* and *NSP2*. The importance of cytokinin signalling in nodulation is further demonstrated by the finding that a key cytokinin biosynthesis gene (*CKX*) is upregulated in *L. japonicus* during nodule initiation, and disrupting this significantly reduces infection thread formation, and therefore overall nodule number (Reid et al., 2016). However, overexpression of *CKX* from *Arabidopsis* (At*CKX3*) and maize (ZmCKX1) in *L. japonicus* also resulted in decreased nodule number (Lohar et al., 2004), suggesting cytokinin plays both a promotional and inhibitive effect on nodulation, depending on level, location and timing. In support of this, whilst cytokinin-activating genes *LONELY GUY 1* and *2* (*LOG1*/*LOG2*) are upregulated in early *M. truncatula* nodule primordia, both RNAi and overexpressing *LOG1* plants exhibit significantly reduced nodule number (Mortier et al., 2014).

As with other aspects of root development as discussed earlier, polar auxin transport is vital in nodulation. The importance of auxin signalling during the initial signalling stage is illustrated by the upregulation of auxin-responsive genes within the root hair transcriptome that are induced by rhizobia or Nod factors (Breakspear et al., 2014). During initiation of nodulation, suppression of rootward polar auxin transport creates concentrated auxin peaks/maxima below the rhizobia-root interaction site which stimulates cortical cell division

and thus leads to nodule organogenesis. Pseudonodules can be induced through inhibition of polar auxin transport through exogenously applied auxin efflux inhibitors (Rightmyer and Long, 2011). The effect of auxin is dependent on appropriate concentration and spatiotemporal positioning. 1 μM of synthetic auxin applied exogenously on roots was found to lead to reduced nodule number on *M. truncatula* roots (Roy et al., 2017), whereas 50 μM induced pseudonodule formation on both *M. truncatula* and *O. sativa* root systems (Hiltenbrand et al., 2016). Accumulation of auxin in rhizobial infection sites is also required for normal nodule formation. Auxin transporter *Medicago truncatula LIKE AUXIN RESISTANT 2* (*MtLAX2*), is expressed in the cortex and nodule primordia, and *mtlax2* mutant lines exhibit decreased infection thread and nodules formation (Roy et al., 2017). Flavonoids are phenylpropanoid-derived secondary metabolites; some flavonoids can act as auxin transport inhibitors, through stabilising PIN dimers and redirecting PIN-mediated auxin fluxes (Teale et al., 2021). RNAi silencing of flavonoid biosynthesis disrupts the initial rhizobia-triggered auxin transport downregulation, and decreases nodule formation (Wasson et al., 2006), suggesting that flavonoids play a key role in nodule auxin flux.

Strigolactones have been found to regulate nodulation, including the nodulation-essential transcription factors *NSP1* and *NSP2* which are required for strigolactone biosynthesis (Liu et al., 2011). Liu et al. (2011) found that key strigolactone biosynthesis genes were strongly downregulated in *nsp1, nsp2 and nsp1/nsp2* mutant *M. truncatula* lines. There appears to be a direct role for strigolactone in early nodulation events, as transcription of strigolactone biosynthesis genes is upregulated by rhizobia and Nod factors (Breakspear et al., 2014). The role for strigolactones in nodulation appears to be dose-dependent; low concentrations of *rac*-GR24 significantly increased nodule number, whereas high concentrations reduced it (De Cuyper et al., 2015).

Unlike the aforementioned phytohormones, ethylene signalling has a predominantly inhibitive role in nodulation. Loss of expression of the *M. truncatula* ortholog of ethylene insensitive *AtEIN2*, *SICKLE* (*MtSKL1*), in the *mtskl1* mutant, has a hypernodulation and hyperinfection phenotype (Varma

Penmetsa et al., 2008), as does the *L. japonicus ein2a ein2b* double mutant (Reid et al., 2018). Many rhizobial genomes contain genes which encode ACC deaminases (acdS), which degrade ACC, reducing ethylene levels and promoting relieving ethylene-mediated nodulation suppression (as reviewed in Nascimento et al., 2016), illustrating how rhizobial activity can modulate the host.

1.3 Flavonoids, ROS and phytohormone interplay on root system architecture

Flavonoids are a major family of plant secondary metabolites, derived from the overarching phenylpropanoid metabolic pathway, which have important roles across an exceptionally wide range of plant developmental processes, mediating stress responses and plant-microbe communication. Subclasses of flavonoids include anthocyanins, chalcones, flavanones, flavones, flavonols and proanthocyanins. These metabolites are widely known for being pigments and key determinants of flower colouration, ranging from yellows, reds, blues, or a combination of these. Differential accumulation of flavonoids in flowers and fruits attracts pollinators and dispersers, increasing reproductive success (Sheehan et al., 2016).

The first committed step in flavonoid synthesis is the conversion of 4-coumaroyl CoA and malonyl CoA to naringenin chalcone via chalcone synthase (encoded by CHS) (Figure 1.9). In the *chs* mutant, no flavonoids are accumulated, thus *chs* plants can be used to evaluate the broad role of flavonoids in plant development. Phenotypically, Arabidopsis *chs* seeds are pale, lacking the wildtype brown pigment conferred by anthocyanins to the seed coats. Studies have found that polar auxin transport in *chs* is altered, with *chs* plants having higher root basipetal auxin transport, and delayed root gravitropism compared to wildtype (Buer and Muday, 2004). Flavonoids have also been implicated in negative phototropism, acting as positional signals which regulate the rate and direction of root light avoidance. It was shown that light induces flavonoid accumulation in *A. thaliana* roots, and that this

accumulation promotes asymmetrical cell elongation through decreasing auxin signalling and the PLETHORA gradient (Silva-Navas et al., 2016).

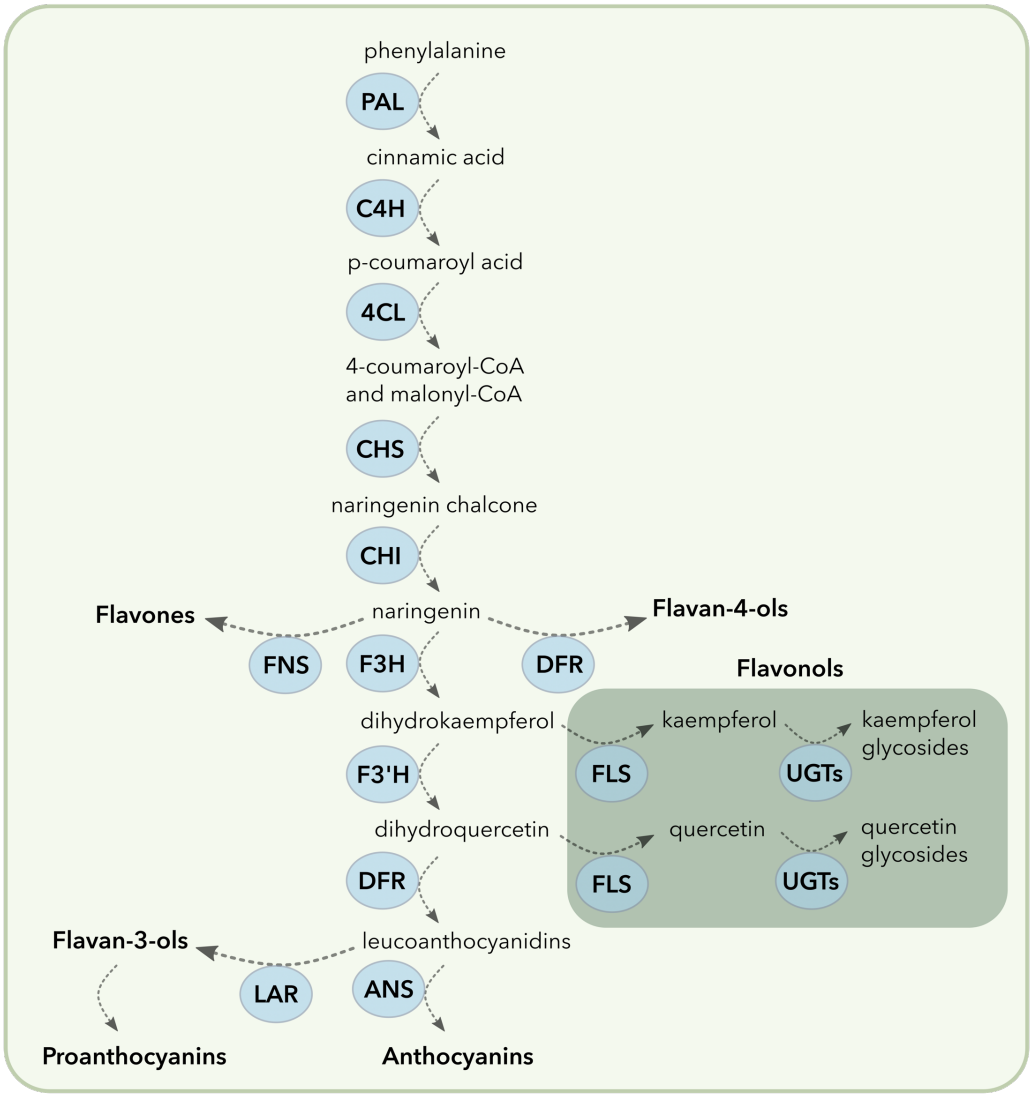

Figure 1.9 Flavonoid biosynthesis in *Arabidopsis thaliana*. Schematic diagram showing flavonoid biosynthesis in *A. thaliana*. PAL, phenylalanine ammonia lyase; CHS, chalcone synthase; CHI, chalcone isomerase; F3H, flavonone 3-hydroxylase; DFR, dihydroflavonol reductase; FLS, flavonol synthase; ANS, anthocyanin synthase; LAR, leucoanthocyanidin reductase; UGT, UDP-glucose: flavonoid 3-O-glucosyltransferase. Adapted from Richmond et al. (2022).

Flavonoids have an important role in scavenging ROS, and this is important in regulation of plant development. ROS partially function as signalling molecules, with local increases in ROS acting as various

developmental cues. For example, within the root system, local increases in ROS have been associated with regulation of primary root elongation, lateral root emergence, root hair elongation, root cell elongation in the root apex, as well as regulation of root gravitropism and phototropism (as reviewed in Mase and Tsukagoshi, 2021). However, ROS are also produced through metabolism and stress, and so mechanisms exist in order to maintain the low basal ROS level, to avoid oxidative damage, whilst at the same time enabling ROS signalling. One such mechanism is the production of antioxidant metabolites, such as flavonols; mutants in the flavonol biosynthesis pathway have elevated ROS levels in root hairs (Gayomba and Muday, 2020) and guard cells (Postiglione and Muday, 2020).

Through their radical scavenging activity, flavonoids are important players in the defence against plant stress and damage. For example, it has been demonstrated that flavonoids mitigate drought stress, both by lowering drought-induced ROS levels (Nakabayashi et al., 2014), and inducing closure of stomata through modulating phytohormone signalling (Brunetti et al., 2018). Another means by which flavonoids act as damage protectants is through photoprotection; flavonoids absorb ultraviolet-B light (UV-B) in the 280nm-320nm region and flavonoid biosynthesis mutants have been shown to be less tolerant to UV-B than wildtype (Ryan et al., 2001). Illustrating their importance as photoprotectants, it has previously been shown that UV-B treatment stimulates the transcription of flavonoid biosynthesis genes (Tohge et al., 2011), and a recent metabolomic study revealed that UV-B treatment (280-320 nm) increases flavonoid levels in Arabidopsis (Tsurumoto et al., 2022).

1.3.1 Flavonoid involvement in plant-microbial interactions

Another protective characteristic of flavonoids is their ability to confer resistance to biotic stressors, such as pathogenic attack. Flavonols have been demonstrated to protect plants against damage from pathogens. For example, anthocyanin-enriched tomato fruits have a lower susceptibility to *Botrytis cinerea* (Zhang et al., 2013), a fungal necrotrophic pathogen which infects many host species. This is thought to be due to the higher level of

anthocyanins interrupting the ROS burst which would typically occur with *B. cinerea* infection, promoting cell death (as reviewed in Heller and Tudzynski, 2011). In *Malus* crab-apple tree tissue infected with the fungal pathogen *Gymnosporangium yamadai*, expression levels of flavonoid biosynthesis genes were found to be significantly upregulated, with *CHS* in particular showing more than a 10-fold increase compared to non-infected tissues (Lu et al., 2017).

One way in which plants may attempt to protect themselves against pathogenic attack or other environmental stressors is through a hypothesised "cry-for-help" scenario, whereby plants secrete specific metabolites, including flavonoids, in their root exudates, to assemble beneficial microbes for a health-promoting rhizobiome. A recent study found that an increase in flavonoid levels in the root microbiome attracted microbes which were able to increase overall plant resistance to dehydration (He et al., 2022). He et al. (2022) demonstrated that higher flavonoid levels can lead to there being altered root microbiome community composition, with the family *Aeromonadaceae* being particularly flavonoid-responsive. The authors also saw that this mutualism enhanced plant drought resistance by regulating stomatal closure, preventing further water content loss.

Via their downstream signalling being involved in shaping the rhizospheric microbial community, flavonoids can also aid in mitigation of nutrient-deficiency in nutrient-poor soils. For example, flavonoid signalling is involved in around 80% of vascular plants during their formation of symbiotic interactions with arbuscular mycorrhizal (AM) fungi. This mutualism boosts plant nutrient uptake by increasing the root nutrient-scavenging surface area with long filamentous hyphae, in return for the carbon-rich photosynthates exuded from the roots of the host plant. Early studies on the AM symbiosis between *M. truncatula* and *Glomus intraradices* found an upregulation of the *AtCHS* homolog *MtCHS1* after initial contact between the host and symbiont (Bonanomi et al., 2001), suggesting that this early interaction induces flavonoid biosynthesis. In addition, flavonoids have been shown to accumulate in host roots during different stages of mycorrhization (Larose et al., 2002;

Schliemann et al., 2008). Flavonoids released in the root exudates are important pre-symbiotic signals in the establishment of plant-AM mutualisms, stimulating spore germination and hyphal growth (Scervino et al., 2005). Interestingly, a flavonoid mixture extracted from white clover mycorrhizal root exudates had different effects on the growth of AM fungi – hyphal branching was increased in Gigaspora, but there was no change in Glomus species (Scervino et al., 2005). This strongly suggests that there is specificity between flavonoid compounds and AM fungi species.

1.3.2 Flavonoid involvement in nodulation

Flavonoids are also essential to the formation of N-fixing symbioses between legumes and rhizobia. The most prominent function of flavonoids in this symbiosis is that they induce expression of rhizobial nodulation (*nod*) genes (Figure 1.8). Previously, Wasson et al. (2006) found almost no flavonoid compounds in the roots of CHS RNAi (*chs*) *M. truncatula*, as well as significantly reduced nodulation (Wasson et al., 2006). In a parallel study in *Glycine max*, the enzyme responsible for the biosynthesis of isoflavone, isoflavone synthase (IFS) was silenced (Subramanian et al., 2006) and the authors found there was no isoflavone in *G. max* RNAi *IFS* roots compared to control, and a major reduction in nodulation. The primary *G. max* symbiont is *Bradyrhizobium japonicum*, for which isoflavone is the main *nod* gene inducer, thus flavonoid biosynthesis and release was found to be key in the establishment of legume-rhizobia symbioses.

1.4 Aims and rationale for the work in this thesis

Phytohormones have vast effects on root system architecture development, varying across space (including cell type), time, and interplaying with each other. As a more recently discovered class of phytohormone, the precise developmental effects of strigolactones are not yet fully understood. This is further complicated due to significant molecular overlap with another novel phytohormone, karrikin; strigolactones and karrikins share both signalling components that they interact with, as well as structural similarity that can lead to increased overlapping effects.

To determine the exact role of strigolactone on root development, the root systems of strigolactone biosynthesis and signalling *Arabidopsis thaliana* mutant lines were phenotyped (Chapter 3 Effect of strigolactones on root system architecture and root transcriptome in *Arabidopsis thaliana*). Transcriptomic changes underlying the strigolactone-deficient root phenotypes were explored using RNA-sequencing of root tissue. Analysis of the resulting dataset found flavonoid biosynthesis to be significantly downregulated in the *Arabidopsis* strigolactone/karrikin signalling mutant roots, and so flavonoid staining of root tips and qPCR was used to explore flavonoid deficiency in a strigolactone-specific signalling mutant (Chapter 4 The strigolactone signalling pathway influences flavonoid biosynthesis in *Arabidopsis thaliana*). To assess phenotypic and transcriptomic effects of increased exogenous strigolactone on root development, seedlings were treated with a strigolactone analogue, and gene expression analyses performed (Chapter 5

Phenotypic and transcriptomic response of *Arabidopsis thaliana* to strigolactone analogue GR24^{4DO}). Finally, to explore whether the relationship between strigolactones, flavonoids and root system architecture is conserved between Arabidopsis and leguminous plants where strigolactones are known to be involved in the regulation of nodulation, phenotyping studies using *Medicago truncatula* strigolactone biosynthesis mutants were performed (Chapter 6 Role of strigolactones in regulation of root system architecture, nodulation, and flavonoid biosynthesis in *Medicago truncatula*).

1.4.1 Hypotheses, aims and objectives

In this thesis, the following hypotheses were proposed: strigolactone plays a role in root development in *A. thaliana* and *M. truncatula,* flavonoid biosynthesis requires strigolactone signalling in *A. thaliana*, and there is a D14-independent pathway for strigolactone signalling in *A. thaliana*. Each experimental chapter aimed to test these hypotheses, as follows:

1) Determine the role of strigolactone on root development in *A. thaliana*.

> Objectives: Phenotype root systems of *A. thaliana* strigolactone biosynthesis and signalling mutant lines and analyse transcriptomic changes underlying strigolactone-deficient root phenotypes through RNA-sequencing of root tissue.

2) Assess flavonoid biosynthesis in strigolactone-deficient *A. thaliana* mutants.

> Objectives: Quantify flavonoid accumulation in root tips via confocal microscopy and quantify flavonoid gene transcription via RT-qPCR in *A. thaliana* strigolactone biosynthesis and signalling mutant lines.

3) Test the effect of exogenous strigolactone treatment on root development.

> Objectives: Phenotype root systems of *A. thaliana* seedlings treated with a strigolactone analogue and analyse transcriptomic changes underlying the root phenotypes through RNA-sequencing of root tissue.

4) Explore whether the role of strigolactone in root development is conserved in *M. truncatula*.

> Objectives: Phenotype root systems of strigolactone-deficient *M. truncatula* mutant lines, quantify levels of flavonoid accumulation in the root tip via confocal microscopy and quantify levels flavonoid gene transcription via RT-qPCR.

Chapter 2 Materials and Methods

2.1 Biological material

2.1.1 *Arabidopsis thaliana*

For *Arabidopsis thaliana* experiments, mutants in the Col-0 background were used: *max1-1* (Booker et al., 2005) and *max2-1* (Stirnberg et al., 2002), *max3-9* (Booker et al., 2004) and *max4-1* (Sorefan et al., 2003), which were kindly donated by Dr Amanda Rasmussen (University of Nottingham, UK), and *d14-1* (Waters et al., 2012) and *kai2-2* seeds were kindly donated by Prof Caroline Gutjahr (Technical University of Munich, Germany) (Waters et al., 2012) (Table 2.1).

Table 2.1 Summary table of *A. thaliana* mutants employed in this work.

Line	Gene	Mutation detail	References
max3-9	*MAX3*	16 nucleotides in exon 2 replaced with 42 nucleotides, results in truncated protein	(Booker et al., 2004)
max4-1	*MAX4*	Transposon insertion in intron 1	(Sorefan et al., 2003)
max1-1	*MAX1*	Point mutation from proline to leucine	(Booker et al., 2005)
max2-1	*MAX2*	Point mutation from aspartic acid to asparagine	(Stirnberg et al., 2002)
d14-1	*D14*	T-DNA insertion within first 100 bp, results in undetectable full-length transcripts	(Waters et al., 2012)
kai2-2	*KAI2*	*Ds* insertion in intron 1	(Waters et al., 2012)

A. thaliana seeds were surface sterilised in 100% ethanol for 5 min, followed by 7% sodium hypochlorite solution for 5 min, then washed 5 times in sterile water. Cleaned seeds were suspended in 0.2% agar and sown onto 0.8% agar plates containing 0.5x Murashige and Skoog (MS) growth medium (Sigma-Aldrich M0529) supplemented with sucrose (1%) (adjusted to pH 5.7 with KOH). Plates were sealed using microporous tape and moved to 4°C in

the dark for stratification. After 2 days, plates were moved to a Sanyo growth chamber (MLR-351H, Sanyo, E&E Europe BV, Loughborough, UK) with a 12 hr light/12 hr dark photoperiod (or 8 hr light/16 hr dark, if otherwise stated), 50 mmol m^{-2} s^{-1} and 22°C during 'day' and 21°C 'night'. For experiments involving GR24, plates either contained 1 µm *rac*-GR24 (Chiralix) or the stereoisomer $GR24^{4DO}$ (StrigoLab) resuspended in acetone or an equivalent volume of acetone as a control.

2.1.2 *Medicago truncatula*

Medicago truncatula var. Jemalong A17 seeds were obtained from the Aberystwyth seed biobank; *nsp2-2* seeds were obtained from Professor Giles Oldroyd (Oldroyd and Long, 2003); *M. truncatula* ecotype R108 seeds were a Gifford lab stock and R108 background *ccd7-1* and *ccd8-1* seeds were kindly donated from Dr Soizic Rochange (Toulouse III - Paul Sabatier University, France) (Lauressergues et al., 2015) (Table 2.2).

Table 2.2 Summary table of *M. truncatula* mutants employed in this work.

Line	Gene	Mutation detail	References
ccd7-1	*CCD7*	*Tnt1* insertion in coding sequence, leading to premature STOP codon	(Lauressergues et al., 2015)
ccd8-1	*CCD8*	*Tnt1* insertion in coding sequence, leading to premature STOP codon	(Lauressergues et al., 2015)
nsp2-2	*NSP2*	Deletion in coding sequence	(Oldroyd and Long, 2003) (Kaló et al., 2005)

M. truncatula seeds were scarified in 95% sulfuric acid for 20-30 mins, or until dark spots appeared on all seeds. Sulfuric acid was removed, and seeds were washed 5 times with water. Seeds were then surface-sterilised in 7% sodium hypochlorite solution for 5 minutes and washed 8 times in sterile water, then were then sown onto 1.5% water agar plates. Sterile water was added to each seed and allowed to be imbibed; this was performed 3 times. Once water was absorbed, sterilised filter paper soaked in sterile water was

placed on the inner lid of the plate to provide humidity. The plate was then sealed with microporous tape and moved to 4°C in the dark for seed stratification. After 2-4 days, plates were then moved to a Sanyo growth chamber with a 16 hr light/8 hr dark photoperiod at 50 mmol m^{-2} s^{-1} and a constant 25 °C.

2.1.3 *Sinorhizobium meliloti*

S. meliloti 1022 was grown on (20 mM HEPES, 0.5% tryptone, 0.3% yeast extract, 6 mM $CaCl_2$ and 1.5% bactoagar, adjusted to pH 6.8-7.0 with KOH and supplemented with 50 µg/mL chloramphenicol) for 2 days at 28 °C. Liquid cultures were prepared by inoculating 20 mL of sterile TY/Ca^{2+} media (5 g/L Bacto Tryptone, 3 g/L yeast extract, 6 mM $CaCl_2$, adjusted to pH 6.8-7.0 with KOH and supplemented with 50 µg/mL chloramphenicol) with a single colony of *Sinorhizobium meliloti* 1022 and incubating for 24 hr in a shaking incubator at 28 °C and 220 rpm. Rhizobial inoculum was prepared by centrifugation at 4000 rpm and 4 °C for 10 min, and resuspension of rhizobial cells in sterile water to an OD_{600} of 0.05.

2.2 Methods

2.2.1 Root system architecture measurement

A. thaliana seedlings were grown as described (Section 2.1.1) on media containing 1 µm *rac*-GR24 (Chiralix) or $GR24^{4DO}$ (StrigoLab) resuspended in acetone or an equivalent volume of acetone as a control. 12-day-old seedlings were imaged via a flatbed scanner at 200 dpi, and images analysed using Fiji (Schindelin et al., 2012). For each seedling, the following measurements were recorded: primary root length, lateral root lengths, number of lateral roots, and lateral root density (number of lateral roots per cm of primary root). The first section of fully elongated root hairs from the root tip were imaged using a Leica MZ FLIII fluorescence stereomicroscope (Leica), and the following measurements were recorded via Fiji: root hair lengths and root hair density (root hair number per 3 mm area).

1-day-old germinated *M. truncatula* seedlings grown as described (Section 2.1.2), were transferred to a nitrogen-free modification of Fåhraeus medium (MFM) 1.5 % agar plates (as described by Catoira et al. 2000): 1 mM $CaCl_2$, 0.5 mM $MgSO_4.7H_2O$, 0.7 mM KH_2PO_4, 0.8 mM $Na_2HPO_4.2H_2O$, 20 μM FeNa-EDTA, 8 μM $MnSO_4.H_2O$, 4 μM $CuSO_4.5H_2O$, 7.34 μM $ZnSO_4.7H_2O$, 16 μM H_3BO_3 and 4.13 μM Na_2MoO_4, adjusted to pH 6.5 prior to autoclaving). Germinated seedlings were placed in a growth pouch directly in contact with the MFM agar (CYGTM Germination Pouch, Mega International, Newport, MN, USA) and treated with a further 25 mL liquid MFM media. Plates were then sealed with micropore tape and returned to the Sanyo growth chamber. After 2 days of growth on MFM media, seedlings were imaged. For each seedling, the 10 mm section of root hairs from the root tip on one side of the root were imaged using a Leica MZ FLIII fluorescence stereomicroscope (Leica), and the following measurements were recorded via Fiji: root hair surface area per 10 mm root and longest root hair length.

For both *A. thaliana* and *M. truncatula* root systems, significant differences between mutant samples and wildtype were calculated in R Studio; measurements were considered statistically significantly different if they had a $p < 0.05$ (analysis of variance and post hoc Tukey or pairwise Wilcoxon rank-sum test with FDR adjustment). All experiments were performed in triplicate, with each replicate consisting of 5-20 seedlings. Once imaged, whole root systems were flash-frozen in liquid N and stored at -80 °C for RNA extraction (Section 2.2.4).

2.2.2 Flavonoid quantification in *A. thaliana* and *M. truncatula*

10-day-old *A. thaliana* (Section 2.1.1) or 5-day-old *M. truncatula* (Section 2.1.2) seedlings were immersed in a solution containing 0.01% Triton X-100 and 2.52 mg/mL diphenylboric acid-2-aminoethyl ester (DPBA) for 7 minutes, then rinsed with distilled water for a further 7 minutes (Sanz et al., 2014). Primary root tips were mounted in distilled water and visualised on a Zeiss 880 Laser-Scanning Confocal Microscope (Carl Zeiss Microimaging) (excitation at 458 nm, emission band pass 500–630 nm, Zeiss EC Plan-Neofluar ×10

objective lens). Integrated density was measured using Fiji software (Schindelin et al., 2012) from the beginning of peak fluorescence in the root elongation zone. This location was selected in order to account for differences in the growth of different genotypes. Significant differences between treated/mutant samples and controls were calculated in R Studio using Student's *t*-test; measurements were considered statistically significantly different if they had a $p < 0.05$.

2.2.3 *M. truncatula* nodulation assay

3-day-old germinated *M. truncatula* seedlings (Section 2.1.2) with root systems > 2 cm were transferred to FP11 pots containing autoclaved perlite with ~ 1.5 cm layer of autoclaved vermiculite on top. Pots were watered with a nitrogen-free nutrient solution (1 mM $CaCl_2.2H_2O$, 1 mM KH_2PO_4, 75 μM FeNa-EDTA, 1 mM $MgSO_4.7H_2O$, 0.25 mM K_2SO_4, 6 μM $MnSO_4.H2O$, 20 μM H_3BO_3, 1 μM $ZnSO_4.7H_2O$, 0.5 μM $CuSO4.5H_2O$, 0.05 μM $CoSO_4.7H_2O$, 0.1 μM $Na_2MoO_4.2H2O$, adjusted to pH 6.5 using KOH). Two days after transfer to pots, seedlings were inoculated with 250 μL *S. meliloti* inoculum, as described previously (Section 2.1.3), or mock-treated with 250 μL sterile water. Pots were incubated at a constant 24 °C under a 16 hr light/8 hr dark photoperiod and watered with nutrient solution as needed. 4 weeks after inoculation, plants were imaged and the following measurements were taken per plant: shoot weight, root weight, nodule number and nodule weight. Measurements were considered statistically significantly different if they had a $p < 0.05$ (analysis of variance and post hoc Tukey or pairwise Wilcoxon rank-sum test with FDR adjustment). This experiment was performed in triplicate, with each replicate consisting of 5-8 seedlings.

2.2.4 RNA extraction

Root or whole seedling tissue for RNA extraction were homogenised into a fine powder using a pestle and mortar chilled on liquid N. RNA was extracted from homogenised sample using the Monarch Total RNA Extraction Kit (New England Biolabs), including the recommended on-column DNase treatment.

For samples for RNA sequencing (RNAseq), the quantity and quality of extracted RNA was checked with a Bioanalyzer 2100 RNA 6000 Pico Total RNA Kit (Agilent Technologies). RNA was stored at -80°C.

2.2.5 RT-qPCR

Extracted RNA was converted to cDNA using the ProtoScript II cDNA Synthesis Kit (New England BioLabs) according to the 'Standard Protocol', using 300 ng of total RNA. cDNA was stored at -20 ˚C. Primers for RT-qPCR were taken from literature or designed using the following parameters: primer melting temperature between 59-61°C, product size 50-250 bp and a GC-content between 45-55% (Table 2.3).

Table 2.3 List of primers used for RT-qPCR analysis. Primers were diluted to a working stock of 10 µM and stored at -20 °C (F, forward primer; R, reverse primer).

Target		Sequence (5'-3')	Reference
AtACTIN2	F	TGTGCCAATCTACGAGGGTTT	(Zhang et al., 2020)
(*AT3G18780*)	R	TTTCCCGCTCTGCTGTTGT	(Zhang et al., 2020)
AtACTIN7	F	AGGCACCTCTTAACCCTAAAGC	(Liang et al., 2020)
(*AT5G09810*)	R	GGACAACGGAATCTCTCAGC	(Liang et al., 2020)
AtCHS	F	TGTGCCAATCTACGAGGGTTT	(Jiang et al., 2015)
(*AT5G13930*)	R	TTTCCCGCTCTGCTGTTGT	(Jiang et al., 2015)
AtCHI	F	CATCGATCCTCTTCGCTCTC	(Jiang et al., 2015)
(*AT3G55120*)	R	AGGTGACACACCGTTCTTCC	(Jiang et al., 2015)
MtTUB	F	CCTGTTGCCGGTTCATAATC	N/A
(*Medtr2g041670*)	R	CCCAAACATAGATTGCTGCT	N/A
MtCHI	F	CACGCTGTTTCCCCTGATCT	(Li et al., 2016a)
(Medtr1g115840)	R	TCAACAACGCCGGTAATCTTG	(Li et al., 2016a)
MtCHS	F	CCACGACACCATCCTAAATTGTATC	(Li et al., 2016a)
(*Medtr5g007713*)	R	TGGTGTGACTAATGCCTTTTTGAC	(Li et al., 2016a)

RT-qPCR was performed in triplicate in 96-well plates on an Agilent Technologies Stratagene Mx3005P (Real-time PCR) system with a reaction volume of 10 µL per well, consisting of 1 µL cDNA, 500 nm of each primer and 0.5X SYBR Green JumpStart *Taq* ReadyMix (Sigma-Aldrich). Thermocycling

conditions were as follows: 95°C preincubation for 5 min, followed by 40 cycles of 95°C for 10 s, 58°C or 60°C for 10 s and 72°C for 10 s. After amplification, a dissociation cycle (with continual acquisition of fluorescence from 65 °C to 95°C) was used to confirm amplification of single amplicons per primer pair. The expression levels of genes of interest were normalised against reference genes via the ΔΔCt method (Schmittgen and Livak, 2008); significant differences between mutant samples and wildtype were calculated in R Studio using Student's *t*-test.

2.2.6 RNA sequencing processing

Extracted *A. thaliana* root tissue RNA from three biological replicates of samples were sequenced on an Illumina NovoSeq 6000 (Novogene UK). Sequencing was paired-end and unstranded, with 150 bp read-length sequences, and a sequencing depth of at least 20 million reads per sample. Quality control of the initial raw data was performed using FastQC. Trimmomatic v0.33 (Bolger et al., 2014) was used to trim and remove adaptors from raw reads with the following parameters: LEADING = 20, TRAILING = 20, SLIDINGWINDOW = 4:20, MINLENGTH = 75 and using PHRED33 quality scores. Quality control of the newly clean reads was performed again using FastQC. Trimmed paired reads were aligned using STAR (Dobin et al., 2013); STAR index files were created using the TAIR10 genome and genome annotation (the sjdbOverhang parameter was set to 149 which is the read length −1). Raw counts data for 32,833 genes in the *A. thaliana* genome were obtained from the STAR alignment files. DESeq2 was used to execute differential expression analysis (Love et al., 2014); genes were considered to be differentially expressed genes (DEGs) if they had a $\log_2$ fold change >1 and or <−1, as well as a Bonferroni-corrected $p < 0.05$. These DEGs were clustered into groups that responded similarly using K-means clustering and queried for overrepresented gene ontology (GO) terms using the 'enrichGO' function from the R package clusterProfiler 4.0 (Wu et al., 2021). GO terms which had a $p < 0.05$ were considered overrepresented. Raw RNA-seq data from this work which has been published has been deposited in the NCBI SRA database (PRJNA784414) (Richmond et al., 2022).

Chapter 3 Effect of strigolactones on root system architecture and root transcriptome in *Arabidopsis thaliana*

3.1 Introduction

3.1.1 Strigolactone biosynthesis and signalling in the model plant *A. thaliana*

Strigolactone biosynthesis in *Arabidopsis* begins with the conversion of carotenoid precursor all-*trans*-β-carotene into 9-*cis*-β-carotene via carotenoid isomerase DWARF27 (D27) (Abuauf et al., 2018; Booker et al., 2004) (Figure 3.1). 9-*cis*-β-carotene is sequentially cleaved by carotenoid cleavage dioxygenases 7 and 8 (CCD7 and CCD8) to form carlactone (Booker et al., 2004; Sorefan et al., 2003).

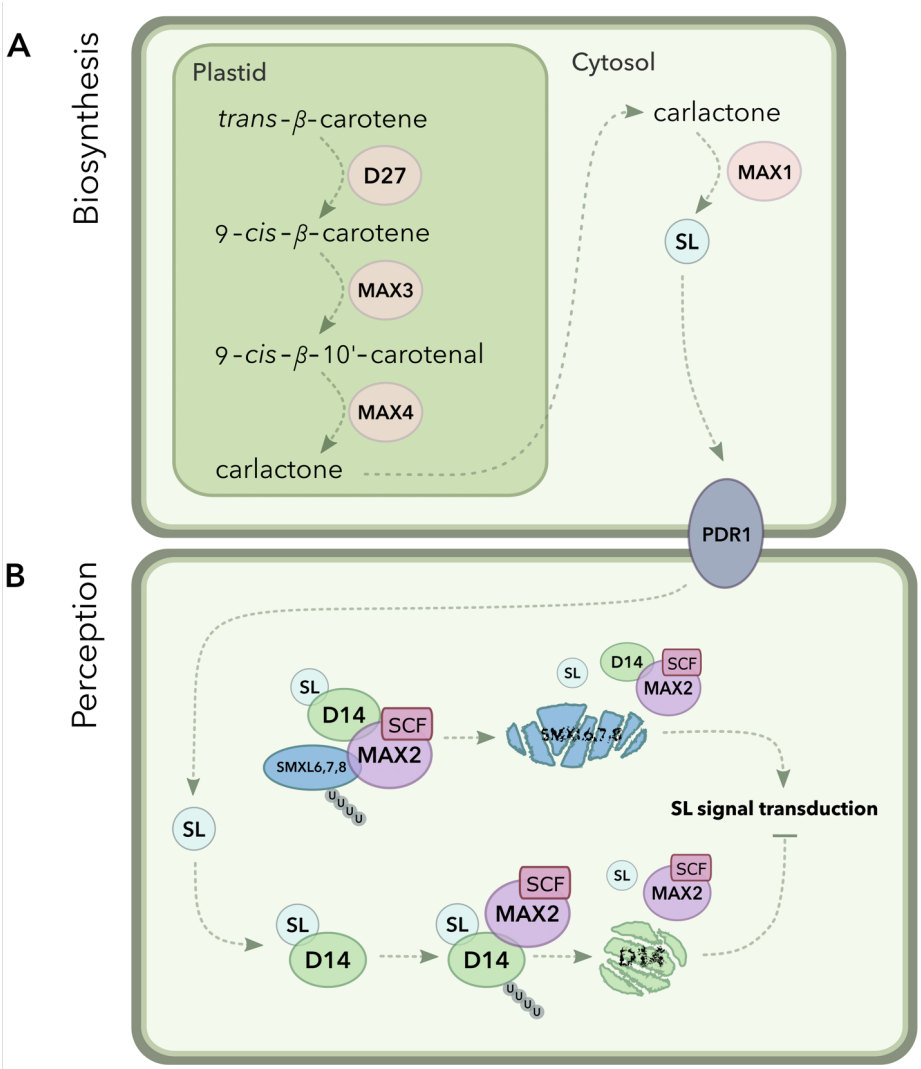

Figure 3.1 Strigolactone biosynthesis in *Arabidopsis thaliana.* A) Strigolactone (SL) biosynthesis occurs through the successive action of DWARF27 (D27) and MORE AXILLARY GROWTH (MAX) proteins 3 and 4, which ultimately convert all-*trans*-β-carotene into SL precursor carlactone. MAX1 converts carlactone into carlactonoic acid, which is then converted into SL. B) SL is transported via PLEIOTROPIC DRUG RESISTANT1 (PDR1) transporters, where it is perceived in cells by its receptor D14. Once activated by SL, D14 undergoes a conformational change and is able to associate with MAX2, which acts as the adaptor of the S-phase kinase associated protein 1-Cullin-F-box (SCF) E3 ubiquitin ligase, forming SCF^{MAX2}. The D14-SCF^{MAX2} complex polyubiquitinates SL signalling repressors SUPPRESSOR OF MAX2 1-LIKE (SMXL) 6, 7 and 8, targeting them for degradation. SCF^{MAX2} can also polyubiquitinate D14, limiting SL signal transduction. Adapted from Richmond et al. (2022).

Given the identified role of SLs in shoot branching, *CCD7* and *CCD8* are also termed *MORE AXILLARY GROWTH* (*MAX*) *3* and *4*, respectively. The Class III cytochrome P450 monooxygenase MAX1 is responsible for the cytosolic oxidisation and hydroxylation of carlactone to form carlactonoic acid (Booker et al., 2005), which is then further converted through yet unknown mechanisms to form SLs. PLEIOTROPIC DRUG RESISTANT1 (PDR1) transporters carry SLs to other cells where they induce downstream responses. SLs are perceived in these cells via the SL receptor and α/β-fold hydrolase DWARF14 (D14).

The binding of SL to D14 induces protein conformational changes, allowing the formation of complexes with its signalling counterparts (Figure 3.1B). One such assembly of proteins is comprised of MAX2, alongside the S-phase kinase associated protein 1-Cullin-F-box (SCF) complex, forming SCF^{MAX2}. The SCF complex is an E3 ubiquitin ligase which catalyses polyubiquitination of proteins, targeting them for degradation. MAX2, is an F-box leucine-rich repeat protein, acting as the substrate-binding subunit for the SCF^{MAX2} complex (Stirnberg et al., 2007). For downstream SL signalling, the D14-SCF^{MAX2} complex has been shown to bind and polyubiquitinate known repressors of SL signalling, including SUPPRESSOR OF MAX2 1 (SMAX1) and SMAX1-LIKE (SMXL) family proteins (Soundappan et al., 2015). In this way, their repression is alleviated, and SL signalling can occur. D14 itself is also one of the degradation targets of SCF^{MAX2}, forming a negative feedback loop to regulate the intensity and duration of SL signalling (Chevalier et al., 2014).

3.1.1.1 Strigolactone and karrikin interplay

MAX2 is a receptor of SL, and it is also a receptor of similar small butenolide molecules called karrikins (KARs). KARs are exogenously derived from the smoke of burning plant material, through the pyrolysis of simple carbohydrates, such as cellulose, glucose and xylose. Once deposited onto the soil surface, they stimulate the germination of dormant seeds in many plant species (as reviewed in Meng et al., 2017). Like many plants, Arabidopsis

does not typically colonise environments prone to wildfires, but nonetheless responds to KARs. Endogenous karrikin-like compounds – KAI2-ligands (KLs) – are also found in plants, acting as signalling molecules. The KAR and KL receptor, KARRIKIN INSENSITIVE2/HYPOSENSITIVE TO LIGHT (KAI2/HTL, KAI2 henceforth) is an α/β-fold hydrolase, and a paralogue of D14 (Waters et al., 2012). Intriguingly, both D14 and KAI2 require MAX2 for downstream SL and KAR signalling, and both target paralogous repressors in the SMXL family. The evolutionary history of KAR and SL signalling is also heavily entwined; phylogenetic analyses imply that the SL receptor D14 is derived from the duplication and differentiation of the eu-KAI2 lineage in land plants, explaining their signalling overlaps and similarities (Bythell-Douglas et al., 2017).

The roles of SL and KAR signalling also converge, meaning it is difficult to correctly attribute certain roles to either pathway. To illustrate, both pathways have been implicated in key plant developmental processes, including germination (Holbrook-Smith et al., 2016; Nelson et al., 2009; Wang et al., 2018), photomorphogenesis (Kim et al., 2022; Xie et al., 2020; Zheng et al., 2020) and root system shaping (Oláh et al., 2021; Rasmussen et al., 2012; Villaécija-Aguilar et al., 2019). Both D14 and KAI2 signalling systems confer tolerance to abiotic stressors, including osmotic stress and drought (Ha et al., 2014; Haider et al., 2018; Li et al., 2017a; Li et al., 2020a). Both pathways have also been associated with the formation of beneficial plant-microbe interactions. For example, as components of plant root exudates, SLs are known to be rhizospheric signals for symbioses, both with arbuscular mycorrhizae and rhizobia. SL-deficient pea and *Glycine max* plants have reduced nodule numbers, demonstrating the role of SLs in promoting nodulation (Foo et al., 2013; Rehman et al., 2018). KAI2-mediated signalling also appears to regulate interactions with soil arbuscular mycorrhizae, in *Oryza sativa* and Brachypodium (Gutjahr et al., 2015; Meng et al., 2022). The use of the same components and their seemingly highly related developmental functions, makes deciphering SL and KL downstream pathways very difficult, but further experiments with *kai2* and *d14* mutants, will make the roles easier to discern.

3.1.2 Variation in structure and bioactivity of strigolactone and strigolactone analogues

SLs are a diverse family of sesquiterpene lactones. So-called canonical SLs share the same core chemical structure of two lactone moieties; a butenolide (D-ring) part connected to a tricyclic γ-lactone (ABC-ring) by an enol-ether bridge (Figure 3.2A). Given that the D-ring is present in all known naturally occurring SLs, it seems likely to have a crucial role in SL agonistic activity. These SLs can be further subdivided into strigol- and orobanchol- types, depending on the stereochemistry of the C-ring, whilst the D-ring remains in the same *R* configuration. It is currently thought that strigol-type SLs are derivative of 5-deoxystrigol (5DS) whilst orobanchol-type SLs derive from 4-deoxyorobanchol (4DO). Non-canonical SLs are those which do not feature the A, B, and/or C parts, though the D-ring is still attached to the molecule via the same enol-ether bridge.

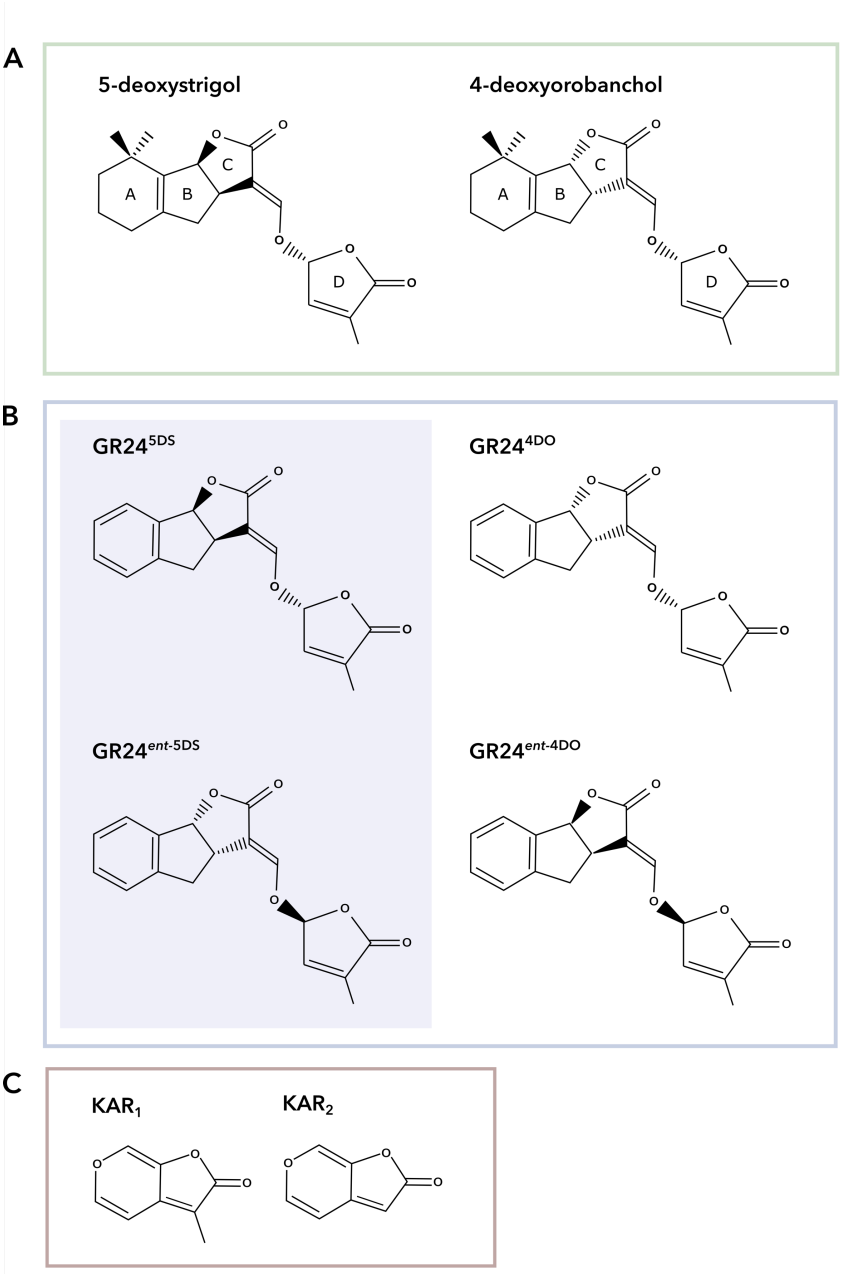

Figure 3.2 Chemical structures of canonical strigolactones (SLs), GR24 stereoisomers and KARs. A) Structures of canonical SLs, 5-deoxystrigol (5DO) and 4-deoxyorobanchol (4DO). A, B and C denote the tricyclic lactone, D represents the butenolide ring. B) Structures of GR24 synthetic SL analogues; highlighted blue in is $GR24^{5DS}$ and its enantiomer $GR24^{ent\text{-}5DS}$ which comprise *racemic* GR24. C) Structures of karrikins, KAR_1 and KAR_2.

Studies on the downstream role of SLs on root system architecture have oftentimes used racemic GR24 (*rac*-GR24) - a synthetic SL mixture composed of $GR24^{5DS}$ and $GR24^{ent\text{-}5DS}$ (Figure 3.2B) - due to its relative affordability in comparison to separated stereoisomers; it is typically 3 times

less expensive. $GR24^{5DS}$ binds the SL receptor D14 as a ligand and activates D14-mediated SL signalling through MAX2 (Scaffidi et al., 2014). However, despite the evident structural similarities between *rac*-GR24 and the canonical SLs, it has been demonstrated that there are also considerable structural similarities to karrikins (Figure 3.2C), thus the $GR24^{ent\text{-}5DS}$ enantiomer is able to bind and activate the KL receptor KAI2 (Flematti et al., 2016). Because of this, *rac*-GR24 is by no means a perfect SL analogue, but it is a useful tool for investigating the general function of MAX2 and downstream signalling, preferentially via D14.

3.1.3 Aims and Objectives

The aim of this work was to determine the role of SLs in Arabidopsis root development because of the significant overlap between the roles of SL and KL (Section 1.4.1). Previous work on SL/KL signalling and its role in plant development have been somewhat contradictory. For example, some authors find that *rac*-GR24 promotes root hair elongation (Kapulnik et al., 2011b), whereas others do not (Villaécija-Aguilar et al., 2019). Thus, the impact of the SL/KL mimic *rac*-GR24 on root development was assessed, as well as the root phenotypes in SL/KL mutants, in order to define how SL and/or KL signalling impacts root system architecture.

Next, transcriptomic analyses of SL mutant plants were analysed to determine the mechanisms behind root system architectural changes that were found.

3.2 Results and Discussion

3.2.1 Mixed synthetic SL reduces lateral root length and number but not in strigolactone signalling mutant

To identify root system architectural traits which may be attributed to SL signalling, *max3-9, max4-1,* and *max1-1* mutants in the Arabidopsis SL biosynthesis pathway were obtained, as well as the SL- and KAR-insensitive mutant *max2-1*. Seedlings were grown for 12 days on mock media, or one

containing 1 μM *rac*-GR24, and root system architecture compared to the wildtype Col-0.

The length of the primary root was not found to be affected by *rac*-GR24 in any of the mutants. However, *max4-1* had a significantly shorter primary root length than Col-0 in both the mock and *rac*-GR24 treatment (*p* values: 9.9E−09 and 6.2E−09, respectively) (Figure 3.3A, E). Lateral root lengths were significantly shorter with *rac*-GR24 treatment compared to mock in Col-0 (*p* = 8.2E−05), *max3-9* (*p* = 3.3E−08), *max4-1* (*p* = 6.9E−06) and *max1-1* (*p* = 1.6E−03), but not for *max2-1* (Figure 3.3B, E). Lateral root number per seedling was significantly lower with *rac*-GR24 treatment in Col-0 (*p* = 0.005), *max3-9* (*p* = 2.1E−09), *max4-1* (*p* = 2.8E−02) and *max1-1* (*p* = 0.03) though not in *max2-1* (Figure 3.3C, E). Lateral root density – calculated as the number of lateral roots divided by primary root length (cm) – was also decreased compared to Col-0 with *rac*-GR24 addition (*p* = 5.8E−05), *max3-9* (*p* = 3.3E−10), *max4-1* (*p* = 2.8E−07) and *max1-1* (*p* = 2.6E−03), though not in *max2-1* (Figure 3.3D, E).

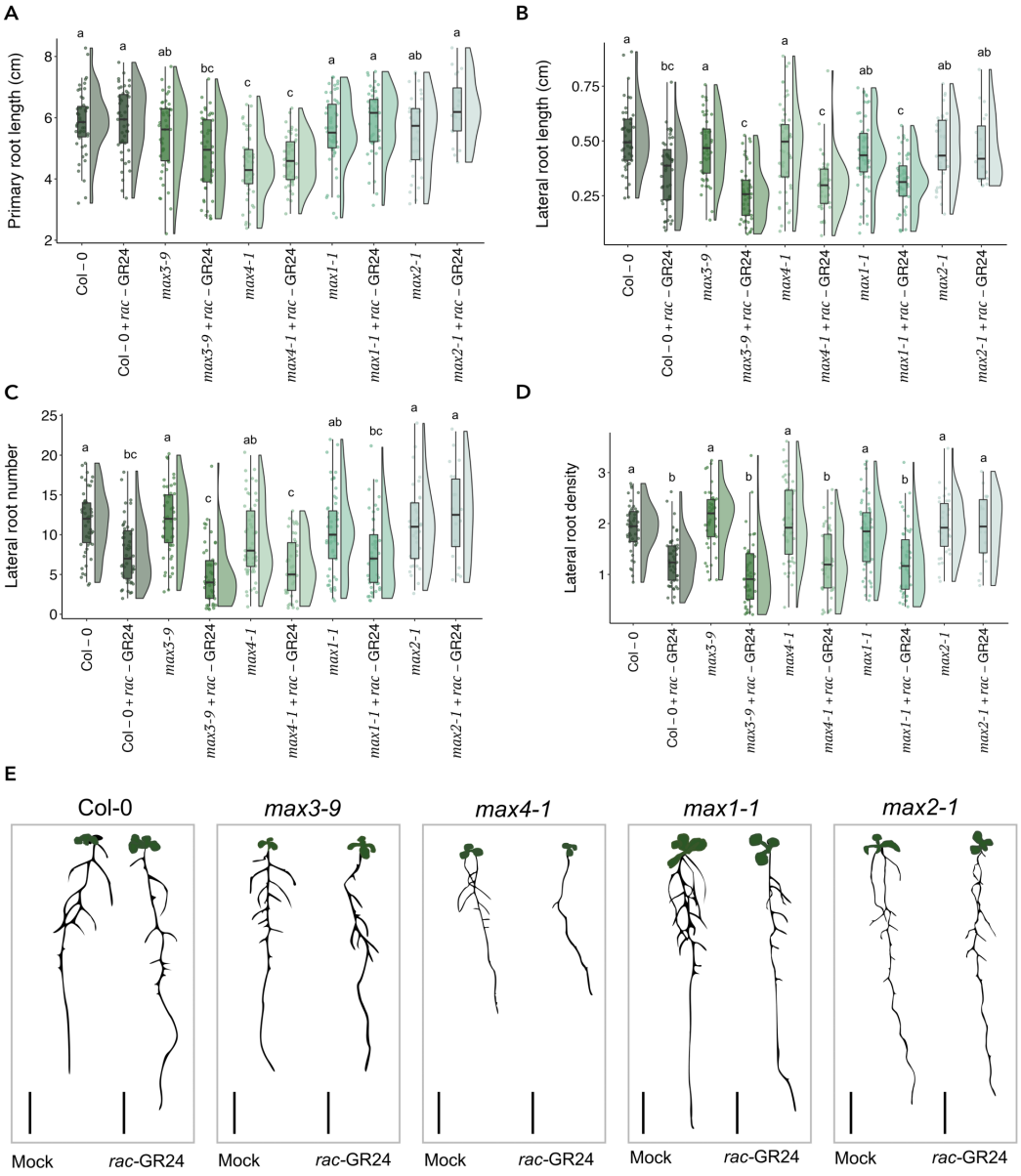

Figure 3.3 Lateral root length, number, and density of 12-day-old Col-0 and SL biosynthesis mutants are reduced upon *rac*-GR24 treatment compared to mock treatment. (A) Primary root length (cm) of 12-day-old Col-0, *max3-1, max4-1, max1-1* and *max2-1* seedlings after growth on 1 µM rac-GR24 media in 12 h light/12 h dark photoperiod. (B) Lateral root average length (cm), (C) lateral root number and (D) lateral root density. (E) Representative images converted to bitmap for each genotype-treatment combination, bars represent 1 cm. Different letters indicate statistically significant differences, determined by ANOVA, post hoc Tukey: $p < 0.05$; (A) $F_{9,429} = 13.183$, (B) $F_{11,535} = 13.919$, (C) $F_{11,535} = 11.52$, (D) $F_{11,535} = 17.297$, 5–20 seedlings per biological repeat, four biological repeats). Adapted from Richmond et al. (2022).

Given that the effect of *rac*-GR24 is sustained in the *max4-1*, *max1-1*, and *max3-1* lines, this suggests that the impact of *rac*-GR24 on lateral root development is independent of these genes. Meanwhile, the *max2*-insensitivity to *rac*-GR24 highlights a dependency on *MAX2* for shaping lateral root architecture in response to *rac*-GR24. This concurs with previous studies which also found a *rac*-GR24 induced decrease in lateral root length and number compared to mock (Jiang et al., 2016; Kapulnik et al., 2011a; Ruyter-Spira et al., 2011).

3.2.2 Lateral root length, number, and density in karrikin signalling mutant is not altered by mixed synthetic SL treatment

Rac-GR24 can stimulate both SL and KL signalling through MAX2, so therefore the next step was to discern whether one or both pathways affected the lateral root developmental changes that were seen. An experiment was designed to discern the role of KAI2 and KL signalling in *rac*-GR24-induced root architectural changes and in particular the *max2-1 rac*-GR24 insensitive response (Section 3.2.1). Root architectural phenotyping was therefore performed using the KL receptor mutant *kai2-2* and the SL receptor mutant *d14-1*.

Primary root length was found not to be affected by *rac*-GR24 treatment, in *d14-1*, *kai2-2* or Col-0 (Figure 3.4A, E), but in mock conditions *d14-1* had a significantly longer primary root than Col-0 (p = 0.037). With *rac*-GR24 treatment, the lateral root length was shorter compared to mock conditions in both Col-0 (p = 4.1E−09) and *d14-1* (p = 0.024), though not in *kai2-2* (Figure 3.4B, E). There were fewer lateral roots in *rac*-GR24 treated seedlings for Col-0 (p = 0.024) and *d14-1* (p = 0.001), but again, not *kai2-2* (Figure 3.4C, E). The absence of lateral root architectural inhibition in response to *rac*-GR24 in *kai2-2* suggests that the regulation of this response could be primarily driven by KL signalling.

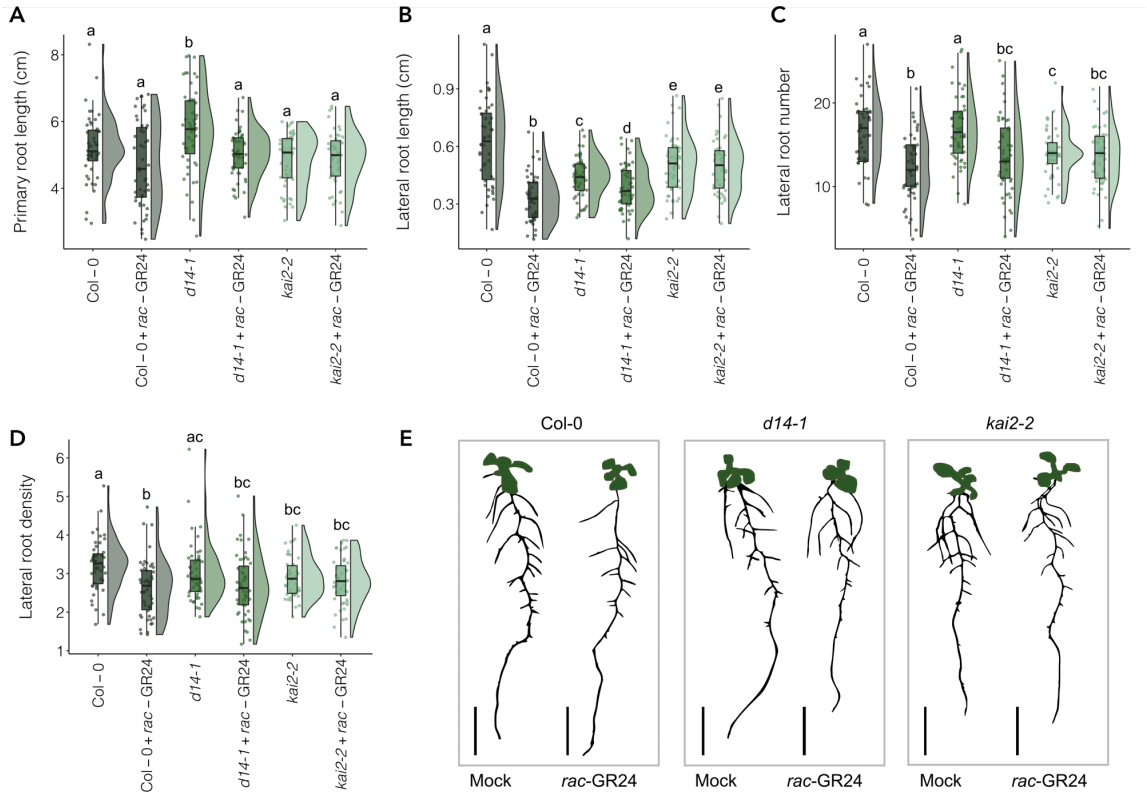

Figure 3.4 *Rac*-GR24 compared to mock treatment reduces the length and number of lateral roots in 12-day-old Col-0 and *d14-1* roots, but not those of *kai2-2*. (A) Primary root length (cm) of 12-day-old Col-0, *d14-1*, and *kai2-2* seedlings after growth on 1 µM rac-GR24 media in 12 hr light/12 hr dark photoperiod, (B) lateral root average length (cm) of the same plants, (C) lateral root number and (D) lateral root density. (E) Representative images converted to bitmap for each genotype-treatment combination, bars represent 1 cm. Different letters indicate statistically significant differences, determined by pairwise Wilcoxon rank sum test (FDR-adjusted $p < 0.05$; n = 12–20 seedlings per biological repeat, three biological repeats). Adapted from Richmond et al. (2022).

The longer primary root in *d14-1* compared to Col-0 under mock-treated conditions contradicts the short primary root phenotype seen in *max4-1*. Interestingly, Villaécija-Aguilar et al (2019) found the opposite – that the primary root lengths of *d14-1* mutants were shorter than Col-0 – under their 16-h light/8-h dark photoperiod. Whilst the results presented here suggest a role for SL signalling in primary root development, it appears that the effects may be subtle and largely dependent on external conditions, such as daylength.

Links have also been made between SL/KL synthesis and signalling, nitric oxide (NO) and primary root growth inhibition. It has been suggested that NO could be both a negative regulator of SL production, as well as an inducer of SL signalling. The enzyme S-nitrosoglutathione (GSNOR) reductase maintains homeostasis of NO and S-nitrosothiol (SNO), and thereby regulates the levels of reactive nitrogen species and intracellular NO levels, and the processes mediated by them. Intriguingly, both up- and down-regulation of GSNOR levels have been shown to result in a significant decrease in primary root length in Arabidopsis. Oláh et al (2020) found that *max1-1*, *d14-1, max2-1* and *kai2-3* root tips had elevated NO levels, with decreased S-nitrosoglutathione (GSNO) reductase (GSNOR) protein abundance and activity (Oláh et al., 2021, 2020). Therefore, the lack of D14-mediated SL signalling in the *d14-1* mutant may result in primary root growth promotion through changes to NO signalling.

Interestingly, lateral root density only changed in response to *rac*-GR24 compared to mock treatment in Col-0 (p = 0.001), but not in either *d14-1* nor *kai2-2* (Figure 3.4D, E). As both *d14-1* and *kai2-2* have a *rac*-GR24 insensitive phenotype in terms of lateral root density, it suggests that this response is co-regulated through both SL and KL signalling, as hypothesised by Villaécija-Aguilar et al. (2019). In fact, both *d14-1* and *kai2-2* had significantly shorter lateral roots than Col-0 in the mock treatment (p = 4.9E−05 and 0.01, respectively), and lateral root number and density was also significantly decreased in the *kai2-2* mutant (p = 0.001 and 0.032, respectively). Therefore, it appears that both D14 and KAI2 are to some extent both involved in lateral root responses to *rac*-GR24 and lateral root development as a whole.

3.2.3 The SL biosynthesis mutant *max4-1* has a shorter primary root length than Col-0 under a 12 light/12 dark photoperiod

Whilst phenotyping the root systems of the SL mutants, the short primary root phenotype of *max4-1* was evident. However, a literature search demonstrated contrary results; for example, Villaécija-Aguilar et al. (2019) found no such difference in primary root length between Col-0 and *max4-1* (Villaécija-Aguilar et al., 2019). In reviewing the work, differences in the experimental photoperiods used were noted; the work presented here uses a 12 hr light/12 hr dark photoperiod, whilst Villaécija-Aguilar et al. (2019) use a 16 hr light/8 hr dark photoperiod.

In order to measure whether daylength affects the primary root length in *max4-1*, the experiment was therefore repeated, with both Col-0 and *max4-1* grown under both photoperiods. Under a 16 hr light/8 hr dark photoperiod, all plants had significantly shorter primary root lengths compared to those grown in 12 hr light/12 hr dark. Consistent with our initial findings, *max4-1* seedlings had significantly shorter primary roots compared to Col-0 under the 12 hr light/12 hr dark conditions (p = 9.4E−15), but not in the 16 hr light/8 hr dark photoperiod (Figure 3.5A, E). The *rac*-GR24 induced decreases in lateral root length and density in *max4-1* were maintained in a 16 hr light/8 hr dark photoperiod (p = 0.007 and 4.8E-09, respectively). Combined, this suggests that the shorter primary root length in *max4-1* is at least partially regulated by photoperiod, and not rescuable by *rac*-GR24 treatment.

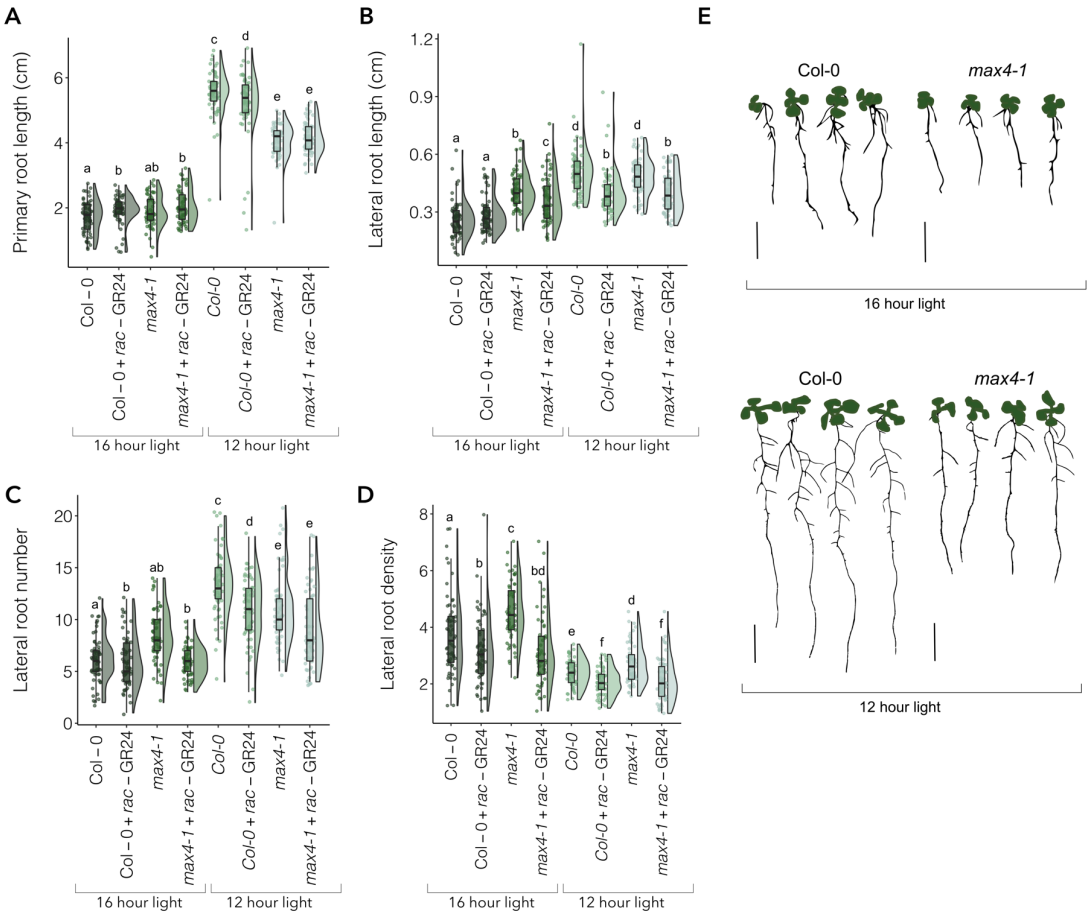

Figure 3.5 Photoperiod affects the short primary root length phenotype of *max4-1*. (A) Primary root length (cm) of 12-day-old Col-0 and *max4-1* seedlings after growth on 1 µM treatment in either a 12 hr light/12 hr dark photoperiod, or a 16 hr light/8 hr dark photoperiod, (B) lateral root average length (cm), (C) lateral root number and (D) lateral root density of the same plants. (E) Representative images converted to bitmap; bars represent 1 cm. Different letters indicate statistically significant differences (pairwise Wilcoxon rank sum test [FDR-adjusted $p < 0.05$]; n = 5–20 seedlings per biological repeat, four biological repeats). Adapted from Richmond et al. (2022).

Other recent studies have also supported this finding, enabling the SL pathway to be linked to light signal perception. In *Solanum lycopersicum*, expression of *SlCCD*s is upregulated with an increase in light intensity and are positive regulators of photoperiod-regulated light-harvesting genes (Mayzlish-Gati et al., 2010). Furthermore, D14 and the MAX4 homolog DWARF10 (D10) have been shown to be regulated by the circadian clock in *Oryza sativa*; overexpression of the *O. sativa* CIRCADIAN CLOCK ASSOCIATED1 (*OsCCA1*) positively regulates both *OsD14* and *OsD10* expression levels by

binding directly to their promotor regions (F. Wang et al., 2020). CCA1 is a key regulator of the plant circadian clock, controlling rhythmic expression of morning-phased and evening-phased genes. If *AtD14* and *AtMAX4* are also entrained to the circadian clock as with *OsD14* and *OsD10*, it could affect SL and SL-precursor levels, potentially explaining the photoperiod-related changes in primary root length seen in *max4-1*.

To evaluate changes to *MAX4* and *D14* transcript abundance depending on daylength, normalised microarray expression data was explored from the DIURNAL database (Mockler et al., 2007). *MAX4* transcripts did not appear to oscillate rhythmically, though *MAX4* expression is known to be regulated via D14-mediated degradation of SMXL6/7/8 (Wang et al., 2020c). *CCA1* and *D14* transcript abundance oscillated rhythmically under both 12 hr light/12 hr dark (long days) and 8 hr light/16 hr dark (short days) (Figure 3.6). However, the rhythm of *D14* oscillations appears to change under these different daylengths. Under short days, *CCA1* and *D14* transcript levels peaked every 24 hr. Under long days, *CCA1* peaked every 24 hr, but *D14* appears to have two peaks per 24 hr period, with larger peaks at 12 hr. Therefore, it is possible that *D14* levels are also different in a 16-hr light/8-hr dark photoperiod. In *max4*, the lack of functional MAX4 would lead to less accumulation of SL precursor carlactone, which has been shown to be able to interact with D14 *in vitro* (Abe et al., 2014). It is possible that this interaction may have a downstream effect in plant growth; indeed, *MAX4* is strongly expressed in *Arabidopsis* primary root tips, suggesting biological significance (Bainbridge et al., 2005).

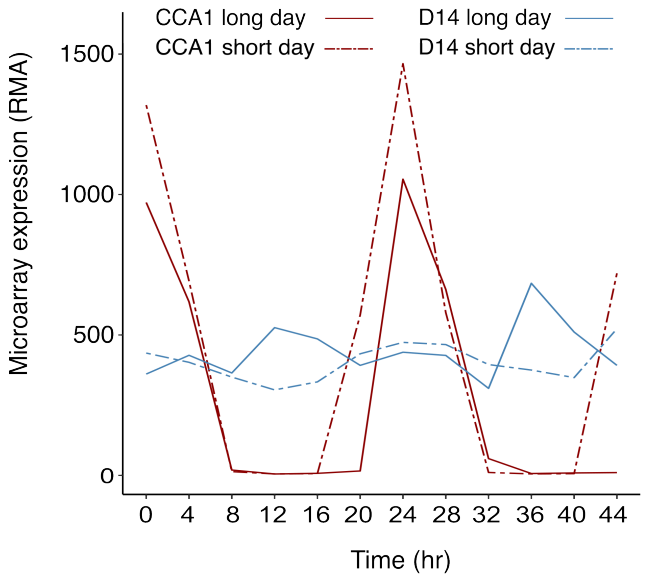

Figure 3.6 Circadian oscillations of *CCA1* and *D14* transcripts. Microarray data (Robust Multichip Average [RMA]) from Diurnal (Mockler et al., 2007) was used to assess how *D14* transcripts oscillate with *CCA1* according to daylength; long days (12 hr light/12 hr dark), short days (8 hr light/16 hr dark).

Combined with daylength, the potential role of carlactone and D14 on root system architecture needs to be further studied. Col-0, *d14-1* and *max4-1* seedlings could be grown across a range of photoperiods, and root systems phenotyped, to link the short primary root phenotype. To assess the effect of carlactone on root system phenotype, a MAX4-overexpressing line could be phenotyped, potentially crossed with a *max1* knockout mutant to suppress conversion from carlactone to SL.

3.2.4 Root hair number increases in response to mixed synthetic SL in Col-0 and SL biosynthesis mutants, but not in SL signalling mutant

In previous mentioned works using a 16 hr light/8 hr dark photoperiod, some authors observed significant increases in root hair length with *rac*-GR24 addition in Col-0 and *max4-1* (Kapulnik et al., 2011a), whilst others found none (Villaécija-Aguilar et al., 2019). The next logical step to understand *rac*-GR24 effects was to assess the effect of *rac*-GR24 on root hair development across the *max* mutants under the 12 hr light/12 hr dark photoperiod used here.

Root hair number was found to increase with *rac*-GR24 treatment (compared to mock-treatment) in Col-0 (p = 6E−04), *max3-9* (p = 0.001), *max4-1* (p = 2E−04) and *max1-1* (p = 9.50E−05), whilst not in *max2-1* (Figure 3.7A,C). Root hairs were significantly more numerous in *max3-9, max4-1 and max1-1* compared to Col-0, but there are significantly less root hairs in *max2-1* (p = 0.047). Root hair length increased with *rac*-GR24 treatment (compared to mock) in Col-0 (p = 0.03) and *max4-1* (p = 0.049) (Figure 3.7B-C), corresponding with the root hair phenotype described by Kapulnik et al. (2011) (Kapulnik et al., 2011a). Villaécija-Aguilar et al. (2019) suggest that *rac*-GR24-mediated root hair elongation is primarily driven through KL signalling, however a significant decrease was observed in root hair length in *max1-1* with *rac*-GR24 treatment compared to mock (p = 4.1E−02). Intriguingly, in mock treated conditions, *max4-1* and *max1-1* had significantly longer root hairs than Col-0 (p = 1.40E−08 and 8.70E−08, respectively) (Figure 3.7B-C).

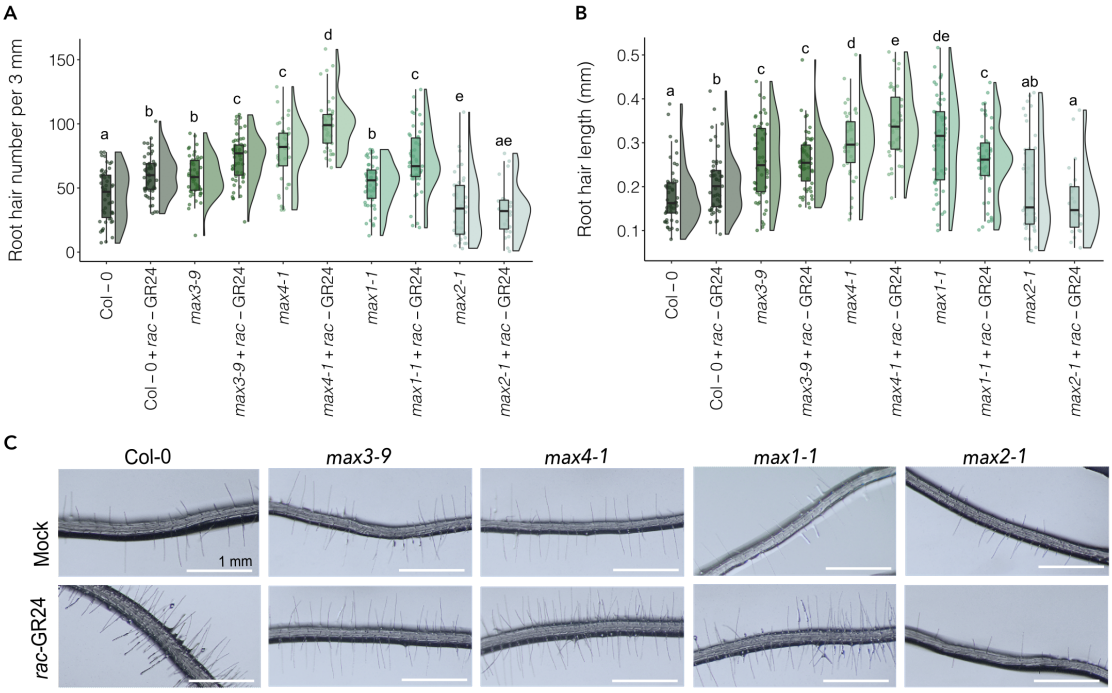

Figure 3.7 Rac-GR24 increases root hair number, except for in *max2-1*. (A) Average root hair number (per 3 mm) of Col-0, *max3-9*, *max4-1*, *max1-1* and *max2-1* roots after growth on 1 µM rac-GR24 in 12 hr light/12 hr dark photoperiod and (B) root hair length of the same plants. (C) Representative images, bars represent 1 mm. Different letters indicate statistically significant difference, determined by pairwise Wilcoxon rank-sum test (FDR-adjusted $p < 0.05$; n = 5–20 seedlings per biological repeat, four biological repeats). Adapted from Richmond et al. (2022).

As carlactone and other SL-precursors are bioactive, accumulation of these in the *max1-1* mutant, alongside *rac*-GR24 treatment, may impact root hair elongation. Equally, if SLs had a positive influence on root hair length and density, it could be predicted that under mock conditions, SL biosynthesis mutants would have shorter and less numerous root hairs than Col-0. In contrast, all *max* biosynthesis mutants tested here were found to have longer and more numerous root hairs than Col-0. This suggests that SL has an impact on root hair development in some way, though the mechanism appears to be complex. On the other hand, as *max2-1* does not show a significant increase in root hair length or number with *rac*-GR24 treatment, it supports the conclusion from previous authors that the *rac*-GR24 root hair response is MAX2-dependent (Kapulnik et al., 2011a).

3.2.5 Root hair number and length in SL receptor mutant is not affected by treatment with mixed synthetic SL

Given that the *rac*-GR24-mediated root hair length and number increase appeared to be MAX2-dependent, the next experiment aimed to discern whether the *rac*-GR24 phenotype is dependent on D14, KAI2 or a combination of both. There is evidence that both SL and KL regulate root hair development – both D14- and KAI2-activating GR24 stereoisomers have been found to promote root hair elongation (Li et al., 2016a) – so it is plausible that both pathways contribute to some extent. Root hair phenotyping with *rac*-GR24 was performed on *d14-1* and *kai2-2* to assess the roles of D14 and KAI2 in the root hair response to *rac*-GR24.

In contrast to the *rac*-GR24-mediated lateral root response, there was found to be an increase in root hair number and length with *rac*-GR24 addition compared to mock in both Col-0 (p = 0.01 and p = 3.11E−02, respectively) and *kai2-2* (p = 0.001 and p = 2.48E−03, respectively) (Figure 3.8A-C). However, there was no significant difference in root hair length or number in *d14-1*, implying that the root hair *rac*-GR24 response may be primarily SL-driven. It is interesting to note that in the mock conditions, both *d14-1* and *kai2-2* root hairs were significantly longer than Col-0 (p = 3.84E−04 and 1.89E−04, respectively) (Figure 3.8B,C), suggesting that SL and KL signalling pathways may both play a role in the regulation of root hair elongation.

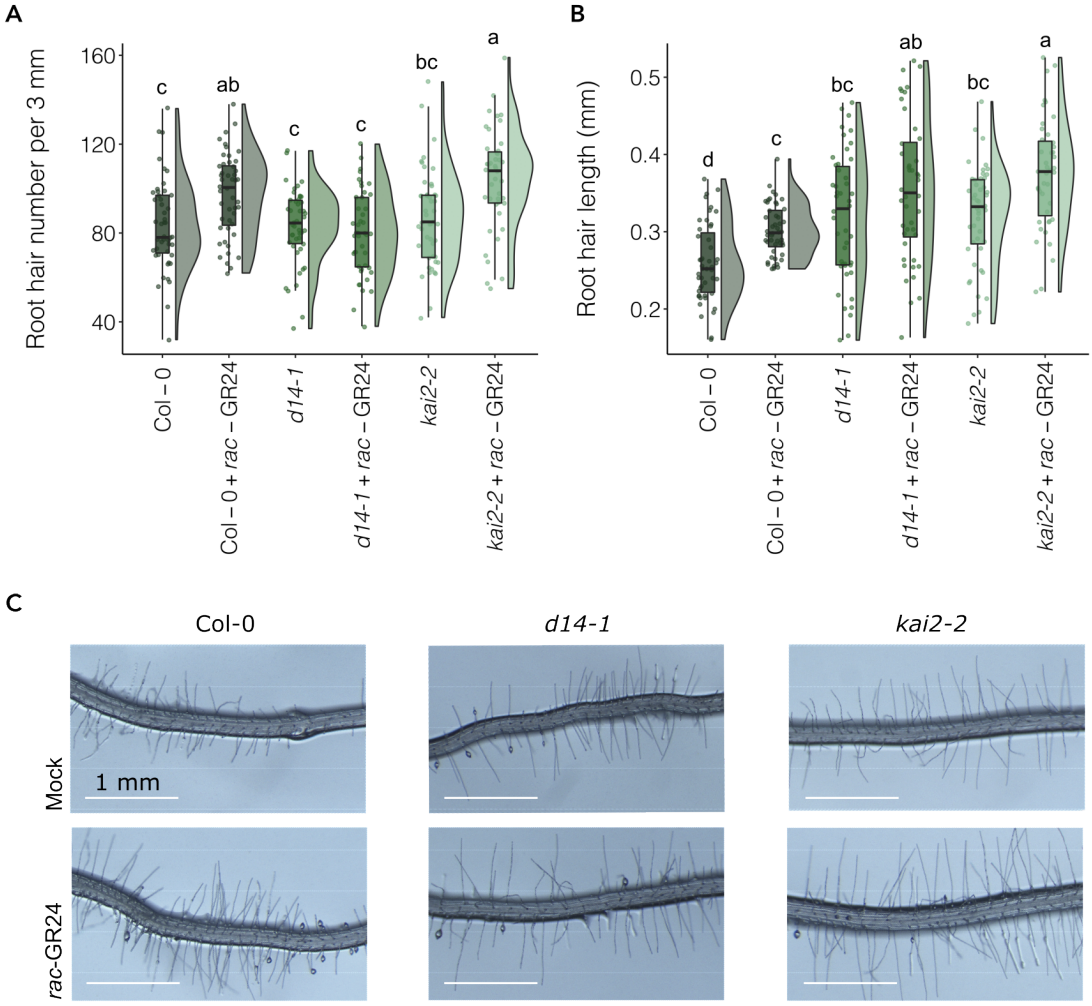

Figure 3.8 Rac-GR24 treatment increases root hair number and length, but not in *d14-1*. (A) Average root hair number (per 3 mm) of 12-day-old Col-0, *d14-1* and *kai2-2* roots after growth on 1 µM rac-GR24 in 12 hr light/12 hr dark photoperiod and (B) average root hair length (mm) of the same plants. (C) Representative images, bars represent 1 mm. Different letters indicate statistically significant difference determined by (ANOVA, post hoc Tukey: $p < 0.05$); (A) $F_{5,270} = 10.203$, (B) $F_{5,270} = 16.211$; n = 12–20 seedlings per biological repeat, three biological repeats). Adapted from Richmond et al. (2022).

Conversely, the KL pathway has been suggested as the main driver of the root hair response to *rac*-GR24, as opposed to SL signalling (Villaécija-Aguilar et al., 2019). In low phosphate conditions - which normally elicits an elongated root hair phenotype - both *KAI2* and *MAX2* transcripts were shown to accumulate in roots (Villaécija-Aguilar et al., 2022). Similarly, in *kai2*

mutants, the authors found an attenuated root hair phenotype, alongside lower accumulation of key root hair regulators, auxin importer AUXIN TRANSPORTER PROTEIN1 (AUX1) and the auxin exporter PIN-FORMED2 (PIN2). Auxin is well-characterised as a positive regulator of root hair development and elongation. This contradicts with the finding presented here that root hairs were significantly longer in both *d14-1* and *kai2-2* compared to wildtype, though plants were not phosphate-deprived. SL signalling has also been associated with regulation of shoot gravitropism via control of auxin in *O. sativa* (Sang et al., 2014). In addition, SMXLs 6, 7 and 8 stimulate shoot branching by supporting polar auxin transport (Soundappan et al., 2015), and there is evidence of SL control on PIN-dependent auxin transport in *A. thaliana* and *P. sativum*, together acting in a mechanism to finetune plant development according to environmental conditions (J. Zhang et al., 2020a). It is possible that the long root hair phenotype seen in both *d14-1* and *kai2-2* is representative of auxin dysregulation through both signalling pathways. This could be tested through single-cell RNA-sequencing analyses on root hair cells from these mutants to ask if auxin-related genes are overrepresented. Low phosphate conditions, which promote root hair growth, also increase expression of SL genes MAX3, MAX4, and D27 in Arabidopsis (Abuauf et al., 2018; Sun et al., 2014). Though the precise role is not yet known, the upregulation of SL genes strongly suggests that they play a part in the phosphate-scavenging root hair response. Single-cell RNA-sequencing analyses could also be employed here, to ask if there is transcriptomic differences between root hair cells of SL signalling mutants and wildtype, when grown on phosphate deplete or replete media.

Intriguingly, transcript levels of TARGET OF MONOPTEROS 5 (TMO5) and TMO5 LIKE1 (TMO5L1) were found to be significantly reduced in Arabidopsis roots when treated with *rac*-GR24 (Struk et al., 2022), which notably increases root hair length (Kapulnik et al., 2011b, 2011a). TMO5 forms a heterodimer with LONESOME HIGHWAY (LHW) and together regulate root hair development in response to low phosphate. Use of single-cell gene expression analyses found an enrichment of TMO5/LHW downstream targets in root hair cells (Wendrich et al., 2020). The authors also found that

misexpression of TMO5 and LHW equally led to increased root hair density cells (Wendrich et al., 2020). According to the findings of Struk et al. (2022), expression of *TMO5L1* is increased in *d14*, *d14;kai2* and *max2*, but not *kai2*, suggesting that it is controlled via the D14/MAX2 signalling cascade, as opposed to KAI2/MAX2 (Struk et al., 2022).

3.2.6 Using RNAseq to identify transcriptomic changes in *max* mutants

To explore the transcriptomic processes underlying the root system architectural differences in *max* mutants, RNA sequencing was performed on root tissue samples from 12-day-old Col-0, *max2-1*, and *max4-1* grown on plates without *rac*-GR24 treatment. These particular mutants were selected due to the short primary root phenotype in *max4-1* with longer and denser root hairs, and the short root hairs and SL insensitivity of *max2-1*. Libraries were prepared and Illumina sequencing performed (Section 2.2.6), then reads were trimmed and mapped to the *A. thaliana* genome annotation TAIR10.

Principal component analysis was next performed to assess whether there were differences between the genotypes. All three genotypes cluster together well, and the first two principal components on the plot account for just under 70% of the total dataset variation (Figure 3.9A). Both *max2-1* and *max4-1* samples are prominently separated from Col-0 according to the first two principal components.

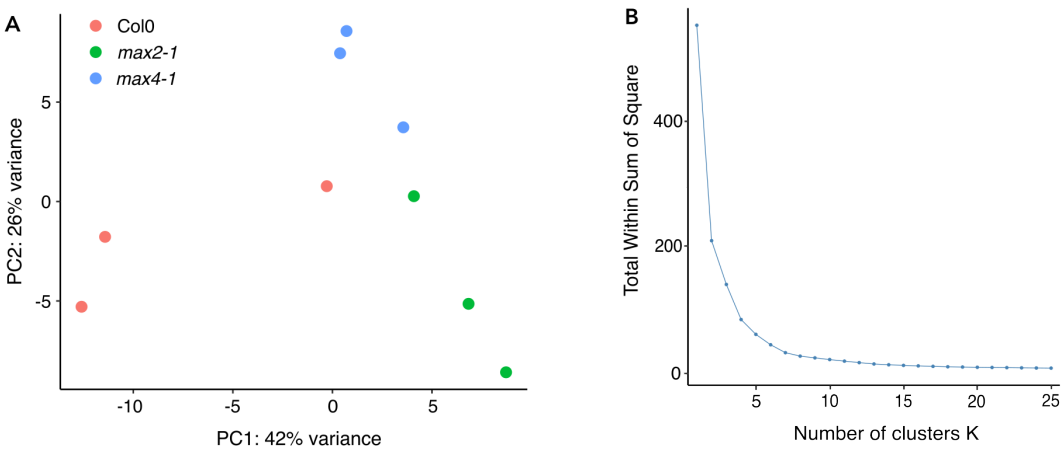

Figure 3.9 Analysis of samples used in RNAseq experiments. A) Principal component analysis (PCA) plot of normalised aligned counted data from 12-day-old root tissue samples from Col-0 (red), *max2-1* (green) and *max4-1* (blue). B) Elbow method of K-means clustering for samples.

There was a total of 292 significantly differently expressed genes (DEGs) (according to a threshold of $-1 < FC > 1$ and $p < 0.05$) between Col-0 and either *max2-1* and *max4-1* roots (Figure 3.9A). The DEGs were grouped into seven clusters as determined by K-means clustering (Figure 3.9B), then overrepresented GO term functions and processes were investigated in each cluster (Figure 3.10) (FDR-adjusted $p < 0.05$).

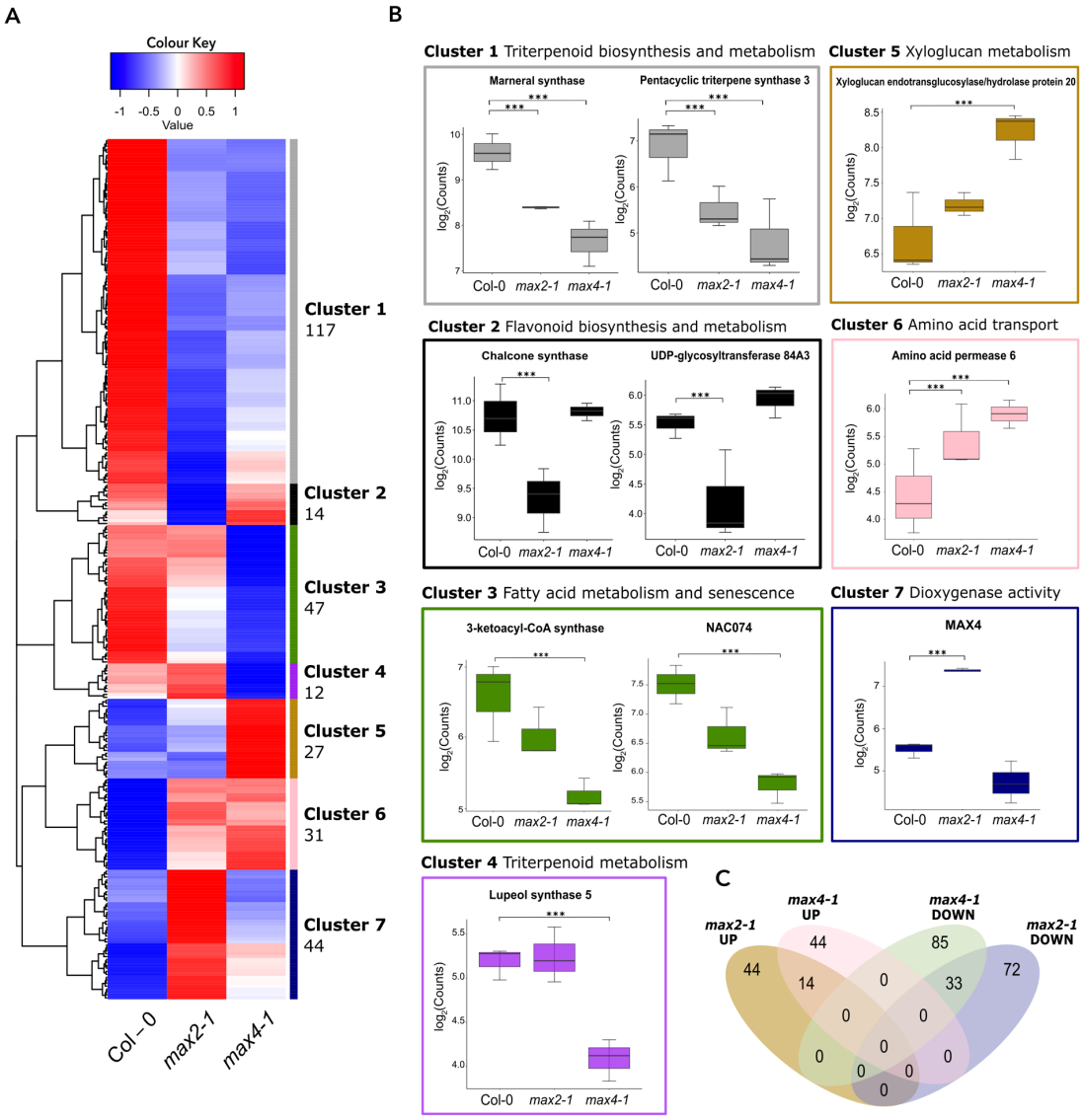

Figure 3.10 Root transcriptome analysis of 12-day-old *max2-1* and *max4-1* seedlings implicates metabolic differences in mediating the *max* phenotypes.

(A) Heatmap of differentially expressed genes between Col-0 and either *max2-1* or *max4-1* grouped into clusters of similar increased/decreased expression patterns. Genes were considered differentially expressed (DE) if they had a $\log_2$ fold change >1 and/or <−1 and had a Bonferroni-corrected $p < 0.05$. (B) Plots of expression values ($\log_2$(counts)) for selected DE genes per cluster. Asterisks indicate statistically significant difference compared to Col-0 as indicated by brackets (***$p < 0.001$; n = 20 pooled root samples per biological repeat, three biological repeats). (C) Venn diagram of 292 DE genes in *max2-1* and *max4-1* root tissue, showing their shared DE genes and number of upregulated and downregulated DE genes per genotype. Adapted from Richmond et al. (2022).

3.2.6.1 Triterpenoid biosynthetic genes are downregulated in both SL mutants

Shared changes between *max2-1* and *max4-1* compared to Col-0 were first assessed, due to the fact that both *MAX2* and *MAX4* regulate with SL signalling, albeit at different steps. Cluster 1, which has lower expression in both *max2-1* and *max4-1*, is the largest of the seven clusters with 117 DEGs. GO term analysis revealed an overrepresentation for genes involved in the biological process (BP) 'triterpenoid biosynthetic process' and 'triterpenoid metabolic process'. Some demonstrative DEGs found in cluster 1 include *MARNERAL SYNTHASE* (*MRN1*) and putative *PENTACYCLIC TRITERPENE SYNTHASE 3* (*PEN3*). As SLs are terpenes themselves, it is consistent that SL biosynthesis and signalling may also regulate synthesis of other terpenoid metabolites.

Cluster 6 comprises 31 genes with higher expression in both *max* mutants, with overrepresented GO terms involved in amino acid transport, including USUALLY MULTIPLE ACIDS MOVE IN AND OUT TRANSPORTERS (UMAMIT28) and AMINO ACID PERMEASE 6 (AAP6). Intriguingly, it has previously been shown that an increased expression of UMAMIT transporters induces particular stress phenotypes in *A. thaliana*, such as impeded growth and an increase in stress marker expression (Besnard et al., 2021). Potentially, this change in amino acid transport is a stress response to the altered SL synthesis and signalling in *max* mutants.

3.2.6.2 Upregulation of xyloglucan metabolism and downregulation of fatty acid metabolism in SL biosynthetic mutant

Despite the overlapping SL-related transcriptomic changes in *max2-1* and *max4-1* as seen in clusters 1 and 6, there were also significant differences observed between them, likely related to their different locations in the SL pathway. Cluster 3 is comprised of 47 genes that have significantly lower expression in *max4-1* whilst no change in expression in *max2-1*. It is overrepresented for GO terms involving 'fatty acid metabolism' – including 'very long-chain fatty acid (VLCFA) metabolism' – wax metabolism, and plant

organ senescence. An exemplar VLCFA-related gene from this cluster is *3-KETOACYL-COA-SYNTHASE 3 (KCS3)*, which catalyses the biosynthesis of VLCFA wax precursors, the closely related *KCS6* was also found in cluster 1. Cluster 3 also included DEGs allied with senescence and the cell cycle, such as *NAC074*, *BIFUNCTIONAL NUCLEASE 1* (*BFN1*) and *YELLOW-LEAF-SPECIFIC GENE 9* (*YLS9*). Given that these genes clustered with – and have a similar expression pattern to – the VLCFA-related genes, the DEGs related to senescence may be linked to the decrease in VLCFA in *max4-1*. It is known that VLCFAs, alongside ethylene, are associated with senescence, as are SLs – for example, MAX4 is upregulated in senescent leaves (Iqbal et al., 2017; Ueda and Kusaba, 2015). In addition, *kcs* mutants with dysregulated VCLFA synthesis have significantly shorter primary root length, both in *A. thaliana* and barley (Lee et al., 2009; Weidenbach et al., 2015); VLCFAs have been shown to promote primary root growth through the activation of ethylene biosynthesis, which stimulates quiescent centre cell division (Ortega-Martínez et al., 2007; Qin et al., 2007). Combined, this could explain the short primary root phenotype seen in *max4-1* but not *max2-1*, given that transcripts involved in VCLFA production are seemingly downregulated in *max4-1* only. It is possible that this decrease in VLCFA metabolism is a stress response to low levels of MAX4 and/or the SL precursor carlactone.

There are 12 genes in cluster 4, which were lower in expression in *max4-1* and no change in *max2-1*. The GO term ‘triterpenoid metabolism’ is overrepresented, specifically including beta-amyrin synthase, lanosterol synthase and oxidosqualene cyclase activity. For example, the terpenoid cyclase gene *LUPEOL SYNTHASE 5* (*LUP5*) features in this cluster, being downregulated in *max4-1* only. This implies that selected SL-related terpene regulation relies on the expression of *MAX4*, but not the downstream *MAX2* which integrates the SL response. As suggested previously, it is plausible that the *MAX4* product carlactone is necessary for this specific terpenoid metabolic process.

In cluster 5, there are 27 genes that have increased expression in *max4-1* but not *max2-1*, overrepresented for BP GO terms related to

'xyloglucan metabolism', and molecular function (MF) GO terms related to polysaccharide and hemicellulose metabolism, and cell wall biosynthesis. Specific xyloglucan-related DEGs include *XYLOGLUCAN ENDOTRANSGLUCOSYLASE/ HYDROLASE PROTEIN 15* and *20* (*XTH15* and *XTH20*) as well as *GLUCURONOXYLAN* 4-*O-METHYLTRANSFERASE-LIKE PROTEIN* (*GXM3*). XTHs control cell wall loosening and expansion, by cleaving and linking cellulose and hemicellulose cross-linkages. Upregulated XTH transcript levels have been associated with stress responses; for example, cellular turgor pressure is increased by drought and salinity stress, and XTH-controlled cell wall remodelling enables cell plasticity to prevent rupture (as reviewed in Tenhaken, 2015). Upregulation of xyloglucan-related DEGs in *max4-1* may therefore be a stress marker, a sign that SLs have a role in alleviating stress. In Arabidopsis, plant cell wall hallmarks such as xyloglucans are recruitment factors for ~40% of root-inhabiting microbes (Bulgarelli et al., 2012) and therefore impact rhizosphere assembly. A split-root experiment demonstrated that expression of multiple *XTH* transcripts were downregulated in roots of plants grown in a high-density microbiome (Korenblum et al., 2020). Upregulation of xyloglucans may function to recruit beneficial microbiota to alleviate abiotic stress. Given the role of xyloglucans for cell expansion, and thus in root hair tip growth and elongation – disrupting xyloglucan metabolism typically results in a severe stunted root hair phenotype (Cavalier et al., 2008) – it could also be that the upregulation of xyloglucan metabolism plays a role in the long and dense root hair phenotype of *max4-1*. As *max2-1* does not have a significantly different root hair length compared to wildtype, nor does it exhibit upregulated xyloglucan metabolism, this process may be MAX2-independent, and reliant on SL or carlactone biosynthesis.

Cluster 7 has 44 DEGs which have increased expression in *max2-1* only, with an enrichment in the GO term 'dioxygenase activity', including 2-oxoglutarate (2OG) and Fe(II)-dependent oxygenase superfamily protein and *GIBBERELLIN 20 OXIDASE 2* (*GA20OX2*). This *max2-1* cluster also includes higher expression of *MAX4,* corroborating the prior finding that there is upregulation of SL biosynthesis in *max2-1*, but not *max4-1* (Kohlen et al., 2011). MAX2 plays a central role in the SL regulatory feedback loop, being

able to target SL receptor D14 for degradation to restrict downstream SL signalling. It is possible that an alternate feedback pathway exists to maintain SL levels, whereby accumulation of D14 without bound SL results in upregulation of SL biosynthetic genes. Though only hypothetical, this may explain the upregulation of *MAX4* in *max2-1* roots. This could be tested through RNA-sequencing analysis of a D14-overexpressing line compared to wildtype, to ask if D14 accumulation upregulates SL biosynthesis.

3.2.6.3 Flavonoid metabolism genes are differentially expressed in SL signalling mutant

Cluster 2 comprises 14 genes with decreased expression in *max2-1*, with an enrichment for GO terms 'flavonoid biosynthesis', 'flavonoid metabolism' and 'anthocyanin-containing compound biosynthesis'. As none of the 14 genes are downregulated in *max4-1* root tissue, this is seemingly a process regulated by MAX2 rather than MAX4. Notably, *CHALCONE SYNTHASE* (*CHS*) – a key flavonoid biosynthesis enzyme – was significantly downregulated in *max2-1* (p = 0.006). CHS converts its substrate into naringenin chalcone, which is the precursor to flavonoids and anthocyanins. As mutant *chs* plants do not synthesise nor accumulate flavonoids, the function of CHS as being crucial to flavonoid biosynthesis is evident (Buer and Muday, 2004). Likewise, *UDP-GLYCOSYLTRANSFERASE 84A3* (*UGT84A3*) was also significantly downregulated in *max2-1* only (p = 0.04). UGT84A3 is a UDP-glycosyltransferase in the phenylpropanoid pathway which glucosylates 4-coumarate. As unglucosylated 4-coumarate is needed for flavonoid biosynthesis, it could be that this is a response to low levels of flavonoid accumulation in *max2-1*, downregulating this otherwise flavonoid-limiting step.

It was previously demonstrated that MAX2 can degrade the major transcription factor BRI1-EMS-SUPPRESSOR 1 (BES1) (Wang et al., 2013), and that BES1 prevents transcription of both *CHS* and *CHALCONE ISOMERASE* (*CHI*), by inhibiting transcription of MYB11, MYB12 and MYB111. These transcription factors promote transcription of *CHS*, *CHI*, as well as other flavonoid biosynthetic genes *FLAVANONE 3-HYDROXYLASE* (*F3H*) and *FLAVONOL SYNTHASE1* (*FLS1*) (Liang et al., 2020). As analysis

of the RNAseq experiment showed a significant downregulation in flavonoid biosynthesis in *max2-1*, in the context of the fact that MAX2 is able to degrade BES1, and BES1 inhibits transcription of flavonoid biosynthesis genes, it was hypothesised that a lack of BES1 degradation by MAX2 in the *max2-1* mutant may explain this finding. This could be tested through a Western blot, quantitating the amount of BES1 protein in *max2-1* cell lysate versus Col-0.

3.2.7 Conclusions

Root systems of SL and KL mutants were phenotyped under both mock conditions and with *rac*-GR24 addition, to assess the roles of SL and KL on shaping root system architecture. Transcriptomic analyses of *max2-1* and *max4-1* roots were then performed to identify gene expression changes which may underlie these developmental differences.

Analysis of root system architecture showed that mutation in *MAX4* leads to a stunted primary root, a phenotype not rescuable by *rac*-GR24 treatment (Figure 3.3), though dependent to some extent on photoperiod (Figure 3.5). There was a decrease in lateral root length, number, and density when treated with *rac*-GR24, but not in *max2* nor *kai2* – suggesting that this response is primarily MAX2/KAI2-driven (Figure 3.4). In contrast, *max2* and *d14* are seemingly insensitive to *rac*-GR24 in terms of their root hair development response, suggesting signalling through the MAX2/D14 system (Figure 3.7).

Through analysis of RNAseq data the mechanisms behind the root phenotypes of *max2-1* and *max4-1* were investigated. Unsurprisingly, there were many shared metabolic differences between *max2-1* and *max4-1*, and Col-0 – such as triterpenoid biosynthesis and amino acid transport – but there were also many interesting variations – such as the upregulation of xyloglucans and downregulation of fatty acids in *max4-1*, but not *max2-1* (Figure 3.10). The downregulation of flavonoid biosynthesis in *max2-1* is also an intriguing finding, and one which is investigated in further chapters.

Chapter 4 The strigolactone signalling pathway influences flavonoid biosynthesis in *Arabidopsis thaliana*

4.1 Introduction

Flavonoids, alongside strigolactones, are key plant metabolites; both regulate aspects of plant development, as well as shape rhizomicrobiome composition. Given that they are both exuded during establishment of symbiotic interactions, it is plausible that expression of flavonoid and strigolactone biosynthesis genes are linked. A complication in this area of research is that the KL signalling pathway has also been linked with promoting flavonoid biosynthesis, as corroborated by a decrease in drought-induced anthocyanin accumulation in *A. thaliana kai2* mutants compared to wildtype (Li et al., 2020b). This has previously been highlighted in a metabolite-profiling study, in which *rac*-GR24 was found to increase the quantity of flavonoid biosynthetic enzymes, which was reduced in *max2-1* (Walton et al., 2016). Given the ability of *rac*-GR24 to stimulate both KAR and SL signalling, the authors also tested flavonoid accumulation after treatment with the purified enantiomers, $GR24^{5DS}$ and $GR24^{ent\text{-}5DS}$, finding that that both stereospecificities gave flavonoid accumulation. A follow-up transcriptomic study found that *CHS* and *FLS* transcript levels were downregulated in both *d14*, *kai2*, and *d14;kai2*, further confirming roles for both SL and KAR pathways in flavonoid biosynthesis (Struk et al., 2022).

The SL signal is transmitted by the degradation of SMXL 6, 7 and 8 which otherwise negatively regulate SL signalling pathways (Figure 3.1). The full extent of downstream SMXL repression has not yet been fully elucidated, however, recent studies have implied a role SL signalling in drought-resistance. Triple mutant *smxl6/7/8* plants have been shown to be more resistant to drought than wildtype, displaying an increase in anthocyanin content during drought (Li et al., 2020c). Whilst it could be that the overall flavonoid biosynthesis pathway is also negatively regulated via SMXL

signalling, *smxl6,7,8* plants exhibit enhanced expression of pivotal anthocyanin-specific biosynthesis genes – such as *DIHYDROFLAVONOL 4-REDUCTASE* (*DFR*) and *ANTHOCYANIDIN SYNTHASE* (*ANS*) – rather than the flavonoid biosynthetic transcripts identified as downregulated in the *max2* RNAseq dataset (Wang et al., 2020). Alternatively, BES1 degradation via SCF^{MAX2} has been implicated in the control of flavonoid biosynthesis. BES1 has been demonstrated to directly bind to, and inhibit, the promotors of three transcription factors – MYB11, MYB12 and MYB111 – which activate flavonol biosynthesis (Liang et al., 2020). When bound to SL, SCF^{MAX2} has been shown to be able to degrade BES1 (Wang et al., 2013), and so control of BES1 via MAX2 is possible. Although both KLs and SLs signal through MAX2, Wang et al. (2013) proposed that BES1 degradation is SL/D14-mediated; the authors found that BES1 degradation in protein extracts from *d14-1* was enhanced by addition of AtD14-His-tagged protein.

4.1.1 Aims and Objectives

The evidence for strigolactone and flavonoid interplay is clear, but the mechanism behind this has yet to be fully elucidated. The aim of this work was to assess flavonoid biosynthesis in strigolactone-deficient *A. thaliana* mutant lines (Section 1.4.1). Based on the evidence described above, the possibility of a BES1-MAX2 link was explored by analysing the *max2* RNAseq dataset to test for an enrichment of downstream BES1 targets. This would also further implicate BES1 in the regulation of flavonoid biosynthesis. The RNAseq analysis presented in Chapter 3 identified a downregulation in flavonoid biosynthesis in *max2-1* but not *max4-1* root tissue, thus the next objective was to determine whether the *max2* flavonoid deficiency is driven by D14 or KAI2 signalling. To do so, *CHS* and *CHI* transcript levels were assessed in tissue from Col-0, *max3-9, max4-1*, *max1-1*, *max2-1*, *d14-1*, and *kai2-2* mutants using RT-qPCR. Next, flavonoid accumulation in Col-0, *max2-1*, *max4-1*, *d14-1*, and *kai2-2* root tips was evaluated via confocal microscopy, to ask whether transcriptomic changes to flavonoid biosynthesis are visible on a metabolic level.

4.2 Results and discussion

4.2.1 BES1 targets are over-enriched in *max2-1* differentially expressed genes

It has been previously demonstrated that MAX2 is able to degrade BES1 (Wang et al., 2013), and that BES1 represses transcription of key flavonoid biosynthesis genes (Liang et al., 2020). Given the finding that there is downregulation of flavonoid-related transcripts in the *max2-1* mutant, the next step was to investigate whether BES1 target genes were enriched amongst the 163 DEGs between Col-0 and *max2-1*.

By combining transcription factor binding motifs and regulatory elements data, 378 direct regulatory interactions between BES1 and other genes have been identified for *A. thaliana* root tissue (Jin et al., 2017; Tian et al., 2020). Of these, eight were identified as DEGs in the *max2-1* dataset of 163 DEGs, which is a 3.7-fold enrichment (hypergeometric test, $p = 0.001$). Of these, three were upregulated – AT1G56600 (GALACTINOL SYNTHASE 2), AT1G58340 and AT3G49620 – and five were downregulated – AT1G06923, AT1G25240, AT1G54970, AT2G01422, AT3G55120 (CHI). If BES1 overaccumulates in *max2-1*, it would be expected that BES1 interactors would be affected according to the direction of BES1 regulation. Previously, researchers identified putative BES1 target transcription factors using gene expression studies and ChIP-chip (Yu et al., 2011). Through using 14-day-old gain-of-function *bes1*-D seedlings which over-accumulate BES1, Yu et al. (2011) explored upregulated and downregulated genes compared to wildtype. From this dataset, 33 of the upregulated and 38 downregulated genes were found to be within the 378 direct BES1 targets in roots (Figure 4.1). In addition, three of the 5 downregulated direct BES1 interactors identified in *max2-1* seedlings (AT1G25240, AT1G54970 and AT2G01422) were also found to be downregulated in *bes1*-D seedlings (Yu et al., 2011). The same comparisons were carried out for the *max4-1* DEG dataset, and there was no significant enrichment of root BES1 target genes found. This further suggests that the BES1-flavonoid link is MAX2-dependent and specific.

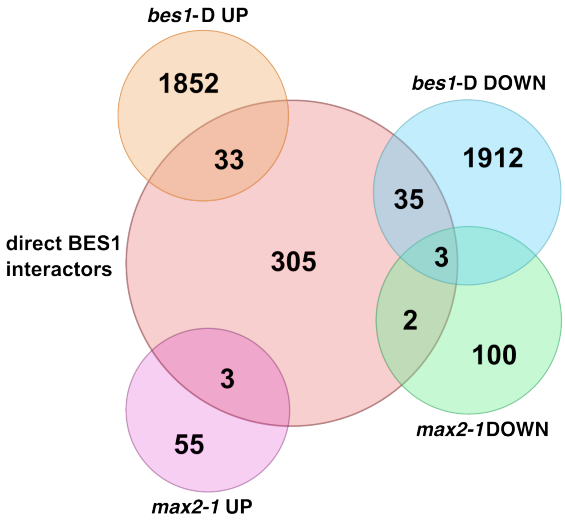

Figure 4.1 Euler diagram of direct BES1 interactors. Direct BES1 targets (red) were identified through online databases (Jin et al., 2017; Tian et al., 2020). The Euler diagram shows the overlap between genes that were identified in the *max2-1* RNA-sequencing upregulated (purple) and downregulated (green) datasets, and genes upregulated (orange) and downregulated (blue) in *bes1*-D seedlings (Yu et al., 2011).

4.2.2 Strigolactone and karrikin receptor mutants as well as signalling mutants have decreased transcription of the key flavonoid biosynthesis gene *CHS*

It is hypothesised that the downregulation of flavonoid biosynthesis genes in *max2-1* is due to overaccumulation of BES1 through lack of degradation by SCF^{MAX2}. In agreement with the hypothesis posed here, an analysis of microarray data from *bes1*-D seedlings found that the most significantly enriched downregulated genes by BES1 were flavonoid biosynthesis-related (Liang et al., 2020). Based on this, next, qPCR was used to assess whether the BES1-targeted flavonoid biosynthesis genes identified in the RNAseq, *CHS* and *CHI*, were also downregulated in whole seedlings.

Both *CHS* and *CHI* transcripts were found to be significantly downregulated in *max2-1* whole seedlings compared to in Col-0 (Student's *t*-test, $p = 0.035$ and 0.015, respectively), but not in *max4-1* compared to in Col-0 (Figure 4.2A). This indicates that the lack of functional *MAX2* affects flavonoid biosynthesis on a whole plant level, not just in root tissue. Given that flavonoids are induced during drought stress, this correlates with previous

findings that MAX2 is a positive regulator of drought stress responses in *A. thaliana* (Bu et al., 2014). The authors found that whilst *max2* was hypersensitive to drought and osmotic stress, the strigolactone biosynthesis mutants, *max3*, *max4* and *max1* were not, corresponding with the finding presented here that *CHS* and *CHI* levels are unchanged in *max4-1*.

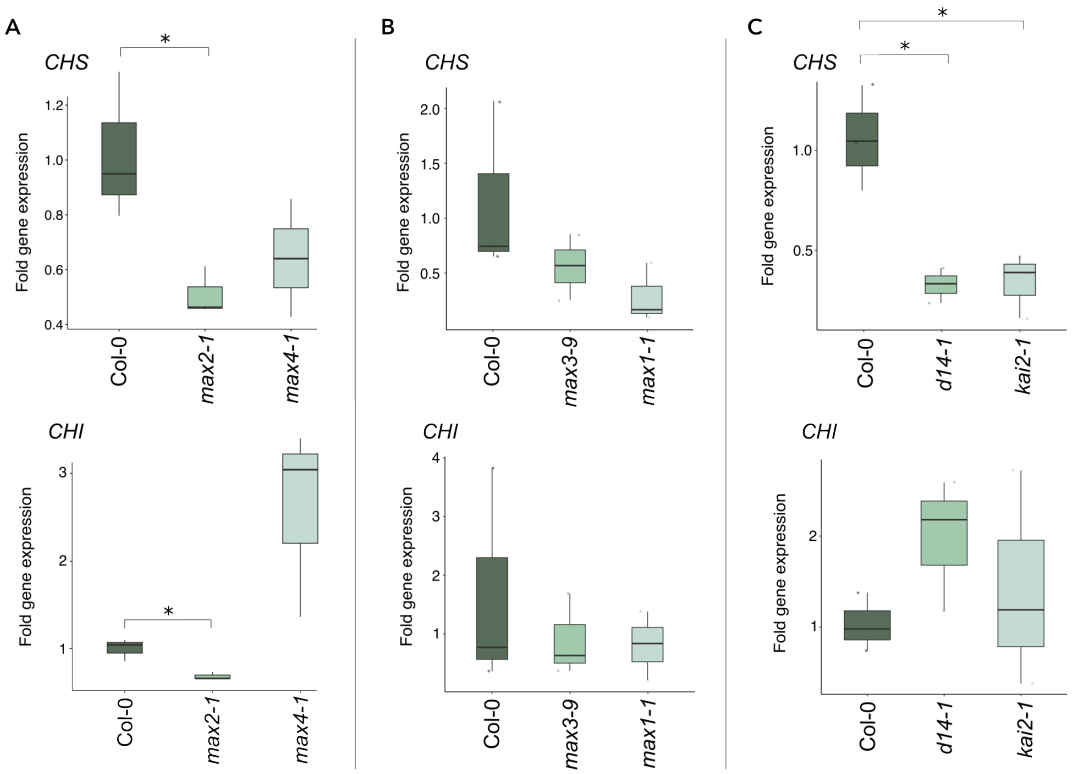

Figure 4.2 A key flavonoid biosynthesis gene, *CHS,* is downregulated in *max2-1*, *d14-1,* and *kai2-2*. RT-qPCR was performed using RNA extracted from 12-day-old seedlings with primers for *CHS* and *CHI* (references were *ACTIN2B* and *ACTIN7*, respectively) (*n* = 20 seedlings per genotype per biological repeat, three biological repeats). A) Col-0, *max2-1,* and *max4-1*; B) Col-0, *max3-9,* and *max1-1*; C) Col-0, *d14-1,* and *kai2-2*. Asterisks indicate statistically significant difference as indicated by brackets (Student's *t*-test, **p* <0.05). Adapted from Richmond et al. (2022).

The levels of *CHS* and *CHI* were also assessed in *max3-1* and *max1-1* to ask whether mutations in other steps in the strigolactone biosynthesis pathway might affect flavonoid gene transcription. Again, in agreement with Bu et al. (2014), neither of these mutant lines had statistically significantly lower levels of *CHS* or *CHI* transcripts in whole plant tissue compared to Col-

0 (Figure 4.2B). However, there does seem to be a slight decrease in these transcript levels, particularly in *max1-1* which would corroborate a previous finding that *MAX1* acts as a positive regulator of flavonoid biosynthesis (Lazar and Goodman, 2006).

Given that both D14 and KAI2 both interact with MAX2, *CHS* and *CHI* transcripts were also evaluated in the *d14-1* and *kai2-2* mutants, to assess whether the MAX2-dependent flavonoid downregulation is D14- or KAI2-driven. Both *d14-1* and *kai2-2* showed significantly lower levels of *CHS* compared to Col-0 (Student's *t*-test, $p = 0.010$ and 0.016, respectively) (Figure 4.2C). This coincides with a recent analysis of 5-day-old seedling root tissue which found significantly less *CHS* expression in both *d14*, *kai2* and *d14;kai2* compared to Col-0 (Struk et al., 2022). There was no statistically significant difference in *CHI* expression in either *d14-1* or *kai2-2* (Figure 4.2C).

Overall, it was found that *CHS,* a key flavonoid biosynthetic gene, is downregulated in both *d14-1* and *kai2-2*.

4.2.3 Strigolactone/karrikin signalling mutants and the strigolactone receptor mutant have decreased accumulation of flavonoids in root tips

In *A. thaliana*, flavonoids accumulate in the root tip, consistent with the shoot-to-root transport of flavonoids (Buer et al., 2013). Using confocal microscopy and diphenylboric acid-2-aminoethyl ester (DPBA) staining, accumulation of flavonoids can be viewed *in situ* and quantified. In order to determine whether the decreased transcription of flavonoid biosynthetic genes has an impact on overall flavonoid levels, accumulation was assessed in 10-day-old Col-0, *max2-1,* and *max4-1* seedling root tips. The *max2-1* mutant had significantly less flavonoid accumulation in the peak root tip zone compared to Col-0 (Student's t-test, $p = 0.019$) with a 0.68-fold decrease in flavonoid level (Figure 4.3A, C). *Max4-1* did not have a significant difference in flavonoid level compared to Col-0. This corroborates with the transcriptomic findings and indicates a role for flavonoid regulation which is MAX2-dependent, but not MAX4-dependent.

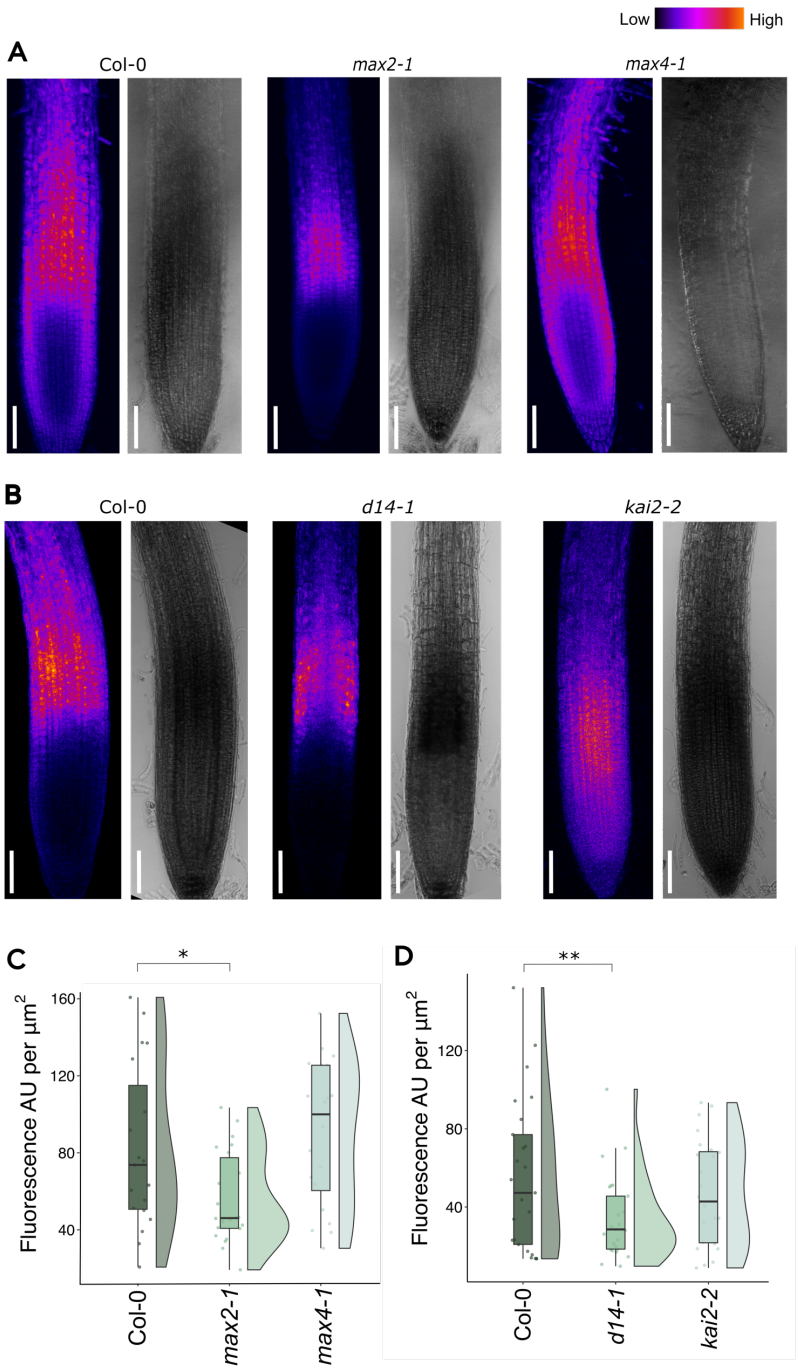

Figure 4.3 Root flavonoid accumulation is downregulated in *max2-1* and *d14-1*, but not in either *max4-1* or *kai2-2*. Ten-day-old seedling root tips were stained with 2.52 mg/mL diphenylboric acid-2-aminoethyl ester (DPBA), which results in flavonoid fluorescence when excited at 458 nm. Representative images of DPBA-stained root tips for A) Col-0, *max2-1,* and *max4-1*; and for B) Col-0, *d14-1,* and *kai2-2*; bars represent 100 µm. Integrated density measurements were taken from the beginning of the peak fluorescence in the elongation zone as fluorescence arbitrary units (AU) per µm^2, for C) Col-0, *max2-1* and *max4-1* and D) Col-0, *d14-1* and *kai2-2*. Asterisks indicate statistically significant difference as indicated by brackets (Student's *t*-test, *$p < 0.05$, **$p < 0.01$.) Adapted from Richmond et al. (2022).

DPBA staining was repeated with Col-0, *d14-1* and *kai2-2* root tips, to ask whether the regulation of flavonoids is affected by the D14-SCF^{MAX2} or KAI2- SCF^{MAX2}, route and help elucidate if it is strigolactone- or karrikin-mediated. Flavonoid accumulation in *d14-1* root tips was significantly reduced (Student's t-test, p = 0.022), with a 0.62-fold change in flavonoid level compared to in Col-0 (Figure 4.3B, D). This is similar to the fold change reduction in flavonoid levels seen in *max2-1* compared to Col-0, suggesting that D14 and MAX2 act together to regulate flavonoid biosynthesis, likely as the D14-SCF^{MAX2} complex. On the contrary, flavonoid accumulation in *kai2-2* root tips was not significantly different to Col-0. This indicates that regulation of flavonoid accumulation through this mechanism is more strongly influenced by the strigolactone pathway than the karrikin pathway.

4.2.4 Conclusion

This chapter aimed to determine whether the *max2* flavonoid deficiency identified in the RNAseq analysis was related or due to D14 and/or KAI2 signalling. Through gene expression analysis using RT-qPCRs, the depletion of *CHS* and *CHI* in whole plant tissue in *max2-1* compared to Col-0 was confirmed, and both *d14-1* and *kai2-1* whole plant tissue had lower *CHS* transcript levels compared to Col-0. This corroborates with previous literature which demonstrate roles of both SL and KL signalling in the overall flavonoid biosynthesis pathway. Root tip flavonoid accumulation was assessed, and *max2-1* and *d14-1* were found to have significantly lower root flavonoid accumulation compared to Col-0, whereas *kai2-1* did not. This suggests that there is a D14- and MAX2-specific mechanism which regulates flavonoid biosynthesis and accumulation, likely via the D14-SCF^{MAX2} complex.

Further work could test this hypothesis through RT-qPCR of *CHS* and *CHI* transcript levels in wildtype, *d14-1* and *kai2-2* root tips treated with the D14-specific stereoisomer GR24^{4DO}. An increase *CHS* and *CHI* transcript levels with GR24^{4DO} treatment in wildtype and *kai2-2*, but not *d14-1*, would further support a D14-mediated mechanism promotion of flavonoid biosynthesis.

Chapter 5 Phenotypic and transcriptomic response of *Arabidopsis thaliana* to strigolactone analogue GR24^{4DO}

5.1 Introduction

Understanding the impact of plant hormones typically involves treating tissue with analogues and then carrying out molecular or phenotypic analysis. *Rac*-GR24, a racemic mixture of GR24^{5DS} and GR24$^{ent\text{-}5DS}$ has been used in previous research as a SL analogue, despite these stereoisomers being able to stimulate KAI2-mediated signalling (Scaffidi et al., 2014) (Figure 5.1). Whilst many studies have been performed previously that examine the phenotypic and transcriptomic effects of *rac*-GR24 (Kapulnik et al., 2011a; Struk et al., 2022), this is not a suitable proxy for focussing on SL signalling, given that KL signalling is also induced. There is added complexity between SL and KL signalling as they both affect similar downstream pathways, regulating the same developmental processes. Signalling through KAI2-SCF^{MAX2} targets SMAX1 and SMXL2 for degradation, relieving repression on their downstream targets (Stanga et al., 2016, 2013) (Figure 5.1). SMAX1 and SMXL2 have both been shown to negatively regulate hypocotyl elongation (Stanga et al., 2013) and drought resistance (Feng et al., 2022). D14-SCF^{MAX2} signalling primarily targets SMXLs 6, 7 and 8 for degradation (Soundappan et al., 2015; L. Wang et al., 2015), though it can also trigger degradation of SMXL2 (L. Wang et al., 2020b) (Figure 5.1). Under the presence of GR24^{4DO}, it was found that SMXL2 co-immunoprecipitates D14 – demonstrating the formation of a complex – and that GR24^{4DO} treatment induces polyubiquitination and degradation of SMXL2 (Wang et al., 2020c). More recently, SMAX1 has also been identified as a D14-SCF^{MAX2} degradation target, though to a lesser extent than the SMXLs (Li et al., 2022b) (Figure 5.1). Like SMAX1 and SMXL2, SMXL6, 7 and 8 are key transcriptional repressors of drought resistance (Li et al., 2020c). Thus, there is much crosstalk between SL and KL signalling, and use of GR24^{4DO} as a SL analogue to investigate SL signalling eliminates at least some overlap.

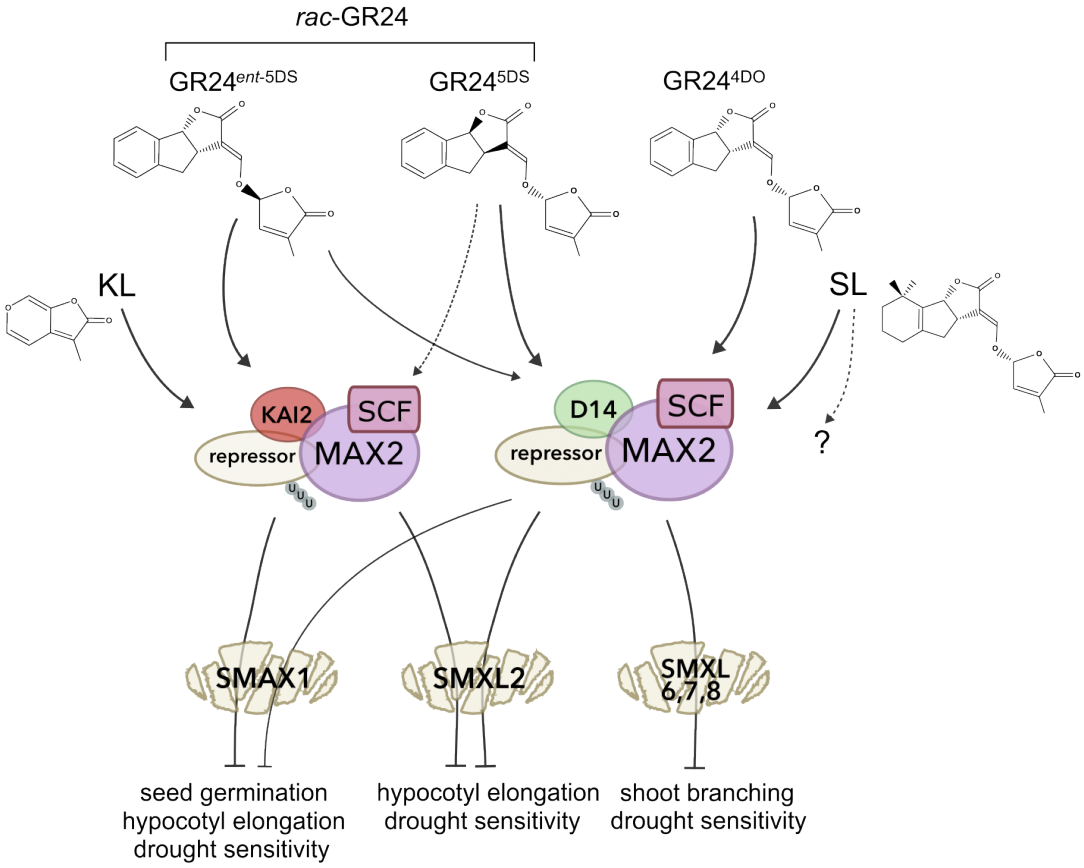

Figure 5.1 Crosstalk between SL and KL signalling pathways. *Rac*-GR24 is a racemic combination of GR24$^{ent\text{-}5DS}$ and GR24^{5DS}. GR24^{5DS} preferentially activates D14, whereas GR24$^{ent\text{-}5DS}$ preferentially activates the KL receptor KAI2, though there is evidence for signalling through D14 and KAI2 for both stereoisomers. Signalling through KAI2-SCF^{MAX2} targets SMAX1 and SMXL2 for degradation. Signalling through the SL receptor D14-SCF^{MAX2} targets SMXL6, 7 and 8 for degradation, as well as SMAX1, to a lesser extent. Selected downstream developmental processes are shown. There is some evidence for a non-canonical D14-SCF^{MAX2}-independent mechanism for SL signalling. Dotted line indicates potential interaction with some evidence. Adapted from Li et al., (2022c).

There has also been suggestion of SL/KL-mediated processes that act independently of the canonical D14/KAI2-SCF^{MAX2} complexes. In *L. japonicus*, it was reported that *rac*-GR24 induces transcriptional changes which are independent of D14, KAI2 and MAX2 (Carbonnel et al., 2021). Furthermore, *MAX2*-independent phenotypic changes in response to *rac*-GR24 have been observed in *A. thaliana*; mutant *max2* plants exhibit *rac*-GR24-induced inhibition of hypocotyl growth (Jia et al., 2014). It has previously been shown that *rac*-GR24 can regulate the nuclear localisation of CONSTITUTIVELY

PHOTOMORPHOGENIC1 (COP1) (Tsuchiya et al., 2010), thus affecting its downstream effects. COP1 is an E3 ubiquitin ligase and a key negative regulator of light signalling, ubiquitinating targets for degradation, such as ELONGATED HYPOCOTYL5 (HY5) and BZR1–1D SUPPRESSOR 1 (BZS1). As a transcription factor, HY5 integrates light and temperature cues to regulate a host of physiological and developmental processes, including photosynthetic capacity, pigment accumulation, nutrient uptake and photomorphogenesis (as reviewed in Xiao et al., 2022). BZS1 integrates brassinosteroid and light signals to regulate photomorphogenesis (Fan et al., 2012), and also positively regulates HY5 expression (Wei et al., 2016). Thus, through regulating COP1 nuclear localisation, *rac*-GR24 may regulate downstream light-mediated HY5 signalling pathways. To support this, it has been shown that 10 μM *rac*-GR24 under light conditions increased HY5 protein accumulation in wildtype Arabidopsis within 5 hr, but not in dark, suggesting a cumulative COP1 inhibition from *rac*-GR24 and light (Jia et al., 2014).

It is therefore of great interest to investigate *D14*-independent responses to $GR24^{4DO}$, to further explore the possibility of non-canonical SL signalling, independent of the D14-SCF^{MAX2} complex.

5.1.1 Aims and Objectives

The aim of this work was to test the effect of exogenous strigolactone on root development in *A. thaliana*, because of the substantial similarities between SL and KL signalling (Section 1.4.1). The GR24 stereoisomer $GR24^{4DO}$ has been shown to preferentially stimulate SL-mediated signalling rather than KL-mediated signalling (Scaffidi et al., 2014), and therefore is an ideal SL analogue for this study. Thus, the impact of $GR24^{4DO}$ on root system architecture was assessed, both on wildtype and on SL and/or KL signalling mutants.

Gene expression changes of the SL signalling mutant and wildtype plants to $GR24^{4DO}$ were analysed to determine the mechanisms underpinning the root system phenotypes that was found. Transcriptomic analysis of the SL

signalling mutant with GR24^{4DO} treatment was also performed to explore the potential existence of a D14-SCF^{MAX2} -independent SL signalling mechanism.

5.2 Results and Discussion

5.2.1 Strigolactone GR24^{4DO} addition increases primary root and lateral root length in Col-0 and SL signalling mutant *d14-1*

In order to determine the effect of SL on root system architecture, root phenotyping was performed on 12-day-old plants grown on media containing 1 µM GR24^{4DO}, compared to mock/control media without GR24^{4DO}. To ask whether GR24^{4DO} growth effect is D14-mediated, the signalling mutant *d14-1* was also compared to Col-0, with and without GR24^{4DO} in the same experiment.

The primary roots of Col-0 seedlings grown on GR24^{4DO} were found to be statistically significantly longer than those grown on mock treatment ($p < 0.0001$) (Figure 5.2A, E). This was interesting, as no effect on primary root length was previously found when Col-0 seedlings were grown on 1 µM *rac*-GR24 compared to mock media (Chapter 3). Primary root lengths were also significantly longer for GR24^{4DO}-treated *d14-1* seedlings compared to mock-treated *d14-1* ($p = 0.013$), indicating that this SL-specific response is not exclusively D14-mediated.

Untreated *d14-1* primary root lengths were found to be significantly longer than untreated Col-0 ($p < 0.0001$). This is an intriguing finding when compared to the short primary root phenotype found in *max4-1*, and it could be that SL levels are responsible for primary root elongation. *Max4* seedlings lack MAX4 to convert carlactone into SLs, whereas *d14* seedlings lack D14 for the SL negative feedback loop, to limit SL production. Indeed, SLs over accumulate in *Osd14* plants compared to wildtype (Arite et al., 2009). In that study, the link between primary root length and endogenous SL levels was assessed and it was found that plants treated with the strigolactone biosynthesis inhibitor TIS108 exhibited significantly decreased primary root lengths. Overall, both GR24^{4DO} application and endogenous SL accumulation

seem to enhance primary root growth. To better understand these links, the next step would be to examine the molecular pathways linking SL signalling and primary root length, for example, using transcriptomic analysis.

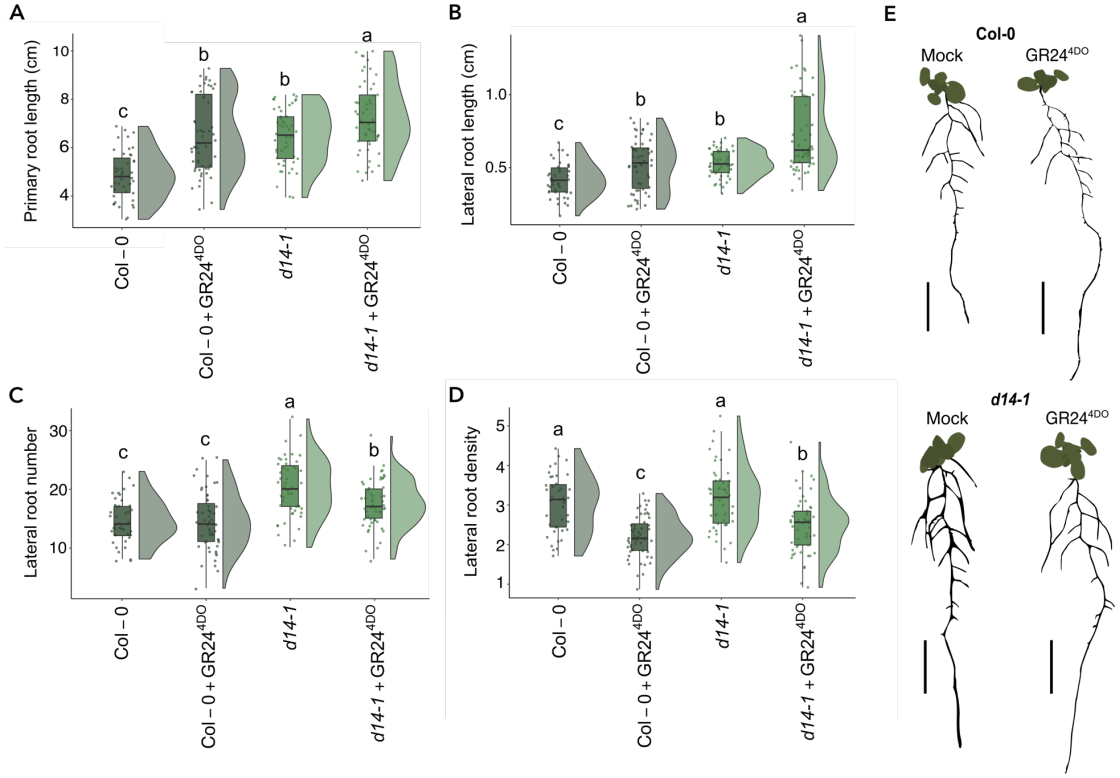

Figure 5.2 GR24^{4DO} increases primary root length and lateral root length and decreases lateral root density compared to mock treatment in 12-day-old Col-0 and *d14-1*. (A) Primary root length (cm) of 12-day-old Col-0 and *d14-1* seedlings after growth on 1 µM GR24^{4DO} media in 12 hr light/12 hr dark photoperiod, (B) lateral root average length (cm), (C) lateral root number and (D) lateral root density, all of the same seedlings. (E) Representative images converted to bitmap for each genotype-treatment combination, scale bars represent 1 cm. Different letters indicate statistically significant differences, determined by ANOVA (post hoc Tukey: $p < 0.05$); n = 10–20 seedlings per biological repeat, three biological repeats); A) $F_{3,197} = 26.27$, B) $F_{3,197} = 26.43$, C) $F_{3,197} = 18.61$, D) $F_{3,197} = 22.41$.

Both Col-0 and *d14-1* lateral roots were found to be significantly longer with GR24^{4DO} treatment compared to their respective mock controls ($p = 0.021$ and < 0.0001, respectively) (Figure 5.2B, E). This indicates a D14-independent mechanism for SL control of lateral root elongation. It is interesting to note that there is a larger increase in average lateral root lengths with GR24^{4DO} treatment compared to mock in *d14-1* (1.38-fold increase) than in Col-0 (1.25-

fold increase). This could be due to higher endogenous levels of SL in *d14-1*, in combination with the exogenous GR24^{4DO} treatment, leading to an enhanced effect, though metabolomic studies of SL levels would be needed to confirm this. The GR24^{4DO}-mediated longer lateral root phenotype is opposite to the decrease in lateral root length seen with 1 µM *rac*-GR24 treatment both in this work (Chapter 3) and in other studies (Kapulnik et al., 2011a; Ruyter-Spira et al., 2011). This suggests that the decrease in lateral root length with *rac*-GR24 treatment may in fact be driven by KL signalling, as it is not seen with GR24^{4DO} treatment. To further support this hypothesis, the *rac*-GR24-mediated shorter lateral root phenotype was not seen in *kai2-2* mutants (Section 3.3.2). It could be that KL signalling typically drives lateral root elongation, whereas SL signalling represses it. To support this, mock-treated Col-0 had significantly shorter lateral roots compared to mock-treated *d14-1* (p = 0.018) (Figure 5.2B, E), indicating that D14-mediated SL signalling plays a role in finetuning lateral root elongation to some extent.

Lateral root number was not found to be statistically significantly different in Col-0 treated with GR24^{4DO} compared to mock treatment. There was a significant decrease in lateral root number in *d14-1* plants treated with GR24^{4DO} compared to mock (p = 0.015) (Figure 5.2C, E), which could again be reflective of increased endogenous SL levels in *d14-1*. To test this, the same experiment could be repeated with increasing concentrations of GR24^{4DO} to ask if a higher concentration produces a similar decrease in lateral root number in Col-0. *Rac*-GR24 treatment also led to a significant decrease in lateral root number in Col-0 and in *d14-1*, but not *kai2-2* (Chapter 3). As with *rac*-GR24 treatment, lateral root density (lateral root number per cm of primary root) was also found to be significantly reduced in both Col-0 (p = 7.5E-08) and *d14-1* (p = 8E-06) plants treated with GR24^{4DO} compared to mock. This suggests that the mechanism controlling lateral root density is D14-independent.

As GR24^{4DO} is D14-specific, KL signalling interplay ought to be reduced compared to with *rac*-GR24 use, however these results indicate that there is

still crosstalk between SL and KL pathways, with both being involved in fine-tuning lateral root initiation.

5.2.2 GR24^{4DO} addition causes shorter and less dense root hairs, independently of D14

Given the long, dense root hair phenotype seen previously in the SL biosynthesis mutants (Chapter 3) - which is non-rescuable by *rac*-GR24 addition - it was theorised that SLs regulate root hair length and density. To test this, root hair number was counted for the seedlings treated with GR24^{4DO}.

Root hairs were analysed per 3 mm of the first fully-elongated root hairs from the root tip. The number of root hairs per 3 mm was found to be significantly less under the GR24^{4DO} treatment compared to mock, in Col-0 (p = 0.001) (Figure 5.3A, C). This supports the theory that SL/GR24^{4DO} inhibits root hair initiation. However, this contradicts the more numerous root hair phenotype induced by *rac*-GR24 that was found earlier (Chapter 3). In recent years, karrikins and KL have garnered more interest for their role in root developmental processes, with many studies suggesting a role in root hair elongation (Carbonnel et al., 2020; Villaécija-Aguilar et al., 2019). It could be that *rac*-GR24 acts through KL signalling more prominently than previously assumed, promoting KAI2-mediated root hair initiation. In this way, GR24^{4DO} treatment would instead highlight the D14-mediated inhibition of root hair initiation. Root hair number was also found to be less for GR24^{4DO} treated *d14-1* mutant seedlings (p = 0.0001), an intriguing finding given that the *d14-1* line is a loss-of-function mutant. This suggests the possibility of a MAX2/D14-independent mechanism for GR24^{4DO}/SL perception and signalling.

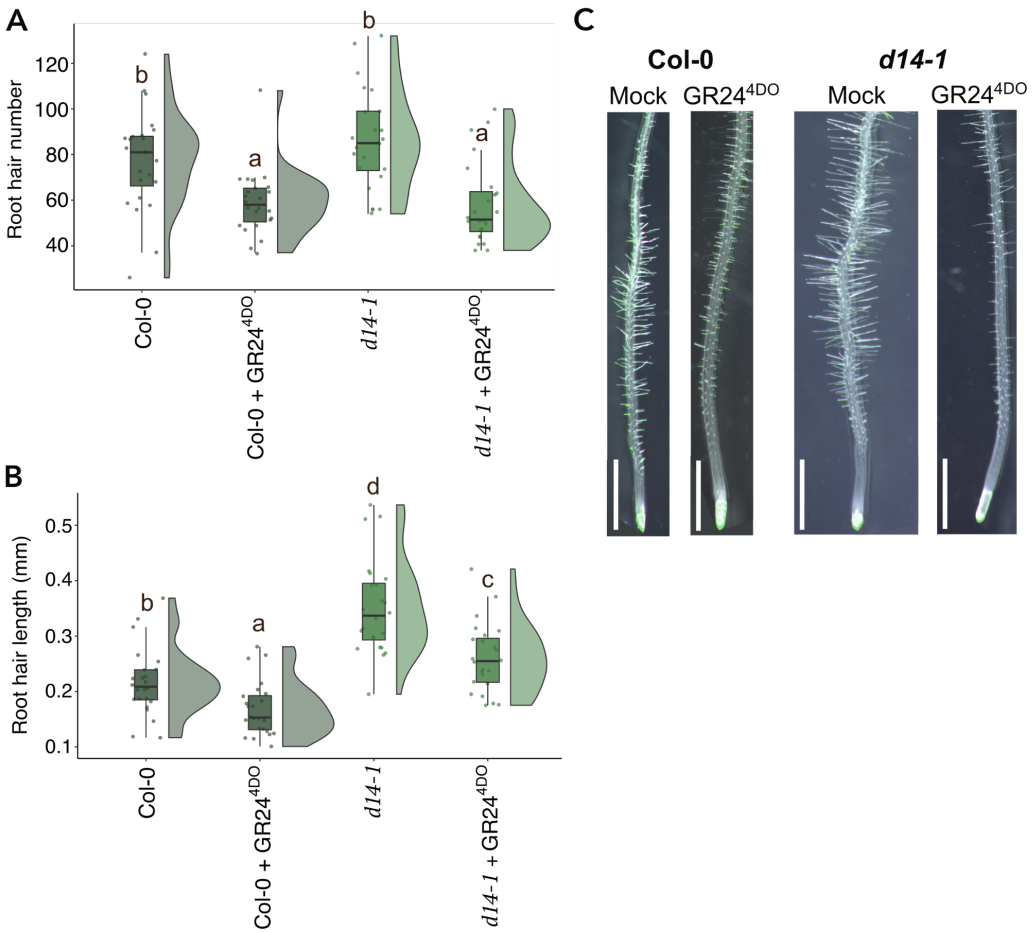

Figure 5.3 GR24^{4DO} decreases root hair length and number compared to mock treatment in 12-day-old Col-0 and *d14-1*. (A) Root hair number per 3 mm of 12-day-old Col-0 and *d14-1* seedlings after growth on 1 µM GR24^{4DO} media in 12 hr light/12 hr dark photoperiod, (B) root hair average length (cm) of the same plants, (C) Representative images for each genotype-treatment combination, bars represent 1 mm. Different letters indicate statistically significant differences, determined by pairwise Wilcoxon rank-sum test (FDR-adjusted $p < 0.05$; n = 10–20 seedlings per biological repeat, three biological repeats).

Root hair average length was found to be significantly shorter under GR24^{4DO} treatment than under mock conditions in both Col-0 (p = 0.004) and *d14-1* (p = 0.0001) seedlings. As this GR24^{4DO}-induced phenotype is shared between Col-0 and *d14-1*, it further supports a D14-independent mechanism of SL signalling, which regulates root hair development. However, as seen previously (Chapter 3), *d14-1* roots have significantly longer root hairs compared to Col-0, under both the mock treatment and the GR24^{4DO}

treatment. This indicates that D14-mediated SL signalling does regulate root hair elongation to some extent. Root hair development is highly sensitive to auxin flux, and SLs are known to be able to modulate the distribution of auxin transporters, in a D14/MAX2-dependent manner (J. Zhang et al., 2020b). It may be that SL-induced auxin dysregulation alters root hair development.

5.2.3 Using RNAseq to identify transcriptomic changes with GR24^{4DO} treatment

To identify the transcriptomic changes underlying the root system architectural differences with GR24^{4DO} treatment, reflective of downstream strigolactone signalling, RNA sequencing was performed on root tissue samples from 12-day-old Col-0 and *d14-1* grown on plates with or without GR24^{4DO}. *d14-1* was also studied, to distinguish D14-independent transcriptomic changes after GR24^{4DO} treatment. Libraries were prepared and Illumina sequencing performed (paired-end, unstranded, read-lengths of 150 bp), then reads were trimmed and mapped to the *A. thaliana* genome annotation TAIR10 (Section 2.2.6).

To evaluate differences between genotypes, principal component analysis was performed. Each of the four treatments cluster together well, and the first two principal components account for 83% of the total dataset variation (Figure 5.4A). According to the first two principal components, the *d14-1* samples are prominently separated from Col-0, and the GR24^{4DO}-treated Col-0 samples are separated from the mock (Figure 5.4A).

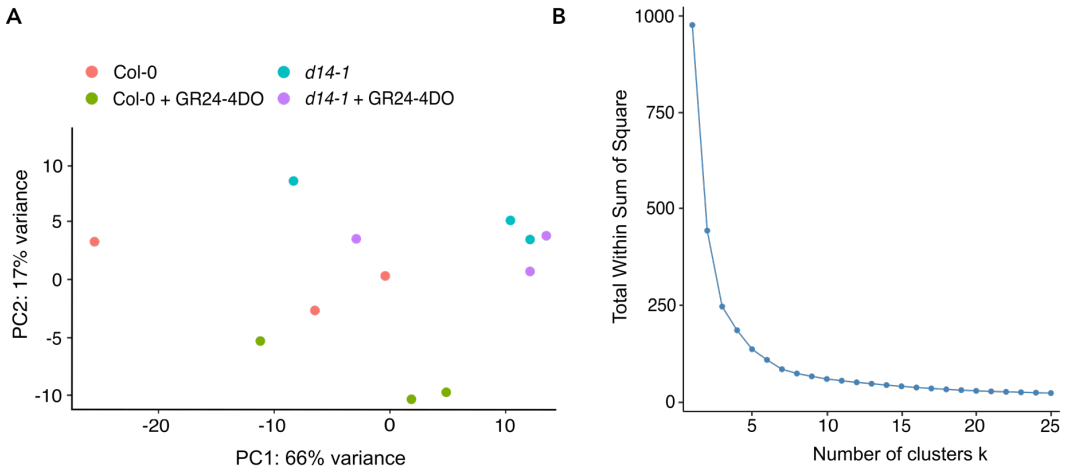

Figure 5.4 Analysis of samples used in RNAseq experiments. A) Principal component analysis (PCA) plot of normalised aligned count data from 12-day-old root tissue samples from Col-0 (red), Col-0 treated with $GR24^{4DO}$ (green), *d14-1* (blue) and *d14-1* treated with $GR24^{4DO}$ (purple). B) Elbow method of K-means clustering for samples.

A total of 338 significantly differently expressed genes (DEGs) (according to a threshold of $-1 < FC > 1$ and $p < 0.05$) were identified between Col-0 and *d14-1* root tissue, either with or without $GR24^{4DO}$ treatment. The DEGs were grouped into six clusters as determined by K-means clustering (Figure 5.4B), then overrepresented GO term functions and processes were investigated in each cluster (Figure 5.5A, B) (FDR-adjusted $p < 0.05$).

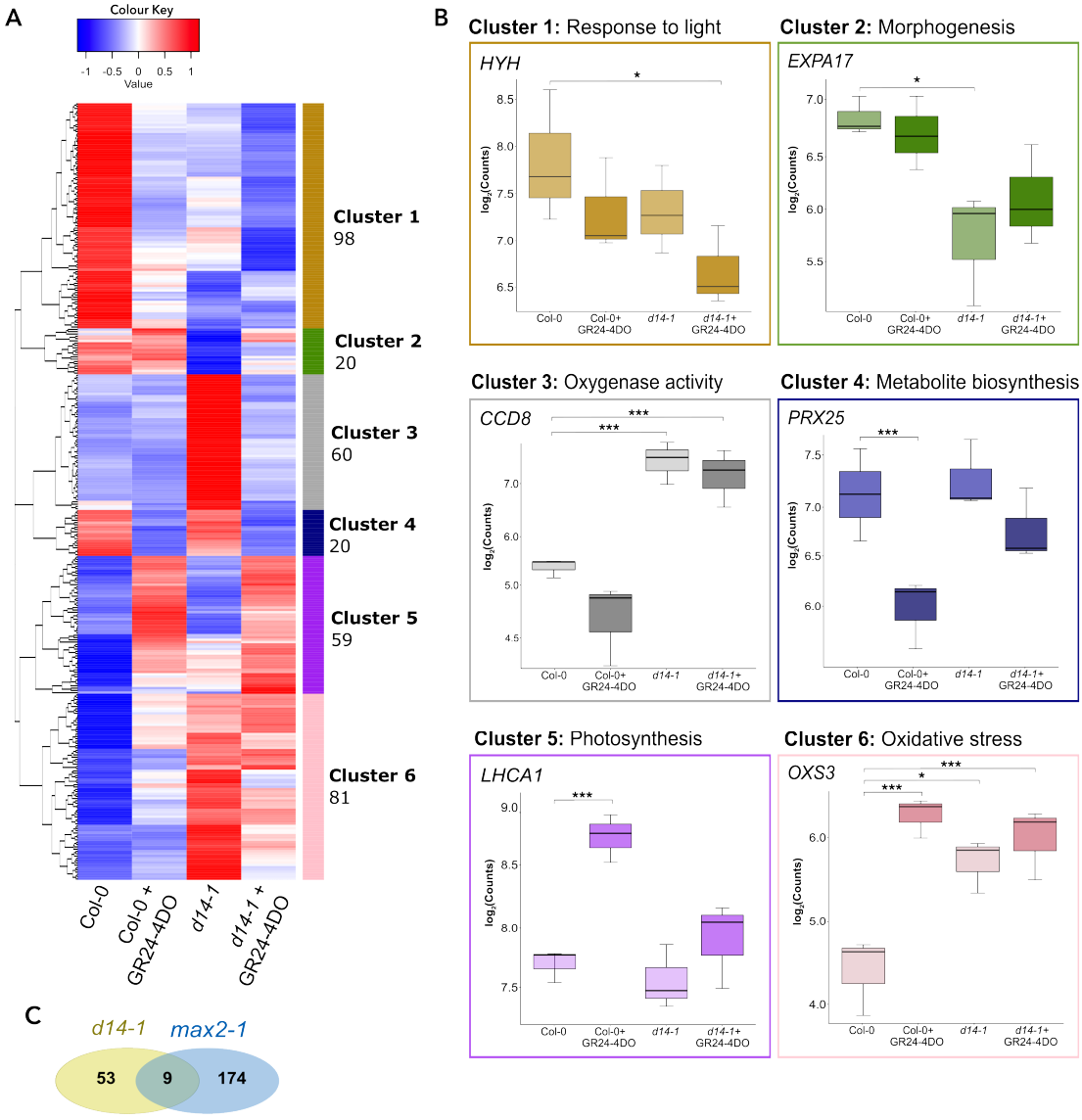

Figure 5.5 Root transcriptome analysis of 12-day-old Col-0 and *d14-1* seedlings, with and without GR24^{4DO} elucidates SL signalling pathways. Heatmap of differentially expressed genes between Col-0 and *d14-1* with or without GR24^{4DO} treatment, grouped into clusters of similar expression patterns. Genes were considered differentially expressed (DE) if they had a $\log_2$ fold change >1 and/or <−1 and had a Bonferroni-corrected $p < 0.05$. (B) Plots of expression values ($\log_2$(counts)) for selected DE genes per cluster. Asterisks indicate statistically significant difference compared to Col-0 as indicated by brackets (*$p < 0.05$, ***$p < 0.001$; n = ~40 pooled root samples per biological repeat, three biological repeats). (C) Venn diagram of DE genes in mock-treated *d14-1* and *max2-1* root tissue, showing their shared DE genes.

There were 9 shared DEGs identified between mock-treated *d14-1* and the *max2-1* dataset (Chapter 3). These include *MAX4*, *CELL WALL INVERTASE5* (*CWINV5*), *ABNORMAL SHOOT4* (*ABS4*), *MYB37*, *OXIDATION-RELATED ZINC FINGER 1* (*OZF1*) and *MTO1-RESPONDING DOWN 1* (*MRD1*). As described previously, the shared upregulation of *MAX4* transcripts in both *d14-1* and *max2-1* is representative of SL feedback regulation (Mashiguchi et al., 2009; L. Wang et al., 2015). *OZF1* promotes the transcription of *MRD1*, and upregulation of both genes has been associated with salicylic acid (SA)-mediated defence and systemic acquired resistance (Singh et al., 2022). This supports a recent study that proposes a role for SLs in SA-mediated systemic acquired resistance (SAR), priming plants for a wide range of biotic stressors (Kusajima et al., 2022). Kusajima et al., (2022) found that SA-induced defence gene transcription was significantly diminished in *max* mutants, particularly *max2-1*, compared to wildtype, suggesting SL signalling supports SA-mediated disease resistance.

5.2.3.1 GR24^{4DO}-treated seedlings have an upregulation of photosynthesis and light-adapted growth genes, and over-enrichment of HY5 downstream targets

GR24^{4DO} signals through the D14-SCF^{MAX2} complex, not KAI2-SCF^{MAX2}, thus downstream SL-specific signalling pathways can be studied through the transcriptomic changes induced by GR24^{4DO} treatment in Col-0. *D14 LIKE 2* (DLK2) has been repeatedly reported to be upregulated by SL treatment (Scaffidi et al., 2013; Waters et al., 2015), thus was used as a proxy transcriptional marker to confirm upregulated SL signalling in the GR24^{4DO}-treated Col-0 root tissue. *DLK2* expression was found to be significantly upregulated in GR24^{4DO}-treated Col-0, compared to untreated Col-0 tissue (Figure 5.6A). Upregulation of *DLK2* was part of cluster 5, comprised of 59 DEGs which are significantly upregulated with GR24^{4DO} treatment (Figure 5.5A-B). In this cluster, GO terms involved in photosynthesis, including ‘light reaction’ and ‘light-harvesting’ are significantly over-represented (Figure 5.6B).

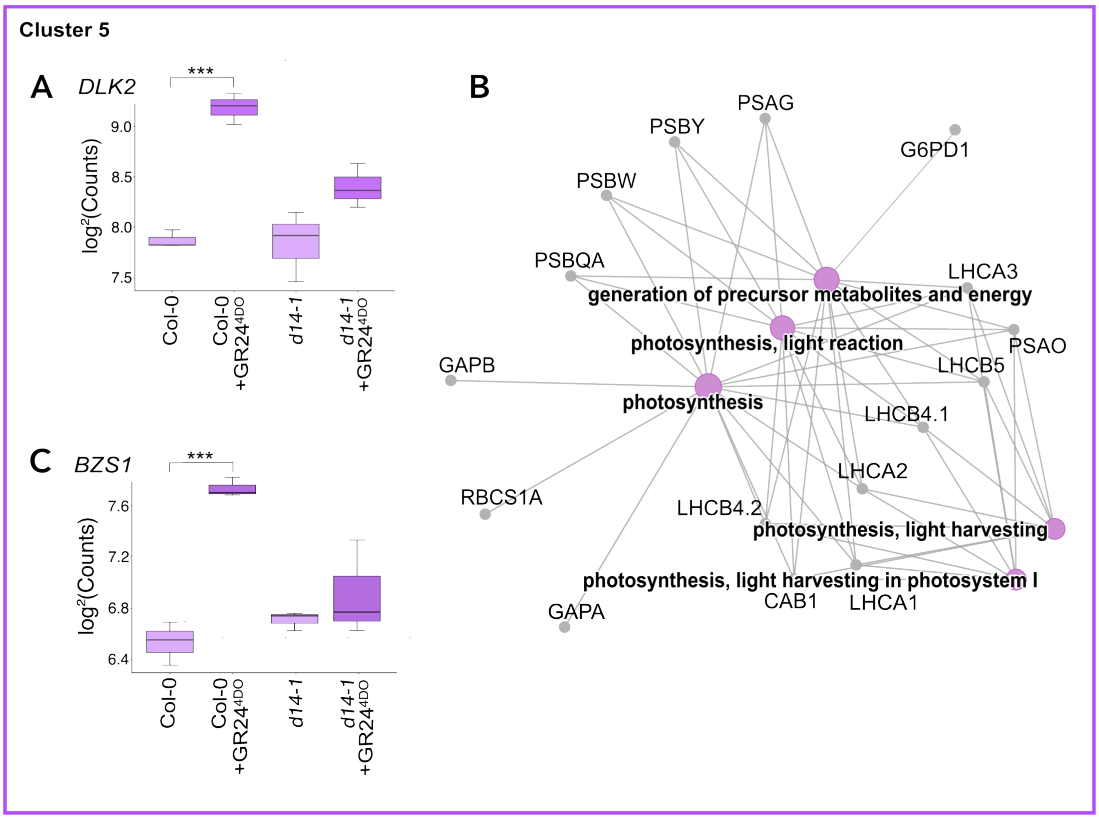

Figure 5.6 Transcriptome analyses identify up-regulation of photosynthetic pathways upon GR24^{4DO} addition in Col-0. A) Counts of selected GO-term associated DEG: *DLK2* transcripts between samples; B) The five most significantly overrepresented GO terms in cluster 5 are shown with associated DEGs; functional enrichment of clusters was performed using the R ClusterProfiler package (FDR-adjusted $p < 0.05$). C) Counts of selected GO-term associated DEG: *BZS1* transcripts between samples. Asterisks indicate statistically significant difference compared to mock-treated Col-0 as indicated by brackets (***$p < 0.001$; n = ~40 pooled root samples per biological repeat, three biological repeats).

Multiple *LIGHT HARVESTING COMPLEX* genes are within cluster 5, including *LHCA1*, *LHCA2* and *LHCA3*, and *LHCB4*, *LHCB4.2* and *LHCB5*. LHC proteins function in photosynthesis by forming light-harvesting complexes (LHC); LHCA subunits form LHC1 and LHCB subunits form LHC2. LHC1 is bound to photosystem 1 (PSI), whereas LHC2 typically binds photosystem 2 (PSII) (as reviewed in Pan et al., 2020). Together, the photosystems perform oxygenic photosynthesis, converting solar energy into chemical energy and forming oxygen through splitting water molecules. Other photosystem component-encoding genes are also within this cluster, including

PHOTOSYSTEM I SUBUNIT (*PSA*) *D1* and *PSAD2*. This striking upregulation of photosynthesis-related genes with $GR24^{4DO}$ treatment is interesting, as it suggests that SL treatment stimulates photosynthesis. In line with this finding, recent studies have noted an increase in photosynthesis with *rac*-GR24 treatment in plants experiencing abiotic stresses which otherwise decrease photosynthesis rate. It was found that application of 5 μM *rac*-GR24 – either applied in irrigation water or by directly spraying onto foliage – significantly increased photosynthesis rate (measured as $\mu M\ CO^2\ m^{-2}\ s^{-1}$) in winter wheat (*Triticum aestivum L.*) when experiencing drought stress (Sedaghat et al., 2021). Thus, the authors concluded that *rac*-GR24 is able to mitigate the effect of drought on photosynthesis. In rapeseed (*Brassica napus L.*), salinity stress – which decreases photosynthesis rate through affecting stomatal conductance – was shown to be alleviated through treatment with *rac*-GR24 (Ma et al., 2017). The net photosynthetic rate of plants grown in 200 mM NaCl was partially rescuable through combined treatment with 0.18 μM *rac*-GR24. Through RNA-seq, the authors next identified that *rac*-GR24 treatment induced upregulation of the KEGG terms 'photosynthesis' and 'photosynthesis-antenna proteins', reflective of the transcriptomic findings described here.

However, the studies by both Sedaghat et al. (2021) and Ma et al. (2017) used *rac*-GR24, of which the $GR24^{ent\text{-}5DS}$ has been proven to be able to stimulate karrikin signalling, and therefore is not a suitable analogue to use for delineating SL signalling. A recent study has partially circumvented this issue by performing transcriptomic analysis of 7-day-old *A. thaliana* seedlings after treatment with $GR24^{5DS}$, a predominantly D14-specific SL stereoisomer (Thula et al., 2022). The authors found upregulation of multiple photosynthesis-related genes with $GR24^{5DS}$ treatment, including multiple *PSA* and *PHOTOSYSTEM II SUBUNIT* (*PSB*) genes. This corroborates with the finding presented here that there is upregulation of light-harvesting genes with $GR24^{4DO}$ treatment, an alternative D14-specific SL analogue.

As *rac*-GR24 regulates COP1 nuclear localisation (Tsuchiya et al., 2010), it could be that the $GR24^{4DO}$ promotion of photosynthesis-related genes

arises through increasing COP1-mediated HY5 and BZR1 protein accumulation. To support this, it has previously been shown that 10 μM *rac*-GR24 increased HY5 protein accumulation in wildtype Arabidopsis (Jia et al., 2014), further suggesting that *rac*-GR24 may regulate downstream light-mediated COP1 signalling pathways. Again, these studies by Tsuchiya et al., (2010) and Jia et al., (2019) have relied on *rac*-GR24 as a SL analogue, where the confabulating effects of KAI2 signalling cannot be ruled out. In this $GR24^{4DO}$-treatment study, it can be seen from the response of DEGs within cluster 5 that $GR24^{4DO}$ promotes photosynthesis in wildtype, potentially through COP1-mediated signalling. To support this hypothesis, the COP1-repressed *BZS1* is also within cluster 5; *BZS1* transcript level is significantly higher in Col-0 with $GR24^{4DO}$ treatment (Figure 5.6C). As BZS1 is a COP1 degradation target, this suggests that $GR24^{4DO}$ may upregulate COP1 downstream targets through inhibition of COP1. Since these findings helped to understand SL signalling, the next step was to investigate whether targets of HY5 – which is inhibited by COP1 activity – were enriched amongst the 178 DEGs between mock-treated Col-0 and $GR24^{4DO}$-treated Col-0.

In previous work, 406 direct regulatory interactions had been identified between HY5 and other genes within *A. thaliana* root tissue (Jin et al., 2017; Tian et al., 2020). Six of these direct HY5 interactors were within the $GR24^{4DO}$-treated Col-0 root dataset of 178 DEGs, representing a 2.4-fold enrichment (hypergeometric test, p = 0.041). Of these, *PSEUDO-RESPONSE REGULATOR 9* (PRR9) was downregulated, and *MA3 DOMAIN-CONTAINING TRANSLATION REGULATORY FACTOR 4* (*MRF4*), *GLUTAMINE AMIDOTRANSFERASE* (*GAT*), *AT4G32480*, *AT2G20670* and *AT3G49790* were upregulated. The direction of regulation of the direct interactors in the other datasets is not yet known (Jin et al., 2017; Tian et al., 2020).

Strikingly, there was also a 2.8-fold enrichment of direct HY5 interactors in the $GR24^{4DO}$-treated *d14-1* root dataset (hypergeometric test, p = 0.007), comprising eight DEGs out of 199. Five DEGs were in common with the HY5 direct interactors identified in $GR24^{4DO}$-treated Col-0 - PRR9, GAT,

AT4G32480, AT3G49790 and AT2G20670, all showing the same expression regulation pattern between Col-0 and *d14-1*. Additionally, AT5G02090, SEED GENE 3 (ATS3) and ATP-BINDING CASSETTE A21 (ATPI21) were upregulated by $GR24^{4DO}$ treatment. Combined, this implies that $GR24^{4DO}$ promotion of HY5 signalling may be D14-independent, and therefore MAX2-independent, thus not involving the D14-SCF^{MAX2} complex. This would explain the enrichment of direct HY5 targets and upregulation of photosynthesis-related genes with $GR24^{4DO}$-treatment in Col-0 and also *d14-1*.

It has been previously shown that *rac*-GR24 inhibits Arabidopsis hypocotyl elongation in a light-dependent manner, likely through COP1 (Tsuchiya et al., 2010). However, Tsuchiya et al. (2010) also showed that *rac*-GR24 concentrations over 50 μM inhibit hypocotyl elongation constitutively, in both light and dark. Later, it was found that 10 μM *rac*-GR24 inhibited hypocotyl elongation in wildtype plants grown in white light, but not in *max2-3* and *max2-4* mutants (Jia et al., 2014). However, 25 μM *rac*-GR24 was found to inhibit hypocotyl elongation in all genotypes grown under white light, and that 50 μM constitutively inhibited hypocotyl elongation in white light and in dark, reflecting the findings of Tsuchiya et al. (2010). This suggests that *rac*-GR24, and potentially $GR24^{4DO}$/SL, likely regulates hypocotyl elongation through both a *MAX2*-dependent and a *MAX2*-independent pathway, which Tsuchiya et al. (2010) pose may be through direct relocalisation of COP1 by SL.

There are differences in experimental conditions between the work presented here and the studies described that may affect overall GR24 response. For the GR24 experiment presented here, plants were grown on media containing 1 μM $GR24^{4DO}$, which is relatively low compared to the 25-50 μM concentrations that were used in the other studies described (Jia et al., 2014; Tsuchiya et al., 2010). Another difference was that in this work the plants were 12-days-old and thus had been exposed to the GR24 for 12 days, compared to 4-day-old seedlings being used in Jia et al. (2014) and 5-day-old seedlings being used in Tsuchiya et al. (2010). There may be a cumulative effect of lower GR24 concentrations over an extended period of time, which

could elicit similar effects as exposure to a high concentration for a shorter period, leading to the same level of D14-SCF^{MAX2}-independent inhibition of COP1 function overall.

It is possible that this D14-SCF^{MAX2}-independent COP1 inhibition by GR24^{4DO} is the driver behind the D14-independent GR24^{4DO} root phenotypes seen previously (Chapter 3). *Cop1-4* mutant plants have longer primary roots compared to wildtype, with larger meristem zones and longer cells in the elongation zone (Lyu et al., 2019). Treatment with GR24^{4DO} may also inhibit COP1 activity, leading to the long primary root phenotype. This theory could also explain the short primary root phenotype seen in *max4-1*. Reduction in SL biosynthesis from a lack of functional MAX4 might result in lack of COP1 repression, and therefore inhibition of primary root growth and elongation. This hypothesis can also help to offer an explanation for the D14-independent lateral root density phenotype that is seen. In *cop1-6* – a weaker *cop1* mutant – initiation of lateral root development is very inhibited compared to wildtype (Ang et al., 1998). Treatment with GR24^{4DO} may result in over-inhibition of COP1, replicating this phenotype. Further experiments, such as this, could be used to test the hypothesised existence of D14-SCF^{MAX2}-independent COP1 inhibition. This could be done through testing nuclear localisation of COP1 under the presence of GR24^{4DO}/GR24^{5DS} in wildtype plants versus a *d14*/*max2* double knockout.

Overall, the significant upregulation of photosynthesis and light-signalling genes in GR24^{4DO}-treated plants supports a role for SL in promoting HY5-mediated upregulation of photosynthesis and light-adapted development.

5.2.3.2 GR24^{4DO}-treated seedlings exhibit downregulation of phenylpropanoid pathway

Within the GR24^{4DO} treatment experiment, there are 20 genes in cluster 4 that are significantly downregulated with GR24^{4DO} treatment (Figure 5.5A-B); this cluster is overrepresented for the KEGG pathway 'phenylpropanoid metabolism'. The genes related to this KEGG term are *CINNAMYL ALCOHOL DEHYDROGENASE 6* (*CAD6*) and *PEROXIDASE 25* (*PRX25*) (Figure 5.7).

The phenylpropanoid pathway produces different metabolites depending on route, including flavonoids, anthocyanins and lignins. PRX25 participates specifically in lignin production; *A. thaliana* T-DNA insertional *prx25* plants have significantly reduced total lignin content compared to wildtype (Shigeto et al., 2015). Previously, downregulation of flavonoid biosynthesis genes was identified in SL signalling mutants *max2-1* and *d14-1* (Richmond et al., 2022), and there is upregulation of flavonoid biosynthesis genes when plants are treated with $GR24^{4DO}$ (Wang et al., 2020b). $GR24^{4DO}$ treatment may therefore induce redirection of the phenylpropanoid pathway to preferentially produce flavonoids and anthocyanins, rather than lignins. Cluster 5 indicated that $GR24^{4DO}$ upregulates photosynthesis and light signalling genes, and so diversion from lignin production to photoprotective flavonoids and anthocyanins would be logical. This could be tested by measuring the lignin versus flavonoids and anthocyanin content in seedlings.

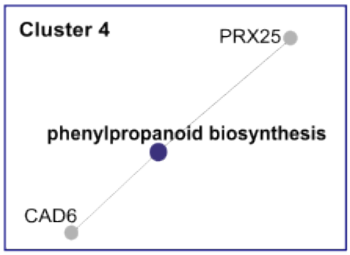

Figure 5.7 Transcriptome analyses identify down-regulation of phenylpropanoid genes with $GR24^{4DO}$ addition in *d14-1*. Associated DEGs are pictured; functional enrichment of clusters was performed using the R ClusterProfiler package (FDR-adjusted $p < 0.05$).

Given the upregulation of light-response signalling identified in cluster 5, it is also plausible that phenylpropanoid regulation is downstream of the same light- and SL-regulated signalling pathway. To support this idea, *PRX25* expression has been found to be negatively regulated by the transcription factor COGWHEEL1 (COG1) (Renard et al., 2020), and COG1 itself is significantly upregulated in plants treated with *rac*-GR24 (Mashiguchi et al., 2009). COG1 stimulates expression of the major light signalling transcription factors PHYTOCHROME-INTERACTING TRANSCRIPTION FACTOR (PIF) 4 and 5, further linking SLs to light response signalling. In a dominant *cog1-D*

line, there was significantly less accumulation of anthocyanins compared to wildtype, indicating that COG1 is a negative regulator of anthocyanin accumulation (Park et al., 2003). This further supports the idea that GR24^{4DO} treatment may redirect phenylpropanoid metabolism to favour anthocyanin biosynthesis. To confirm the expected links, levels of flavonoid and lignin accumulation should be measured in plants treated with GR24$^{4DO.}$

5.2.3.3 Circadian clock and light-responsive genes are downregulated in the d14-1 mutant compared to Col-0

Cluster 1 contains 98 genes which are downregulated in *d14-1* with GR24^{4DO} treatment compared to Col-0 under mock treatment. This cluster is overrepresented for the GO term 'response to light' and contains many light-responsive genes (Figure 5.8A). D14 forms a negative feedback loop to prevent further SL production, thus, it is possible that this downregulation of genes only in *d14-1* plants treated with GR24^{4DO} is the result of a snowballing effect of overaccumulation of endogenous SLs combined with the high level of exogenous GR24^{4DO}. To support this idea, levels of an endogenous SL, 2′-*epi*-5-deoxystrigol, were found to be higher in *O. sativa d14* mutant root tissue compared to wildtype (Arite et al., 2009). Given that *d14-1* is a loss-of-function mutant, differential gene expression with GR24^{4DO} treatment in *d14-1* is also further evidence for D14-independent SL signalling, particularly in the context of regulating light-mediated development.

Gene expression changes in response to light signalling drives plant photomorphogenesis. Repression of light signalling in plants in darkness involves the light-signalling repressor COP1 which forms an E3-ubiquitin ligase complex with SUPPRESSOR OF PHYA-105 (SPA) proteins 1-4. This COP1/SPA complex targets positive light signalling proteins for degradation, suppressing photomorphogenesis. In light, the COP1/SPA complex is inactivated by direct interactors, including cryptochrome photoreceptors (CRYs) and phytochrome A (PHYA). Aboveground characteristics of light-grown seedlings include suppression of hypocotyl elongation and promotion of pigment accumulation (as reviewed in Legris et al., 2019). Light-grown roots

exhibit both primary and lateral root growth promotion, seemingly as a physiological light-avoidance strategy to encourage root growth to darkness (soil). Under light, PHYA and B mediate the degradation of PIFs, relieving PIF-imposed suppression of photomorphogenesis. *A. thaliana* light-grown PHYA-deficient mutants have significantly shorter primary roots, fewer lateral roots and shorter root hairs compared to light-grown wildtype, indicating PHYA-mediated primary, lateral root and root hair growth promotion in response to light (De Simone et al., 2000; Kumari et al., 2019; Yokawa et al., 2013). These root photomorphogenic characteristics are reminiscent of the *d14-1* mutant, which has significantly longer primary roots, more numerous lateral roots, and longer root hairs compared to wildtype (Section 5.2.1). In the context, it could be that photomorphogenesis is promoted in the *d14-1* line. If SLs accumulate within the *d14-1* mutant, the phenotype aligns with the hypothesis that SL inhibits COP1-mediated repression of photomorphogenesis (Sheerin et al., 2015). To test whether *d14-1* does overaccumulate SLs, thus strengthening this concept, metabolomic analyses of SL levels should be performed.

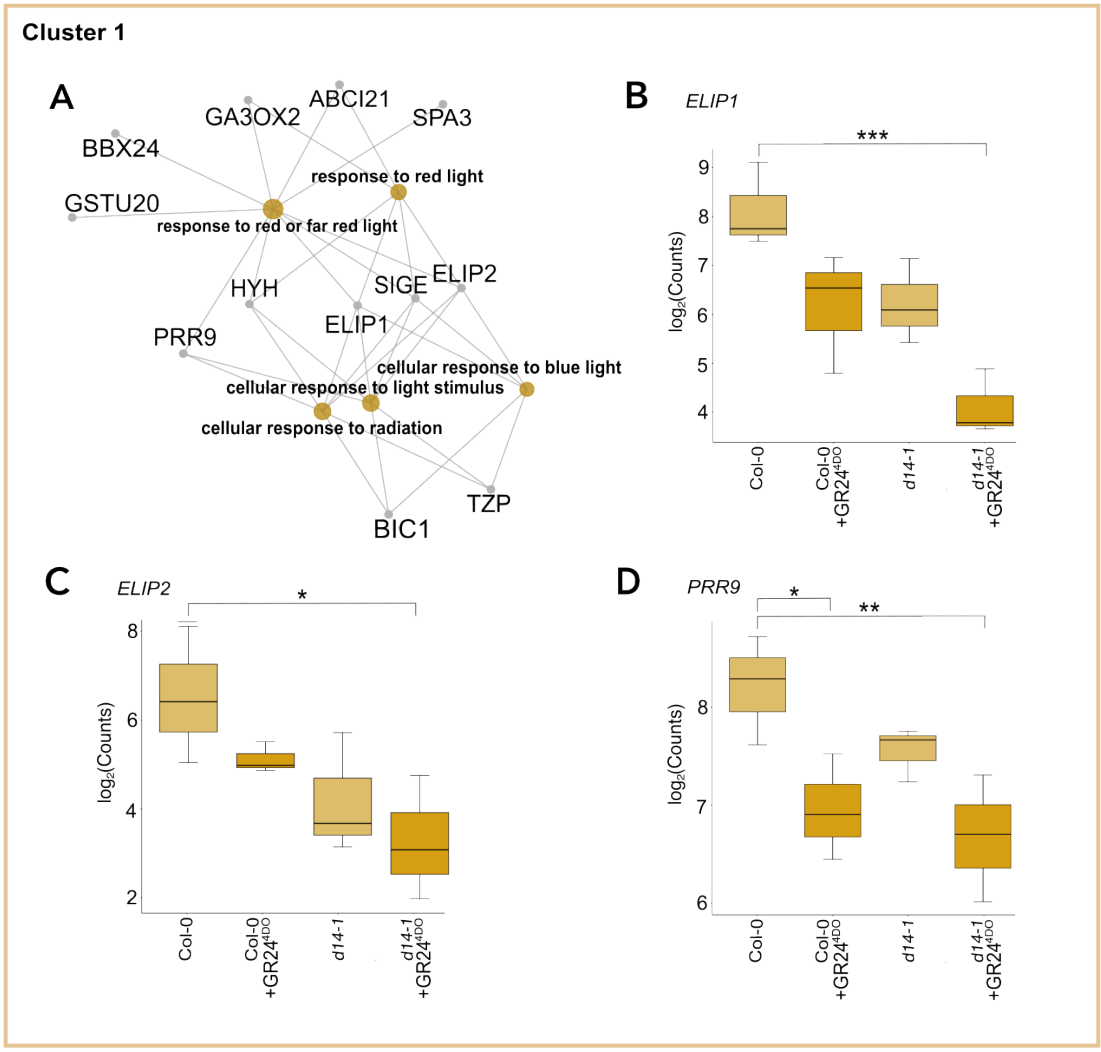

Figure 5.8 Transcriptome analyses identify down-regulation of light-responsive genes with GR24^{4DO} addition in *d14-1*. A) The five most significantly overrepresented GO terms in cluster 1 are shown with associated DEGs; functional enrichment of clusters was performed using the R ClusterProfiler package (FDR-adjusted $p < 0.05$). Counts of selected GO-term associated DEGs: B) *ELIP1* transcripts, C) *SPA3* transcripts and D) *GA3OX2* transcripts. Asterisks indicate statistically significant difference compared to mock-treated Col-0 as indicated by brackets (*$p < 0.05$, **$p < 0.01$, ***$p < 0.001$; n = ~40 pooled root samples per biological repeat, three biological repeats).

Alongside HY5, HY5-HOMOLOG (HYH) is a target of the COP1/SPA complex, with a similar role in photomorphogenesis promotion. In cluster 1, there is no significant difference between *HYH* transcript levels in untreated *d14-1* and GR24^{4DO}-treated Col-0 compared to untreated Col-0, though there appears to be a trend for *HYH* transcript level decrease in both (Figure 5.5B). *HYH* transcript levels are significantly reduced in GR24^{4DO}-treated *d14-1*, compared to untreated Col-0 (Figure 5.5B). This may be due to an additive effect of endogenous SL accumulation and exogenous GR24^{4DO} treatment. In line with the hypothesis that SLs regulate D14-independent COP1 inhibition, *HYH* transcription may be downregulated through a negative feedback loop: overaccumulation of HYH protein from a lack of COP1/SPA-mediated HYH protein degradation might signal for *HYH* repression. SL-mediated COP1 inhibition may induce constitutive light signalling, leading to photomorphogenic root phenotypes. This would explain the longer primary and lateral root lengths with GR24^{4DO} addition and *d14-1* mutation (Section 5.2.1). To test this hypothesis, quantification of HY5/HYH protein accumulation should be performed in the *d14-1* line and Col-0, with and without GR24^{4DO}; if HYH/HY5 protein accumulation is found in both the Col-0 and *d14-1*, this would support the hypothesis.

In GR24^{4DO}-treated *d14-1* there were longer and more numerous lateral roots compared to GR24^{4DO}-treated Col-0 (Section 5.2.1). This phenotype could be explained by the downregulation of *HYH*, as it was recently shown that HY5/HYH-mediated signalling regulates light-induced root growth, independently of light signalling in the shoot (Zhang et al., 2017). *HY5* was found to be abundantly expressed within early lateral root primordia, and *HYH* was found to be expressed within lateral root vascular root tissue (Zhang et al., 2019). Similar to the GR24^{4DO}-treated *d14-1* phenotype, Zhang et al. (2019) found that the lateral roots of *hy5* plants were significantly longer than wildtype, whether grown in light or dark. To support that SLs may harness HY5/HYH-mediated signalling to modulate plant development, other studies have implicated SLs and HY5/HYH signalling in other photomorphogenic changes including hypocotyl elongation (Jia et al., 2014) and seed germination (Toh et al., 2012). Many of the DEGs within this cluster are associated with

the GO term ‘response to light stimulus’, further suggesting that SLs play a role in photomorphogenesis. To illustrate, cluster 1 features significant downregulation of *EARLY LIGHT-INDUCABLE PROTEIN 1* and *2* (*ELIP1/2*) in $GR24^{4DO}$-treated *d14-1* compared to mock-treated Col-0 (Figure 5.8A-C). Chloroplastic proteins ELIP1 and ELIP2 protect PSII against photooxidative stress, and so the downregulation of ELIPs in cluster 1 suggests that SLs are involved in cellular adaptation to light stress.

COP1-mediated HY5 signalling also acts to regulate the light input of the circadian clock. In plants, the circadian rhythm is maintained through entrainment to daily cues, the most potent being the light/dark cycle. In cluster 1, there is significant downregulation of *PRR9* (Figure 5.8A, D), which is a key morning loop clock gene. PRR9 acts as a transcription repressor of other morning loop genes *CCA1* and *LHY* (Nakamichi et al., 2010), which in turn positively regulate PRR9, forming a feedback loop. SLs have previously been associated with the rice circadian clock, as *OsD14* expression has been shown to be positively regulated by *OsCCA1* (F. Wang et al., 2020). PRR proteins have also been shown to suppress COP1 degradation of some targets (Hayama et al., 2017). Combined with the results presented here, this suggests that SLs may act in a complex feedback module with circadian genes to regulate photomorphogenesis and light-induced adaptations.

As this finding implicates SLs with entrainment of the circadian clock, a time course experiment should be performed with SL biosynthesis mutants, to analyse via RT-qPCR whether SL-deficiency affects rhythmic expression of key clock components, including *PRR9* and *CCA1*. If SLs regulate HY5-mediated circadian clock entrainment to light, it would be expected that circadian clock function is disrupted.

5.2.3.4 Downstream SL signalling appears to regulate oxidative stress and root growth

Cluster 3 includes DEGs which are upregulated in mock-treated *d14-1* compared to mock-treated Col-0*,* with an over-enrichment of the GO term ‘plant organ formation’ (Figure 5.9). Many DEGs in this cluster are also

upregulated in GR24^{4DO}-treated *d14-1*, suggesting that this cluster represents downstream effects of inhibiting D14-mediated signalling. A lack of functional D14, would lead to overaccumulation of SMXL6, 7 and 8, and SMAX1, which are transcriptional repressors of downstream SL signalling. Consistent with a previous study which shows that SLs accumulate in SL signalling mutants due to lack of negative feedback (Arite et al., 2009), cluster 3 includes significant upregulation of both *CCD7/MAX3* and *CCD8/MAX4* in *d14-1*. In a *smax1* overexpressing line it was previously found that *MAX3*, *MAX4* and *MAX1* genes were more highly expressed compared to wildtype (Zheng et al., 2021). These expression differences were implicated in phenotypic changes including plants having larger leaves and less shoot branching (Zheng et al., 2021). Analysis of cluster 3 thus helps to implicate SMXL/SMAX signalling pathways in the SL response.

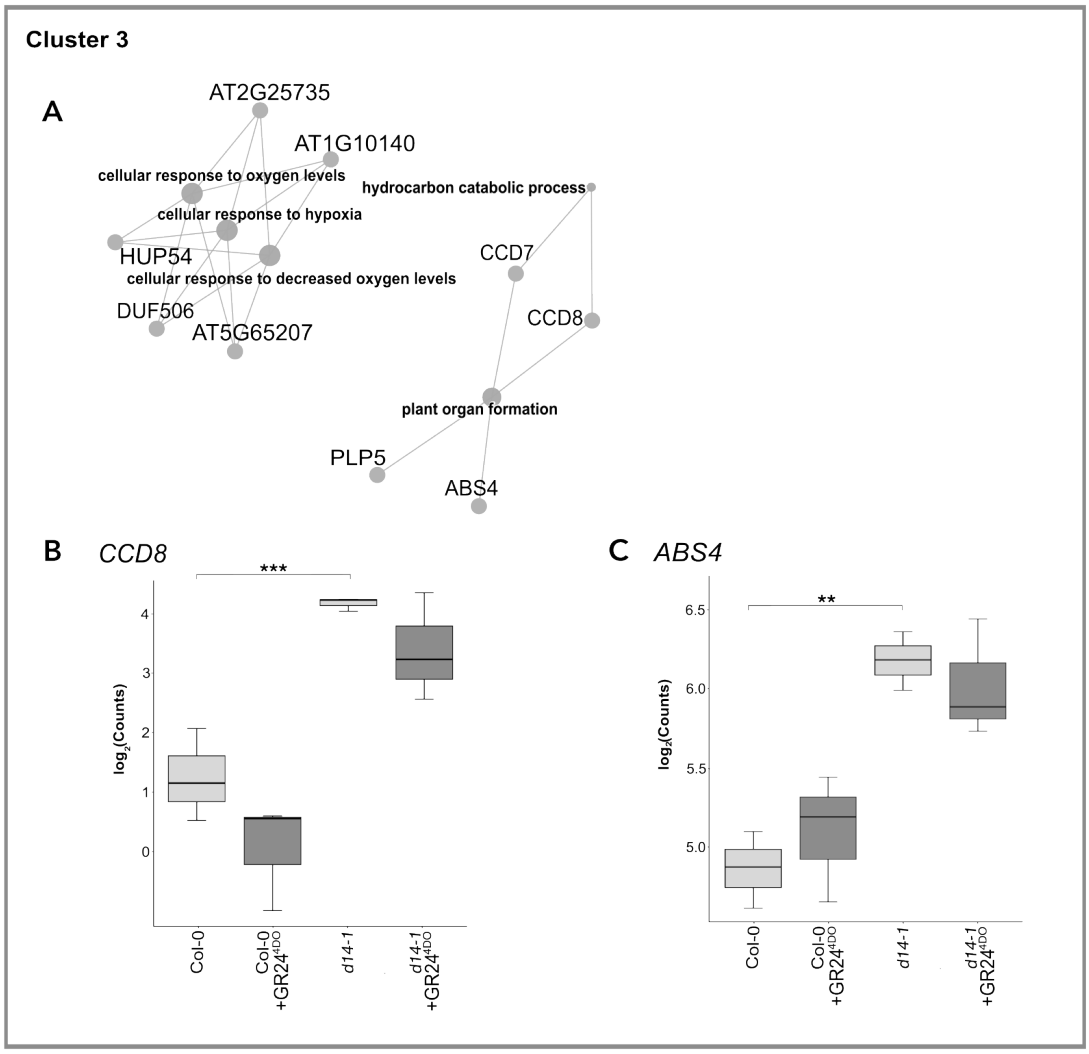

Figure 5.9 Transcriptome analyses identify upregulation of plant growth-related genes in mock-treated *d14-1* compared to Col-0. A) The five most significantly overrepresented GO terms in cluster 3 are shown with associated DEGs; functional enrichment of clusters was performed using the R ClusterProfiler package (FDR-adjusted $p < 0.05$). Counts of selected GO-term associated DEGs: B) *CCD8/MAX4* transcripts, and C) *ABS4* transcripts. Asterisks indicate statistically significant difference compared to mock-treated Col-0 as indicated by brackets (**$p < 0.01$, ***$p < 0.001$; n = ~40 pooled root samples per biological repeat, three biological repeats).

There is a significant upregulation of *ABS4,* a Multidrug and Toxic Compound Extrusion (MATE) family efflux transporter which has been implicated in morphogenesis, in *d14-1* compared to Col-0 (Figure 5.9C). In an *ABS4*-overexpressing line (*ABS4*-OE), hypocotyl cell elongation in the dark was significantly reduced compared to wildtype, indicating a de-etiolation or

constitutive photomorphogenesis phenotype (Wang et al., 2015). This would corroborate the findings from analysis of cluster 1, which identified a significant upregulation of photomorphogenesis-related processes, such as chloroplast development, and light signalling response genes. Comparing the root phenotypes of Col-0, *d14-1*, *ABS4-OE* and *cop1* (which has a constitutive photomorphogenesis phenotype), with and without $GR24^{4DO}$ treatment would be informative as to what extent D14-mediated SL signalling through SMXL/SMAX1 also regulates photomorphogenesis.

It has also been established that SLs regulate plant drought resistance, through functional analysis of SL signalling mutants. Triple mutant *smxl6,7,8* plants are more drought-resistant compared to wildtype, such as through increased anthocyanin biosynthesis, reduced cuticle permeability and oxidative stress tolerance (Li et al., 2020c). Amongst DEGs in cluster 3, there is over-enrichment of GO terms involved in oxidative stress. As these DEGs are upregulated in *d14-1*, it suggests that the *d14-1* mutant has lower oxidative stress tolerance. Flavonoids have antioxidant properties, and the finding that *d14-1* plants have lower expression of a key flavonoid biosynthesis gene, and less root tip accumulation of flavonoids compared to wildtype (Chapter 4), can thus be linked. In further support of this, within, cluster 2 there is a significant downregulation of *MYB37* in mock- and $GR24^{4DO}$-treated *d14-1* (Figure 5.10A-B). MYB37 is a member of the R2R3 family of transcription factors, of which the majority play a role in promoting anthocyanin/flavonoid biosynthesis (as reviewed in Li et al., 2022a). It has been demonstrated that MYB37 overexpression improves drought tolerance, which may well be due to accumulation of flavonoids, due to their ROS-scavenging and antioxidant capabilities (Yu et al., 2016). To support this, in *Perilla frutescens*, MYB37 is predicted to regulate photosensitive anthocyanin production, and in *Salvia miltiorrhiza*, MYB37 is predominantly expressed in stems, which could be linked to a role in lignin biosynthesis (general phenylpropanoid metabolism) (Li and Lu, 2014). *4CL3*, a key phenylpropanoid biosynthesis gene, is downregulated in cluster 2 alongside *MYB37*, providing another link between these processes (Figure 5.10).

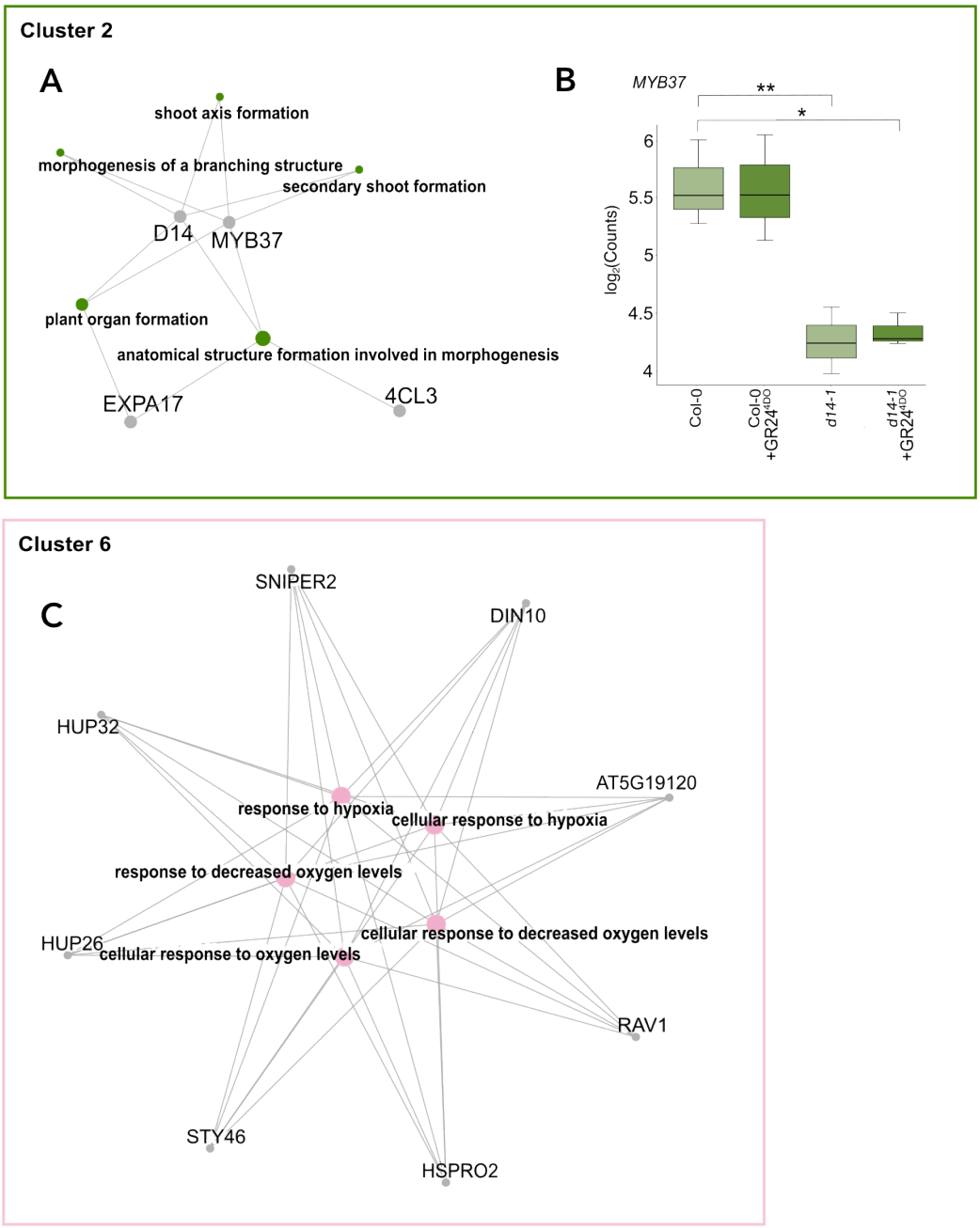

Figure 5.10 Transcriptome analyses identify downregulation of phenylpropanoid-related genes and upregulation of oxidative stress response DEGs in *d14-1* compared to Col-0. The five most significantly overrepresented GO terms in cluster 2 with associated DEGs. B) Counts of selected GO-term associated DEG: *MYB37* transcripts. C) The five most significantly overrepresented GO terms in cluster 6 with associated DEGs. Functional enrichment was performed using R ClusterProfiler package (FDR-adjusted $p < 0.05$). Asterisks indicate statistically significant difference compared to mock-treated Col-0 as indicated by brackets (*$p < 0.05$, **$p < 0.01$; n = ~40 pooled root samples per biological repeat, three biological repeats).

To further illustrate that *MYB37* expression – and therefore flavonol and lignin biosynthesis – might be positively regulated by SL-D14-MAX2^{SCF} degradation of SMXL/SMAX1, significant downregulation of *MYB37* was found in *max2-1* compared to wildtype (Chapter 3). Similar to the stress-resistant phenotype of triple mutant *sxml6,7,8*, overexpression of *MYB37* has been demonstrated to reduce ROS accumulation and oxidative damage in salt-stressed plants (Li et al., 2022d). Moreover, cluster 6 features DEGs which are upregulated in both treated genotypes compared to mock-treatment of these genotypes (Figure 5.5A,B), and the cluster is overrepresented for GO terms associated with oxidative stress, including *OXIDATIVE STRESS 3* (*OXS3*) (Figure 5.10C). Oxidative stress tolerance is ameliorated in *OXS3* overexpressor lines, and diminished in *oxs3* mutants (Blanvillain et al., 2009). This indicates that SL dysregulation, either through exogenous treatment or lack of functional D14, might increase oxidative stress.

Together, this data and analysis suggests a SL signalling through SL-D14-MAX2^{SCF} drives stress tolerance, likely through promoting ROS-scavenging metabolites.

5.2.4 Conclusions

Root systems of wildtype and SL signalling mutant *d14-1* seedlings were phenotyped under both mock conditions and with GR24^{4DO} addition, to assess the roles of D14-mediated SL signalling on shaping root system architecture. Transcriptomic analyses of roots were executed to identify gene expression changes which may cause the phenotypic differences.

Investigation of wildtype root system architecture revealed that GR24^{4DO} addition leads to a longer primary root, longer lateral roots (Figure 5.2) and shorter root hairs (Figure 5.3) compared to mock-treatment. This differed to the lateral root inhibition and root hair promotion induced by *rac*-GR24 treatment (Chapter 3). Root system architecture studies revealed that mutation in *D14* leads to a longer primary root length, longer and more numerous lateral roots, and longer root hairs compared to wildtype. These characteristics are reminiscent of those seen during root

photomorphogenesis. Like wildtype, with GR24^{4DO} addition *d14-1* exhibits longer primary and lateral roots and shorter root hairs compared to untreated *d14-1*, which suggests that there is a D14-independent pathway regulating root response to GR24^{4DO}.

The mechanism behind the root phenotypes of wildtype and *d14-1* in response to GR24^{4DO} were investigated through analysis of RNAseq data. There were transcriptomic differences between mock-treated wildtype and *d14-1* – such as upregulation of morphogenesis-related DEGs – which may contribute to the promotion of primary and lateral root and root hair growth in *d14-1*. Transcriptomic variances between mock-treated and GR24^{4DO}-treated wildtype included a striking upregulation of photosynthesis-related and light-adapted growth genes, implicating SL in light signalling. As indicated by the root system architectural study, there were also many shared transcriptomic differences between Col-0 and *d14-1* to GR24^{4DO} treatment – such as oxidative stress response genes – suggesting the existence of a D14-independent mechanism for SL signalling.

Chapter 6 Role of strigolactones in regulation of root system architecture, nodulation, and flavonoid biosynthesis in *Medicago truncatula*

6.1 Introduction

Through hosting root-microbe symbioses, plants can mitigate growth limitations by abiotic stressors, including nitrogen (N) or phosphorus (P) deficiency (as reviewed in Omae and Tsuda, 2022). The majority of vascular plants can form interactions with arbuscular mycorrhizal fungi (AMF), which lead to an increase in the surface area for plant water/nutrient acquisition, through fungal hyphal branching; the symbiont receives carbon-rich root exudates in return. In legumes, nodulation with symbiotic N-fixing rhizobia provides plants a usable form of N, even in/from low N soils. Strigolactones (SLs) have been implicated in the regulation of initiation and activity of root-microbe symbioses. In many plant species, SL biosynthesis and release via root exudates is increased when plants are under abiotic stress - such as phosphate deficiency (López-Ráez et al., 2008; Mayzlish-Gati et al., 2012; Sun et al., 2014). SL upregulation indicates their importance in mediating responses to stress and plant-microbe interactions.

The SL/KL analogue *rac*-GR24 potently stimulates spore germination and hyphal branching in AMF at subnanomolar concentrations (Besserer et al., 2006). SLs were found to stimulate hyphal branching in the AMF *Gigaspora margarita*, but not KLs (Akiyama et al., 2010), demonstrating that hyphal branching is regulated via SLs rather than KLs. By promoting spore germination and hyphal branching towards the SL-exuding root, SLs may increase the likelihood of root-fungus association. Further, there is reduced promotion of hyphal branching and root colonisation in SL biosynthesis mutants in *P. sativum* (Gomez-Roldan et al., 2008) and *S. lycopersicum* (Vogel et al., 2010). In Os*ccd7* and Os*ccd8*, where SL is not detectable in root exudates, AMF colonisation of the roots is significantly decreased through

reduced attachment of AMF to the root (Kobae et al., 2018). Thus, SLs play an essential and multifaceted role in AMF-root symbioses.

The role of SLs as chemoattractants for parasitic plants has been well-established (Akiyama et al., 2010). It has been suggested that SLs may have similar chemoattractive properties for microbiota; recruiting favourable fungi and bacteria and promoting a more beneficial root microbiome (Liu et al., 2020a). Liu et al. (2020a) found that *G. max D14, MAX2* and *MAX1* overexpression lines have significant differences in their microbiome community composition, showing the importance of SL signalling and biosynthesis to microbial recruitment. Similarly, *A. thaliana max4* and *O. sativa d14* mutants had significantly different fungal (Carvalhais et al., 2019) and bacterial (Nasir et al., 2019) community compositions, respectively. In leguminous plants, SLs could aid in the recruitment of free-living rhizobia to the root microbiome, which increases the likelihood of initiating a successful symbiosis. As with AMF colonisation, SLs appear to promote formation of rhizobia-legume symbioses. To illustrate, application of *rac*-GR24 significantly increased nodule number in rhizobia-treated wildtype *M. sativa* (Soto et al., 2010), *M. truncatula* (De Cuyper et al., 2015) and *P. sativum* (Foo and Davies, 2011). Furthermore, when SL biosynthetic genes are mutated or silenced, nodule number decreases in *G. max* (Rehman et al., 2018), *L. japonicus* (Liu et al., 2013), *M. sativa* (Soto et al., 2010) and *P. sativum* (Foo and Davies, 2011). The key nodulation genes *NSP1* and *NSP2* are essential for SL biosynthesis in *M. truncatula* and *O. sativa* (Liu et al., 2011), suggesting that SL biosynthesis is co-regulated alongside nodulation. Additionally, SL biosynthesis genes are upregulated in *M. truncatula* root hairs by rhizobia and Nod factors (Breakspear et al., 2014), further implicating SLs in early nodule initiation events.

SLs seem to promote infection thread formation during nodule development, with the SL-deficient *P. sativum ccd8-1* mutant forming significantly fewer infection threads compared to wildtype (McAdam et al., 2017). Interestingly, the frequency of infection threads resulting in fully developed nodule formation was not altered in *ccd8-1* compared to wildtype,

suggesting that more nodules are formed to compensate for inefficiency. In conclusion, SLs appear to play a role in nodule formation both exogenously – attracting rhizobia, and endogenously – promoting nodule development.

6.1.1 Aims and Objectives

The aim of this work was to explore whether the role of strigolactone in root development is conserved in *M. truncatula* (Section 1.4.1). As *Arabidopsis thaliana* SL biosynthesis *max3-9* and *max4-1* mutants exhibit longer and more numerous root hairs compared to wildtype, root hairs of *M. truncatula* SL biosynthesis mutants *ccd7-1* and *ccd8-1* were measured to ask if they also exhibit this phenotype. Previous work suggests a promotional role of SLs on nodulation in other leguminous plants, such as *G. max* (Rehman et al., 2018), *L. japonicus* (Liu et al., 2013), *M. sativa* (Soto et al., 2010) and *P. sativum* (Foo and Davies, 2011). Thus, nodule number was also assessed in *M. truncatula ccd7-1* and *ccd8-1*, alongside plant biomass. Given that flavonoids and SLs both influence nodulation, and SL signalling positively regulates flavonoid biosynthesis genes in *A. thaliana*, gene expression analyses of flavonoid biosynthesis genes were also performed on *ccd7-1* and *ccd8-1* root tissue.

6.2 Results and Discussion

6.2.1 Root hair phenotypes of *Medicago truncatula* strigolactone mutants

The root hairs of the *ccd7-1* and *ccd8-1 Medicago truncatula* strigolactone mutants were phenotyped, following the hypothesis that, as with the *A. thaliana* strigolactone biosynthesis mutants, there would be an increase in root hair length and density compared to wildtype. Two strigolactone biosynthesis mutants were selected, *ccd7-1* and *ccd8-1*, which are in the R108 background. To ask whether the nodulation regulatory gene *NSP2* also affects root hair SL responses, the *nsp2-2* mutant was also included in this study, which is in the A17 background. Elongation and increased density of root hairs is a nutrient foraging response when in low phosphate conditions, thus *M. truncatula* seedlings were grown on media containing no phosphate to accentuate any root hair phenotypes.

Five-day-old *M. truncatula* seedlings were imaged, and root hair area (in mm^2) was measured for the first 10 mm of each root tip using Image J. Both *ccd7-1* and *ccd8-1* root tips had a statistically significantly larger root hair area per 10 mm of root tip compared to R108 wildtype (p = 0.006 and 0.002, respectively) (Figure 6.1A, C). Higher root hair density compared to wildtype had also been found for the *A. thaliana* strigolactone mutants (Chapter 3), which suggests that strigolactone-mediated regulation of root hair length and density may be conserved across plant species. There was no significant difference in root hair area between *nsp2-2* root tips and the A17 wildtype.

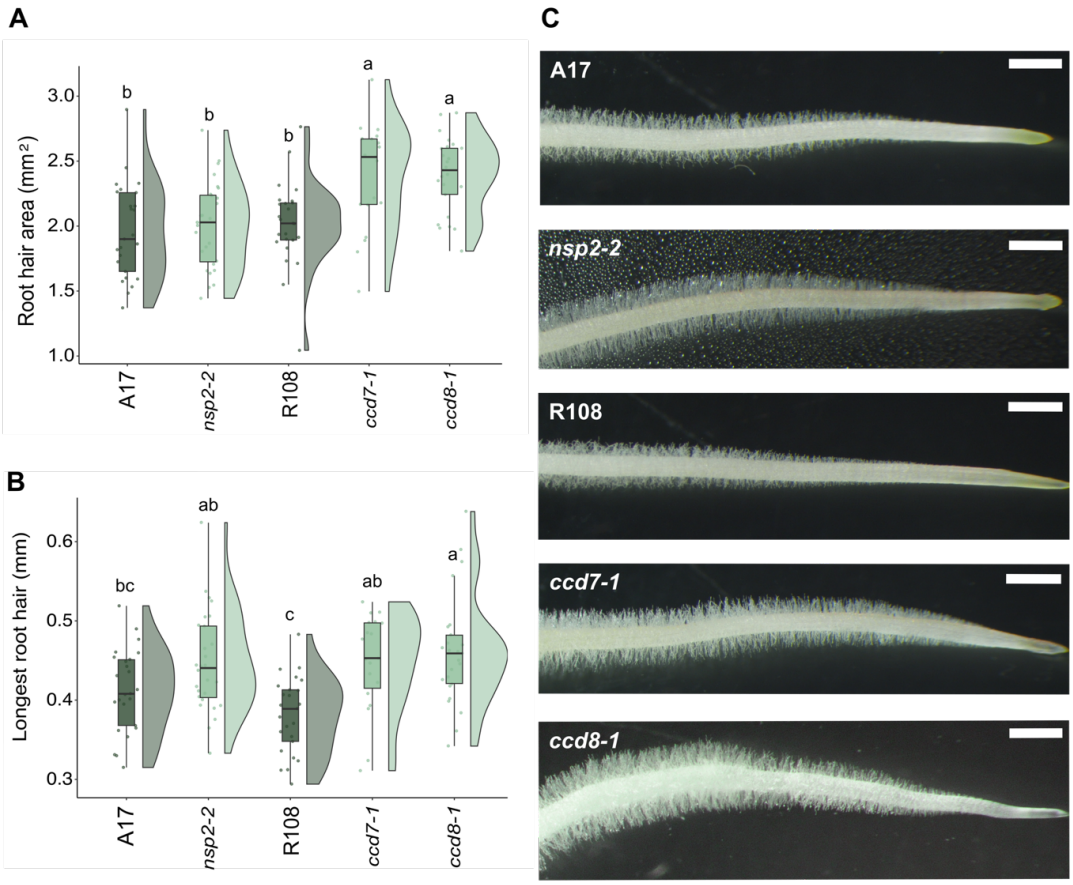

Figure 6.1. Strigolactone biosynthesis contributes to root hair length in *M. truncatula*
Root hair area (per 10 mm) of 5-day-old A17, *nsp2-2*, R108, *ccd7-1* and *ccd8-1* roots after growth on no phosphate media and (B) longest root hair length (mm) of the same plants. (C) Representative images, bars represent 1 mm. Different letters indicate statistically significant difference determined by ANOVA (post hoc Tukey: $p < 0.05$); (A) $F_{4,117} = 9.366$, (B) $F_{4,117} = 7.499$; n = 5–13 seedlings per biological repeat, three biological repeats).

The longest section of root hairs within the same 10 mm section as measured for root hair areas was quantified to measure differences in root hair length. In both *ccd7-1* and *ccd8-1*, the maximum root hair lengths were statistically significantly longer than those of R108 (p = 2.986E-3 and 5.181E-5, respectively) (Figure 6.1B-C). This is again reminiscent of the long root hair phenotype found in the *A. thaliana* strigolactone biosynthesis mutants compared to wildtype (Chapter 3). There was no significant difference in maximum root hair length between *nsp2-2* and A17 (Figure 6.1B-C).

6.2.2 Nodulation phenotypes of *Medicago truncatula* strigolactone mutants

As strigolactone is a component of plant-microbe pre-symbiotic communication, the nodulation phenotypes of the strigolactone *M. truncatula* mutants was assessed. 5-day-old seedlings were inoculated with the symbiont *Sinorhizobium meliloti* strain 1021 and watered with nitrogen-free nutrient solution, which provides conditions in which nodulation occurs. After 4 weeks of growth, plants were sampled, and fresh weights measured.

As expected, nodulating A17 plants had significantly increased fresh shoot weights compared to their uninoculated counterparts (p = 0.034) (Figure 6.2A, C). This aligns an increase in nitrogen acquisition in nodulating plants and therefore higher biomass. Though not significant, there does appear to be lower shoot biomass in the strigolactone mutants compared to R108, particularly for *ccd7-1*. This may be due to lower N_2-fixation efficiency in this mutant line. To test this, it would be interesting to determine whether *ccd7-1* and *ccd8-1* nodules have reduced nitrogenase activity g^{-1} nodule by measuring acetylene reduction, which is a proxy measure for nodule efficiency (which can be measured as reduced acetylene g^{-1} nodule). Fresh root weights were not significantly different amongst any genotype or treatment (Figure 6.2B, C). The number of *S. meliloti* nodules that formed on *ccd7-1* plants was significantly reduced compared to wildtype (p = 0.0499) (Figure 6.2D). This indicates a role for SL biosynthesis in initiation of nodulation. Though not significant, there appears to be a similar nodule number reduction on *ccd8-1*

plants. It is interesting to note that the *S. meliloti* nodules on *ccd7-1* plants were uncharacteristically small compared to those on R108 (Figure 6.2E). It has been previously noted that these small numerous nodules are ineffective (Westhoek et al., 2021). Consistently, both the *ccd7-1* and *ccd8-1* nodules appeared paler in comparison to the deep pink of the R108 nodules. This pink colouration is due to the presence of leghaemoglobin, and thus indicative of a higher N_2-fixation efficiency in R108.

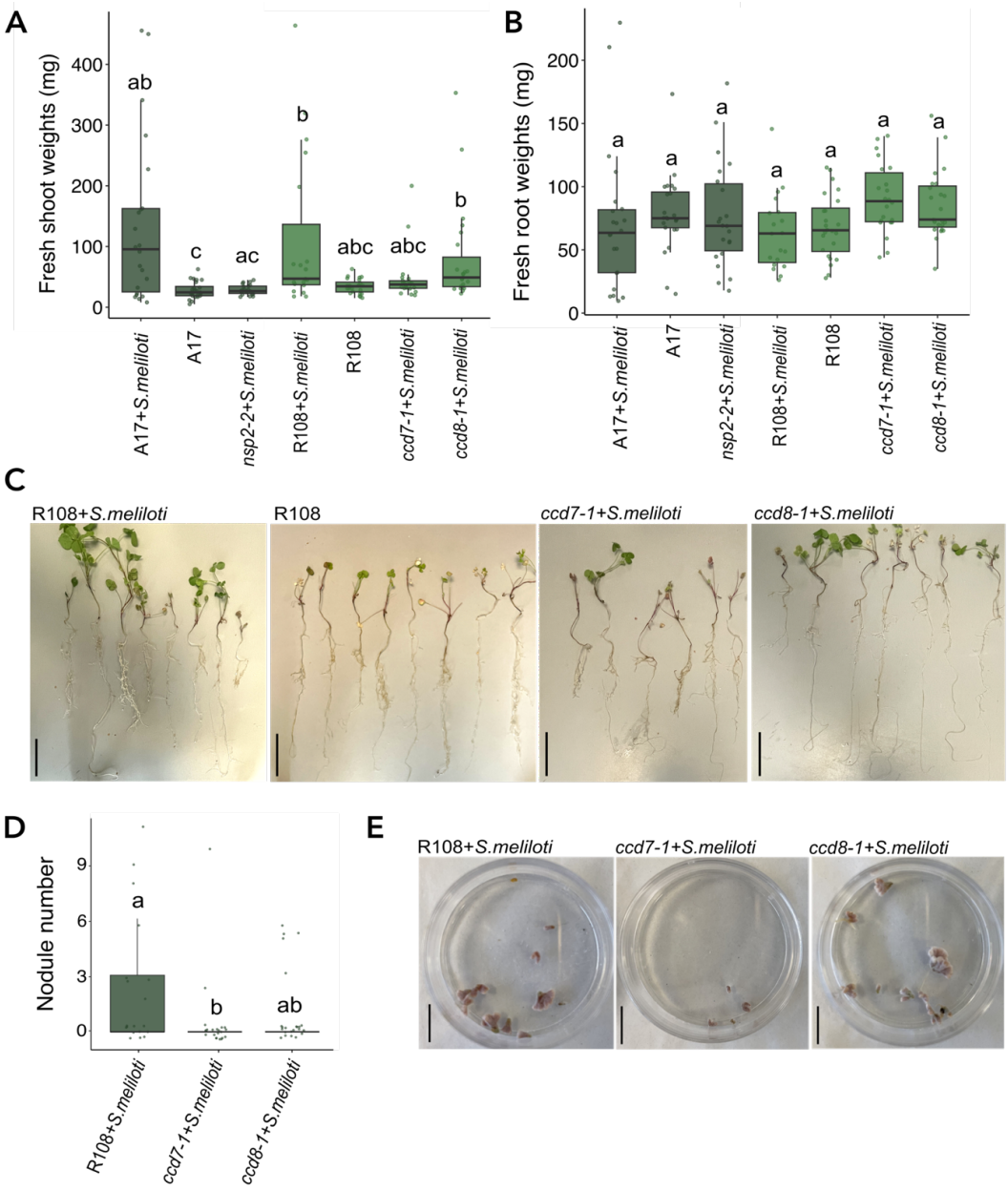

Figure 6.2 Strigolactone biosynthesis affects nodule development in *M. truncatula* Phenotypes of 4-week-old A17, *nsp2-2*, R108, *ccd7-1* and *ccd8-1* plants with or without *S. meliloti* inoculation. (A) fresh shoot weights (mg), (B) fresh root weights (mg), (C) representative images of plants, bars represent 5 cm, (D) nodule number and (E) representative images of nodules, bars represent 1 cm. Different letters indicate statistically significant difference determined by pairwise Wilcoxon rank-sum test (FDR-adjusted $p < 0.05$; n = 5–8 seedlings per biological repeat, three biological repeats).

6.2.3 Analysis of flavonoid-related gene expression and flavonoid expression in *M. truncatula* strigolactone mutants

Given the flavonoid depletion seen in *A. thaliana* strigolactone signalling mutants *max2-1* and *d14-1,* flavonoid biosynthesis and regulatory gene expression and root tip accumulation was assessed. The *M. truncatula* roots used to assess root hair development were stained with DPBA, as described previously (Section 4.2.3). There were no significant differences between fluorescence AU per micron^2 across any of the genotypes compared to their respective wildtype (Figure 6.3A, B). In addition, RT-qPCR analyses showed no significant differences in *M. truncatula CHS* and *CHI* gene expression in root tissue (Figure 6.3C and D, respectively). However, there appears to be a slight decrease in *CHI* and *CHS* expression in *ccd7-1* and *ccd8-1* compared to R108. The slight decrease in *MtCHI* and *MtCHS* expression in *ccd7-1* and *ccd8-1* matches the small but not significant changes seen in *AtCHI* and *AtCHS* in the orthologous *A. thaliana* mutants *max3-9* and *max4-1*. In *A. thaliana* the *max2* gene was found to have the most significant flavonoid differences, and thus would be of note to study. Although not available at the time of this work, a *M. truncatula max2* Tnt1 insertional mutant has since been identified (NF18521) (Li et al., 2022c). RT-qPCR of *CHI* and *CHS* should be performed in this mutant line to assess whether there is a similar correlation between strigolactone signalling and flavonoid biosynthesis in *M. truncatula max2* as there is in *A. thaliana max2-1*.

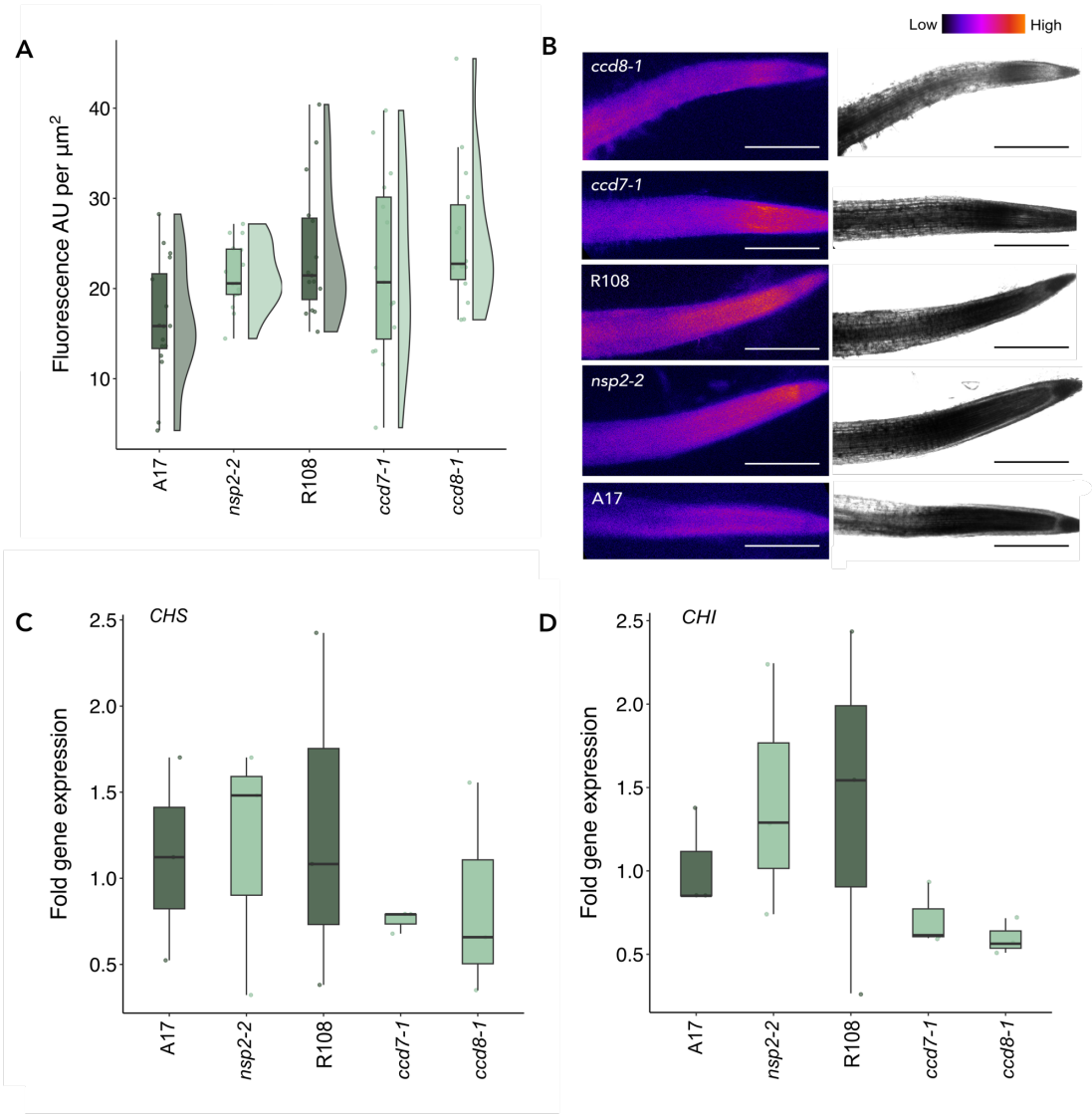

Figure 6.3 Flavonoid biosynthesis and accumulation is not significantly altered in *M. truncatula* SL biosynthesis mutant roots. 5-day-old seedling root tips were stained with 2.52 mg/mL diphenylboric acid-2-aminoethyl ester (DPBA), which results in flavonoid fluorescence when excited at 458 nm. (A) Roots were imaged, and integrated density measurements were taken from the beginning of the peak fluorescence in the elongation zone as fluorescence arbitrary units (AU) per μm^2; (B) representative images of DPBA-stained root tips, bars represent 100 μm. RT-qPCR was performed using RNA extracted from 5-day-old seedlings with primers for (C) *CHS* and (D) *CHI* (*MtTUB* was used as a reference); (n = 20 seedlings per genotype per biological repeat, three biological repeats).

6.2.4 Conclusions

The *ccd7-1 M. truncatula* SL biosynthesis mutant appears to have a mild nodulation deficiency phenotype. As root-exuded SLs have been implicated in shaping the plant microbiome, it could be that the deficiency in SLs is preventing recruitment of free-living rhizobia. In this phenotyping experiment, plant roots were directly inoculated with rhizobia. In future, adding rhizobia to the soil/growth media rather than the root would enable us to ask if the mild nodulation reduction in *ccd7-1* is due to altered rhizobial attraction. As seen in *A. thaliana* SL biosynthesis mutants, there does not appear to be an effect on flavonoid biosynthesis and accumulation in *M. truncatula* SL biosynthesis mutants. Therefore, the *ccd7-1* nodulation deficiency cannot be directly attributed to a reduction in rhizobial recruitment through altered levels of flavonoids in root exudates.

Nodules of both *ccd7-1* and *ccd8-1* mutants are paler in comparison to wildtype, suggestive of less leghaemoglobin and therefore less efficient nitrogen fixation. Given the known effect of SLs on mediating auxin flux (J. Zhang et al., 2020b), perhaps the reduction in nodulation can be attributed to lower levels of endogenous SLs, thus affecting nodule development post-initiation. If SL-deficiency leads to aborted nodule development and reduced nitrogen fixation efficiency, this could explain the paler, lighter pink appearance of *ccd7-1* and *ccd8-1* nodules compared to wildtype. As a proxy measure for nitrogen fixation efficiency, the nitrogenase activity g^{-1} nodule should be tested in both *ccd7-1, ccd8-1* and *max2* compared to wildtype, to ascertain the role of SL biosynthesis and signalling in nodule development. Given the pale nodules of the SL biosynthesis mutants, reduced nodule nitrogen fixation efficiency is expected, which would implicate SLs in nodule productivity.

Chapter 7 General discussion

7.1 New insight into how strigolactones shape plant root architecture from study in *A. thaliana* and *M. truncatula*

Plant root systems exhibit a high degree of plasticity in their ability to adapt to biotic and abiotic changes in the environment. Regulation of these developmental processes are governed by hormonal interplay. The regulation of root system developmental changes by the phytohormone strigolactone (SL) was explored through combining phenotypic studies with gene expression analyses.

The SL pathway shares signalling components with the karrikin-like ligand (KL) signalling pathway, thus root phenotypic differences were studied in both SL biosynthesis *A. thaliana* mutants and SL and KL signalling *A. thaliana* mutants in order to unravel SL- and KL-specific responses (Chapter 3 Effect of strigolactones on root system architecture and root transcriptome in *Arabidopsis thaliana*). SL biosynthesis mutants had longer and denser root hairs compared to wildtype, indicating SL regulation of root hair initiation and development (Richmond et al., 2022). When treated with the SL/KL analogue *rac*-GR24, wildtype plants had longer and denser root hairs, and shorter and fewer lateral roots. KL signalling mutants did not exhibit the same *rac*-GR24-induced lateral root reduction and SL signalling mutants did not exhibit *rac*-GR24-induced root hair enhancement. Root hair and lateral root length regulation can therefore be attributed to SL and KL signalling respectively, under these conditions. The gene expression changes underpinning these SL-specific root phenotypes were examined via RNA-sequencing analysis of SL biosynthesis and signalling mutant root tissue. The decrease in flavonoid biosynthetic genes identified in the SL/KL signalling mutant was of particular interest, in alignment with previous work suggesting that SLs promote flavonoid biosynthesis (Lazar and Goodman, 2006; Walton et al., 2016).

To determine whether the downregulation of flavonoid biosynthetic gene expression results in a decrease in flavonoid accumulation, SL/KL

signalling mutant root tips were imaged with a fluorescent flavonoid stain (Chapter 4 The strigolactone signalling pathway influences flavonoid biosynthesis in *Arabidopsis thaliana*). A significant decrease in flavonoid accumulation was seen in the SL/KL signalling mutant, as well as the SL-specific signalling mutant (Richmond et al., 2022). This aligns with a recent study that reports a MAX2- and D14-dependent mechanism for regulation of flavonol biosynthesis (Struk et al., 2022).

To further elucidate the role of SL in root development, RNA-sequencing analysis was employed to determine gene expression changes in response to the SL-specific analogue $GR24^{4DO}$ (0

Phenotypic and transcriptomic response of *Arabidopsis thaliana* to strigolactone analogue $GR24^{4DO}$. This approach revealed a large and surprising upregulation of photomorphogenesis-related genes with $GR24^{4DO}$ treatment in wildtype plants. Root architectural development is dependent on light and circadian cues (as reviewed in Lee et al., 2017), therefore this novel finding posits SLs as key integrators of these stimuli for root photomorphogenesis.

To determine whether SL signalling affects root development similarly in a leguminous plant model, roots of *M. truncatula* SL biosynthesis mutants were phenotyped (Chapter 6 Role of strigolactones in regulation of root system architecture, nodulation, and flavonoid biosynthesis in *Medicago truncatula*). Root hairs of SL biosynthetic mutants in *M. truncatula* were found to have a larger surface area per 10 mm compared to wildtype, indicating that root hairs were longer. This finding suggests a novel conserved mechanism for SL regulation of root hair development. To determine whether disruption of SL biosynthesis affects nodulation, plant biomass and nodule number was quantified in *M. truncatula* SL biosynthesis mutants. While a mild reduction in nodule number was seen in *ccd7-1*, plant biomass was not found to be significantly different compared to wildtype.

7.2 Future directions for this research

7.2.1 Characterising the role of strigolactones in root system architecture

This work provides substantial progress in elucidating the precise role of SLs in root system architecture. However, further research in this area is required to fully describe the mechanisms by which SLs affect root development. For example, the majority of the transcriptomic studies in this work analysed whole root tissue, which, although insightful, may not capture important gene expression changes occurring at an individual root zone level. For example, exclusively analysing the root differentiation zone of $GR24^{4DO}$-treated plants would reveal zone-specific gene expression changes underlying SL-regulated root hair morphogenesis. Nevertheless, these findings provide further understanding of the role of SL signalling in root system architecture.

RNA-sequencing analysis was employed in this work to identify key gene expression changes underpinning root phenotypic differences with SL biosynthesis/signalling gene mutation or exogenous SL treatment in *A. thaliana*. Given the upregulation of photomorphogenesis-related transcripts with $GR24^{4DO}$ treatment, the photoperiod-dependent stunted primary root phenotype of *max4-1* warrants further investigation since these findings raise the possibility that SLs regulate root photomorphogenesis. Further indicating a link between photoperiod and SL biosynthesis, it has been found that *MAX3* and *MAX4* transcripts are light-induced in hypocotyls (Rasmussen et al., 2012). In addition, MAX2-mediated signalling has been implicated in aboveground COP1/HY5 light-adapted development (Jia et al., 2014; Shen et al., 2012; Thussagunpanit et al., 2017), making SL involvement in root photomorphogenesis highly plausible. Given that researchers use varying daylengths and light intensities, light-dependent SL regulation may explain disparities between phenotyping studies with SL addition or SL biosynthesis gene mutants, such as the inconsistency in the *max4-1* short primary root phenotype (Villaécija-Aguilar et al., 2019).

Further work should aim to clarify the mechanism by which SLs regulate root photomorphogenesis and whether it is MAX2-dependent.

As flavonoid production is a key photoprotective, light-adaptive response, the link between SLs and photomorphogenesis is also supported through the finding that SL signalling promotes key flavonoid biosynthetic genes. Given that flavonoids exhibit lower accumulation in the root tips of SL signalling mutants, it is likely that levels of flavonoids in root exudates of these mutants are also reduced. As chemoattractants, flavonoids play a key role in cultivating a beneficial soil microbiome, thus SL signalling mutants might have reduced ability to shape their microbiome. Likewise, research using SL biosynthesis and signalling mutants has shown that SLs also impact soil microbial communities in *A. thaliana* (Carvalhais et al., 2019), *O. sativa* (Nasir et al., 2019) and *G. max* (Liu et al., 2020b). This suggests a dual function of SLs in shaping the rhizomicrobiome: directly, as an exogenous exudate, and indirectly, through modulating production of chemoattractive flavonoids. It would therefore be interesting to analyse levels of flavonoids in SL biosynthesis/signalling mutant exudates and examine the impact on rhizospheric microbial communities through metagenomic sequencing. This would provide a greater understanding as to what extent SL promotion of flavonoid production influences recruitment of the soil microbiome, and whether certain microbial functions might be specifically favoured.

7.2.2 Identifying the role of strigolactones in nodule initiation and development

As *A. thaliana* is not capable of nodulation, *M. truncatula* was used as a system to assess whether SL biosynthesis deficiency affects root symbiotic interactions with rhizobia. Root hairs were found to be significantly longer in SL biosynthesis mutants, and the *ccd7-1* line showed a mild nodule number and putative activity reduction. As early nodule development requires localised changes in root hairs in contact with rhizobia, there may be an underlying mechanism through which SLs positively regulate nodule development through modulating root hair elongation or infection thread formation. Indeed,

it has been shown that *P. sativum* SL-deficient plants form significantly fewer infection threads compared to wildtype (McAdam et al., 2017). Thus, it would be interesting to determine whether infection thread formation is also reduced in *M. truncatula* SL biosynthesis mutants. Further studies should also aim to elucidate the gene expression changes underpinning SL-mediated root hair development, perhaps through single-cell RNA-sequencing of root hair cells in *M. truncatula* SL biosynthesis mutants compared to wildtype.

7.3 Wider impact of this research

Nitrogen (N) availability is a key limiting factor to plant growth and therefore is supplemented in an agricultural setting through the use of artificial/industrially-produced nitrogenous fertilisers. Although using N fertilisers has boosted agricultural intensification and crop yields, it is both economically and environmentally costly. N fertilisers are produced through the energetically expensive Haber-Bosch process. Environmentally, surface run-off of N fertiliser pollutes surrounding soils and waterways, causing algal blooms and eutrophication. The global population is projected to exceed 9 billion by 2050, presenting the significant problem of how to provide enough food for the growing population whilst reducing reliance on N fertilisers. This is further complicated by the effects of climate change, which are increasingly negatively affecting crop yields.

Harnessing knowledge of phytohormone pathways and root development could boost crop growth and health whilst reducing N fertiliser usage. The ability of strigolactones to shape root system architecture and promote a beneficial root microbiome could be employed by applying strigolactones to soils to increase crop yield, reducing current reliance on N fertilisers. Genetically engineering non-leguminous species to be able to host symbioses with beneficial rhizobia to create self-nitrifying crops, would further diminish global need for N fertiliser application. Current research is focussed on applying nodulation machinery to non-leguminous plants, but as this work suggests, it might also be necessary to utilise phytohormones, such as strigolactones, to further improve plant nitrogen use efficiency.

Bibliography

Abe, S., Sado, A., Tanaka, K., Kisugi, T., Asami, K., Ota, S., Il Kim, H., Yoneyama, Kaori, Xie, X., Ohnishi, T., Seto, Y., Yamaguchi, S., Akiyama, K., Yoneyama, Koichi, Nomura, T., 2014. Carlactone is converted to carlactonoic acid by MAX1 in Arabidopsis and its methyl ester can directly interact with AtD14 in vitro. Proc. Natl. Acad. Sci. U. S. A. 111, 18084–18089. https://doi.org/10.1073/PNAS.1410801111

Abuauf, H., Haider, I., Jia, K.P., Ablazov, A., Mi, J., Blilou, I., Al-Babili, S., 2018. The Arabidopsis DWARF27 gene encodes an all-trans-/9-cis-β-carotene isomerase and is induced by auxin, abscisic acid and phosphate deficiency. Plant Sci. 277, 33–42. https://doi.org/10.1016/j.plantsci.2018.06.024

Akiyama, K., Matsuzaki, K., Hayashi, H., 2005. Plant sesquiterpenes induce hyphal branching in arbuscular mycorrhizal fungi. Nature 435, 824–827. https://doi.org/10.1038/nature03608

Akiyama, K., Ogasawara, S., Ito, S., Hayashi, H., 2010. Structural Requirements of Strigolactones for Hyphal Branching in AM Fungi. Plant Cell Physiol. 51, 1104–1117. https://doi.org/10.1093/pcp/pcq058

An, L., Zhou, Z., Sun, L., Yan, A., Xi, W., Yu, N., Cai, W., Chen, X., Yu, H., Schiefelbein, J., Gan, Y., 2012. A zinc finger protein gene ZFP5 integrates phytohormone signaling to control root hair development in Arabidopsis. Plant J. 72, 474–490. https://doi.org/10.1111/j.1365-313X.2012.05094.x

Ang, L.H., Chattopadhyay, S., Wei, N., Oyama, T., Okada, K., Batschauer, A., Deng, X.W., 1998. Molecular Interaction between COP1 and HY5 Defines a Regulatory Switch for Light Control of Arabidopsis Development. Mol. Cell 1, 213–222. https://doi.org/10.1016/S1097-2765(00)80022-2

Arite, T., Umehara, M., Ishikawa, S., Hanada, A., Maekawa, M., Yamaguchi, S., Kyozuka, J., 2009. *d14*, a Strigolactone-Insensitive Mutant of Rice, Shows an Accelerated Outgrowth of Tillers. Plant Cell Physiol. 50, 1416–1424. https://doi.org/10.1093/pcp/pcp091

Bagautdinova, Z.Z., Omelyanchuk, N., Tyapkin, A.V., Kovrizhnykh, V.V., Lavrekha, V.V., Zemlyanskaya, E.V., 2022. Salicylic Acid in Root Growth and Development. Int. J. Mol. Sci. 23, 2228. https://doi.org/10.3390/ijms23042228

Bainbridge, K., Sorefan, K., Ward, S., Leyser, O., 2005. Hormonally controlled expression of the Arabidopsis MAX4 shoot branching regulatory gene.

Plant J. 44, 569–580. https://doi.org/10.1111/j.1365-313X.2005.02548.x

Band, L.R., Wells, D.M., Larrieu, A., Sun, J., Middleton, A.M., French, A.P., Brunoud, G., Sato, E.M., Wilson, M.H., Péret, B., Oliva, M., Swarup, R., Sairanen, I., Parry, G., Ljung, K., Beeckman, T., Garibaldi, J.M., Estelle, M., Owen, M.R., Vissenberg, K., Hodgman, T.C., Pridmore, T.P., King, J.R., Vernoux, T., Bennett, M.J., 2012. Root gravitropism is regulated by a transient lateral auxin gradient controlled by a tipping-point mechanism. Proc. Natl. Acad. Sci. 109, 4668–4673. https://doi.org/10.1073/pnas.1201498109

Besnard, J., Sonawala, U., Maharjan, B., Collakova, E., Finlayson, S.A., Pilot, G., McDowell, J., Okumoto, S., 2021. Increased Expression of UMAMIT Amino Acid Transporters Results in Activation of Salicylic Acid Dependent Stress Response. Front. Plant Sci. 11, 606386. https://doi.org/10.3389/FPLS.2020.606386

Besserer, A., Puech-Pagès, V., Kiefer, P., Gomez-Roldan, V., Jauneau, A., Roy, S., Portais, J.C., Roux, C., Bécard, G., Séjalon-Delmas, N., 2006. Strigolactones Stimulate Arbuscular Mycorrhizal Fungi by Activating Mitochondria. PLOS Biol. 4, e226. https://doi.org/10.1371/journal.pbio.0040226

Bhoi, A., Yadu, B., Chandra, J., Keshavkant, S., 2021. Contribution of strigolactone in plant physiology, hormonal interaction and abiotic stresses. Planta 2021 2542 254, 1–21. https://doi.org/10.1007/S00425-021-03678-1

Blanvillain, R., Kim, J.H., Wu, S., Lima, A., Ow, D.W., 2009. OXIDATIVE STRESS 3 is a chromatin-associated factor involved in tolerance to heavy metals and oxidative stress. Plant J. 57, 654–665. https://doi.org/10.1111/j.1365-313X.2008.03717.x

Bolger, A.M., Lohse, M., Usadel, B., 2014. Trimmomatic: A flexible trimmer for Illumina sequence data. Bioinformatics 30, 2114–2120. https://doi.org/10.1093/bioinformatics/btu170

Bonanomi, A., Oetiker, J.H., Guggenheim, R., Boller, T., Wiemken, A., Vögeli-Lange, R., 2001. Arbuscular mycorrhiza in mini-mycorrhizotrons: first contact of *Medicago truncatula* roots with Glomus intraradices induces chalcone synthase. New Phytol. 150, 573–582. https://doi.org/10.1046/j.1469-8137.2001.00135.x

Booker, J., Auldridge, M., Wills, S., McCarty, D., Klee, H., Leyser, O., 2004. MAX3/CCD7 is a carotenoid cleavage dioxygenase required for the synthesis of a novel plant signaling molecule. Curr. Biol. CB 14, 1232–1238. https://doi.org/10.1016/j.cub.2004.06.061

Booker, J., Sieberer, T., Wright, W., Williamson, L., Willett, B., Stirnberg, P., Turnbull, C., Srinivasan, M., Goddard, P., Leyser, O., 2005. MAX1 encodes a cytochrome P450 family member that acts downstream of MAX3/4 to produce a carotenoid-derived branch-inhibiting hormone. Dev. Cell 8, 443–449. https://doi.org/10.1016/j.devcel.2005.01.009

Bouguyon, E., Perrine-Walker, F., Pervent, M., Rochette, J., Cuesta, C., Benkova, E., Martinière, A., Bach, L., Krouk, G., Gojon, A., Nacry, P., 2016. Nitrate Controls Root Development through Posttranscriptional Regulation of the NRT1.1/NPF6.3 Transporter/Sensor. Plant Physiol. 172, 1237–1248. https://doi.org/10.1104/pp.16.01047

Brady, S.M., Sarkar, S.F., Bonetta, D., McCourt, P., 2003. The ABSCISIC ACID INSENSITIVE 3 (ABI3) gene is modulated by farnesylation and is involved in auxin signaling and lateral root development in Arabidopsis. Plant J. 34, 67–75. https://doi.org/10.1046/j.1365-313X.2003.01707.x

Breakspear, A., Liu, C., Roy, S., Stacey, N., Rogers, C., Trick, M., Morieri, G., Mysore, K.S., Wen, J., Oldroyd, G.E.D., Downie, J.A., Murray, J.D., 2014. The Root Hair "Infectome" of *Medicago truncatula* Uncovers Changes in Cell Cycle Genes and Reveals a Requirement for Auxin Signaling in Rhizobial Infection. Plant Cell 26, 4680–4701. https://doi.org/10.1105/tpc.114.133496

Brumos, J., Robles, L.M., Yun, J., Vu, T.C., Jackson, S., Alonso, J.M., Stepanova, A.N., 2018. Local Auxin Biosynthesis Is a Key Regulator of Plant Development. Dev. Cell 47, 306-318.e5. https://doi.org/10.1016/j.devcel.2018.09.022

Brunetti, C., Fini, A., Sebastiani, F., Gori, A., Tattini, M., 2018. Modulation of Phytohormone Signaling: A Primary Function of Flavonoids in Plant–Environment Interactions. Front. Plant Sci. 9. https://doi.org/10.3389/fpls.2018.01042

Bu, Q., Lv, T., Shen, H., Luong, P., Wang, J., Wang, Z., Huang, Z., Xiao, L., Engineer, C., Kim, T.H., Schroeder, J.I., Huq, E., 2014. Regulation of drought tolerance by the F-box protein MAX2 in Arabidopsis. Plant Physiol. 164. https://doi.org/10.1104/pp.113.226837

Buer, C.S., Kordbacheh, F., Truong, T.T., Hocart, C.H., Djordjevic, M.A., 2013. Alteration of flavonoid accumulation patterns in transparent testa mutants disturbs auxin transport, gravity responses, and imparts long-term effects on root and shoot architecture. Planta 238, 171–189. https://doi.org/10.1007/S00425-013-1883-3/

Buer, C.S., Muday, G.K., 2004. The *transparent testa4* Mutation Prevents Flavonoid Synthesis and Alters Auxin Transport and the Response of

Arabidopsis Roots to Gravity and Light. Plant Cell 16, 1191–1205. https://doi.org/10.1105/TPC.020313

Bulgarelli, D., Rott, M., Schlaeppi, K., Ver Loren van Themaat, E., Ahmadinejad, N., Assenza, F., Rauf, P., Huettel, B., Reinhardt, R., Schmelzer, E., Peplies, J., Gloeckner, F.O., Amann, R., Eickhorst, T., Schulze-Lefert, P., 2012. Revealing structure and assembly cues for Arabidopsis root-inhabiting bacterial microbiota. Nature 488, 91–95. https://doi.org/10.1038/nature11336

Bythell-Douglas, R., Rothfels, C.J., Stevenson, D.W.D., Graham, S.W., Wong, G.K.S., Nelson, D.C., Bennett, T., 2017. Evolution of strigolactone receptors by gradual neo-functionalization of KAI2 paralogues. BMC Biol. 15, 52. https://doi.org/10.1186/s12915-017-0397-z

Cai, X.T., Xu, P., Zhao, P.X., Liu, R., Yu, L.H., Xiang, C.B., 2014. Arabidopsis ERF109 mediates cross-talk between jasmonic acid and auxin biosynthesis during lateral root formation. Nat. Commun. 5, 5833. https://doi.org/10.1038/ncomms6833

Carbonnel, S., Das, D., Varshney, K., Kolodziej, M.C., Villaécija-Aguilar, J.A., Gutjahr, C., 2020. The karrikin signaling regulator SMAX1 controls *Lotus japonicus* root and root hair development by suppressing ethylene biosynthesis. Proc. Natl. Acad. Sci. U. S. A. 117, 21757–21765. https://doi.org/10.1073/pnas.2006111117

Carbonnel, S., Torabi, S., Gutjahr, C., 2021. MAX2-independent transcriptional responses to *rac*-GR24 in *Lotus japonicus roots*. Plant Signal. Behav. 16, 1840852. https://doi.org/10.1080/15592324.2020.1840852

Carvalhais, L.C., Rincon-Florez, V.A., Brewer, P.B., Beveridge, C.A., Dennis, P.G., Schenk, P.M., 2019. The ability of plants to produce strigolactones affects rhizosphere community composition of fungi but not bacteria. Rhizosphere 9, 18–26. https://doi.org/10.1016/j.rhisph.2018.10.002

Cavalier, D.M., Lerouxel, O., Neumetzler, L., Yamauchi, K., Reinecke, A., Freshour, G., Zabotina, O.A., Hahn, M.G., Burgert, I., Pauly, M., Raikhel, N.V., Keegstra, K., 2008. Disrupting Two *Arabidopsis thaliana* Xylosyltransferase Genes Results in Plants Deficient in Xyloglucan, a Major Primary Cell Wall Component. Plant Cell 20, 1519–1537. https://doi.org/10.1105/TPC.108.059873

Chaiwanon, J., Wang, Z.Y., 2015. Spatiotemporal Brassinosteroid Signaling and Antagonism with Auxin Pattern Stem Cell Dynamics in Arabidopsis Roots. Curr. Biol. 25, 1031–1042. https://doi.org/10.1016/j.cub.2015.02.046

Chang, K.N., Zhong, S., Weirauch, M.T., Hon, G., Pelizzola, M., Li, H., Huang, S.C., Schmitz, R.J., Urich, M.A., Kuo, D., Nery, J.R., Qiao, H., Yang, A., Jamali, A., Chen, H., Ideker, T., Ren, B., Bar-Joseph, Z., Hughes, T.R., Ecker, J.R., 2013. Temporal transcriptional response to ethylene gas drives growth hormone cross-regulation in Arabidopsis. eLife 2, e00675. https://doi.org/10.7554/eLife.00675

Chen, Q., Dai, X., De-Paoli, H., Cheng, Y., Takebayashi, Y., Kasahara, H., Kamiya, Y., Zhao, Y., 2014. Auxin Overproduction in Shoots Cannot Rescue Auxin Deficiencies in Arabidopsis Roots. Plant Cell Physiol. 55, 1072–1079. https://doi.org/10.1093/pcp/pcu039

Chen, Q., Sun, J., Zhai, Q., Zhou, W., Qi, L., Xu, L., Wang, B., Chen, R., Jiang, H., Qi, J., Li, X., Palme, K., Li, C., 2011. The Basic Helix-Loop-Helix Transcription Factor MYC2 Directly Represses PLETHORA Expression during Jasmonate-Mediated Modulation of the Root Stem Cell Niche in Arabidopsis. Plant Cell 23, 3335–3352. https://doi.org/10.1105/tpc.111.089870

Chen, R., Jiang, H., Li, L., Zhai, Q., Qi, L., Zhou, W., Liu, X., Li, H., Zheng, W., Sun, J., Li, C., 2012. The Arabidopsis Mediator Subunit MED25 Differentially Regulates Jasmonate and Abscisic Acid Signaling through Interacting with the MYC2 and ABI5 Transcription Factors. Plant Cell 24, 2898–2916. https://doi.org/10.1105/tpc.112.098277

Cheng, Y., Zhu, W., Chen, Y., Ito, S., Asami, T., Wang, X., 2014. Brassinosteroids control root epidermal cell fate via direct regulation of a MYB-bHLH-WD40 complex by GSK3-like kinases. eLife 3, e02525. https://doi.org/10.7554/eLife.02525

Chevalier, F., Nieminen, K., Sánchez-Ferrero, J.C., Rodríguez, M.L., Chagoyen, M., Hardtke, C.S., Cubas, P., 2014. Strigolactone promotes degradation of DWARF14, an α/β hydrolase essential for strigolactone signaling in Arabidopsis. Plant Cell 26, 1134–1150. https://doi.org/10.1105/TPC.114.122903

Choi, J., Lee, T., Cho, J., Servante, E.K., Pucker, B., Summers, W., Bowden, S., Rahimi, M., An, K., An, G., Bouwmeester, H.J., Wallington, E.J., Oldroyd, G., Paszkowski, U., 2020. The negative regulator SMAX1 controls mycorrhizal symbiosis and strigolactone biosynthesis in rice. Nat. Commun. 11, 2114. https://doi.org/10.1038/s41467-020-16021-1

Cook, C.E., Whichard, L.P., Wall, M., Egley, G.H., Coggon, P., Luhan, P.A., McPhail, A.T., 1972. Germination stimulants. II. Structure of strigol, a potent seed germination stimulant for witchweed (*Striga lutea*). J. Am. Chem. Soc. 94, 6198–6199. https://doi.org/10.1021/ja00772a048

De Cuyper, C., Fromentin, J., Yocgo, R.E., De Keyser, A., Guillotin, B., Kunert, K., Boyer, F.D., Goormachtig, S., 2015. From lateral root density to nodule number, the strigolactone analogue GR24 shapes the root architecture of *Medicago truncatula*. J. Exp. Bot. 66, 137–146. https://doi.org/10.1093/jxb/eru404

De Simone, S., Oka, Y., Inoue, Y., 2000. Effect of Light on Root Hair Formation in Arabidopsis thaliana Phytochrome-Deficient Mutants. J. Plant Res. 113, 63–69. https://doi.org/10.1007/PL00013917

De Smet, I., Vassileva, V., De Rybel, B., Levesque, M.P., Grunewald, W., Van Damme, D., Van Noorden, G., Naudts, M., Van Isterdael, G., De Clercq, R., Wang, J.Y., Meuli, N., Vanneste, S., Friml, J., Hilson, P., Jürgens, G., Ingram, G.C., Inzé, D., Benfey, P.N., Beeckman, T., 2008. Receptor-like kinase ACR4 restricts formative cell divisions in the Arabidopsis root. Science 322, 594–597. https://doi.org/10.1126/science.1160158

Dobin, A., Davis, C.A., Schlesinger, F., Drenkow, J., Zaleski, C., Jha, S., Batut, P., Chaisson, M., Gingeras, T.R., 2013. STAR: Ultrafast universal RNA-seq aligner. Bioinformatics 29, 15–21. https://doi.org/10.1093/bioinformatics/bts635

Dubrovsky, J.G., Sauer, M., Napsucialy-Mendivil, S., Ivanchenko, M.G., Friml, J., Shishkova, S., Celenza, J., Benková, E., 2008. Auxin acts as a local morphogenetic trigger to specify lateral root founder cells. Proc. Natl. Acad. Sci. 105, 8790–8794. https://doi.org/10.1073/pnas.0712307105

Dunand, C., Crèvecoeur, M., Penel, C., 2007. Distribution of superoxide and hydrogen peroxide in Arabidopsis root and their influence on root development: possible interaction with peroxidases. New Phytol. 174, 332–341. https://doi.org/10.1111/j.1469-8137.2007.01995.x

Fan, X.Y., Sun, Yu, Cao, D.M., Bai, M.Y., Luo, X.M., Yang, H.J., Wei, C.Q., Zhu, S.W., Sun, Ying, Chong, K., Wang, Z.Y., 2012. BZS1, a B-box protein, promotes photomorphogenesis downstream of both brassinosteroid and light signaling pathways. Mol. Plant 5, 591–600. https://doi.org/10.1093/mp/sss041

Feng, Y., Xu, P., Li, B., Li, P., Wen, X., An, F., Gong, Y., Xin, Y., Zhu, Z., Wang, Y., Guo, H., 2017. Ethylene promotes root hair growth through coordinated EIN3/EIL1 and RHD6/RSL1 activity in Arabidopsis. Proc. Natl. Acad. Sci. 114, 13834–13839. https://doi.org/10.1073/pnas.1711723115

Feng, Z., Liang, X., Tian, H., Watanabe, Y., Nguyen, K.H., Tran, C.D., Abdelrahman, M., Xu, K., Mostofa, M.G., Ha, C.V., Mochida, K., Tian, C., Tanaka, M., Seki, M., Liang, Z., Miao, Y., Tran, L.S.P., Li, W., 2022.

SUPPRESSOR of MAX2 1 (SMAX1) and SMAX1-LIKE2 (SMXL2) Negatively Regulate Drought Resistance in *Arabidopsis thaliana*. Plant Cell Physiol. 63, 1900–1913. https://doi.org/10.1093/pcp/pcac080

Flematti, G.R., Scaffidi, A., Waters, M.T., Smith, S.M., 2016. Stereospecificity in strigolactone biosynthesis and perception. Planta 243, 1361–1373. https://doi.org/10.1007/s00425-016-2523-5

Foo, E., Davies, N.W., 2011. Strigolactones promote nodulation in pea. Planta 234, 1073–1081. https://doi.org/10.1007/s00425-011-1516-7

Foo, E., Yoneyama, K., Hugill, C.J., Quittenden, L.J., Reid, J.B., 2013. Strigolactones and the Regulation of Pea Symbioses in Response to Nitrate and Phosphate Deficiency. Mol. Plant 6, 76–87. https://doi.org/10.1093/mp/sss115

Fu, X., Harberd, N.P., 2003. Auxin promotes Arabidopsis root growth by modulating gibberellin response. Nature 421, 740–743. https://doi.org/10.1038/nature01387

Galway, M.E., Masucci, J.D., Lloyd, A.M., Walbot, V., Davis, R.W., Schiefelbein, J.W., 1994. The TTG gene is required to specify epidermal cell fate and cell patterning in the Arabidopsis root. Dev. Biol. 166, 740–754. https://doi.org/10.1006/dbio.1994.1352

Gayomba, S.R., Muday, G.K., 2020. Flavonols regulate root hair development by modulating accumulation of reactive oxygen species in the root epidermis. Development 147, dev185819. https://doi.org/10.1242/dev.185819

Geisler, M.M., 2021. A Retro-Perspective on Auxin Transport. Front. Plant Sci. 12. https://doi.org/10.3389/fpls.2021.756968

Gifford, M.L., Dean, A., Gutierrez, R.A., Coruzzi, G.M., Birnbaum, K.D., 2008. Cell-specific nitrogen responses mediate developmental plasticity. Proc. Natl. Acad. Sci. U. S. A. 105, 803–808. https://doi.org/10.1073/pnas.0709559105

Gomez-Roldan, V., Fermas, S., Brewer, P.B., Puech-Pagès, V., Dun, E.A., Pillot, J.P., Letisse, F., Matusova, R., Danoun, S., Portais, J.C., Bouwmeester, H., Bécard, G., Beveridge, C.A., Rameau, C., Rochange, S.F., 2008. Strigolactone inhibition of shoot branching. Nature 455, 189–194. https://doi.org/10.1038/nature07271

González-García, M.P., Vilarrasa-Blasi, J., Zhiponova, M., Divol, F., Mora-García, S., Russinova, E., Caño-Delgado, A.I., 2011. Brassinosteroids control meristem size by promoting cell cycle progression in Arabidopsis roots. Development 138, 849–859. https://doi.org/10.1242/dev.057331

Gonzalez-Rizzo, S., Crespi, M., Frugier, F., 2006. The *Medicago truncatula* CRE1 Cytokinin Receptor Regulates Lateral Root Development and Early Symbiotic Interaction with *Sinorhizobium meliloti*. Plant Cell 18, 2680–2693. https://doi.org/10.1105/tpc.106.043778

Guo, D., Liang, J., Li, L., 2009. Abscisic acid (ABA) inhibition of lateral root formation involves endogenous ABA biosynthesis in *Arachis hypogaea L.* Plant Growth Regul. 58, 173–179. https://doi.org/10.1007/s10725-009-9365-0

Gutjahr, C., Gobbato, E., Choi, J., Riemann, M., Johnston, M.G., Summers, W., Carbonnel, S., Mansfield, C., Yang, S.Y., Nadal, M., Acosta, I., Takano, M., Jiao, W.B., Schneeberger, K., Kelly, K.A., Paszkowski, U., 2015. Rice perception of symbiotic arbuscular mycorrhizal fungi requires the karrikin receptor complex. Science 350, 1521–1524. https://doi.org/10.1126/science.aac9715

Ha, C.V., Leyva-González, M.A., Osakabe, Y., Tran, U.T., Nishiyama, R., Watanabe, Y., Tanaka, M., Seki, M., Yamaguchi, S., Dong, N.V., Yamaguchi-Shinozaki, K., Shinozaki, K., Herrera-Estrella, L., Tran, L.S.P., 2014. Positive regulatory role of strigolactone in plant responses to drought and salt stress. Proc. Natl. Acad. Sci. 111, 851–856. https://doi.org/10.1073/pnas.1322135111

Haider, I., Andreo-Jimenez, B., Bruno, M., Bimbo, A., Floková, K., Abuauf, H., Ntui, V.O., Guo, X., Charnikhova, T., Al-Babili, S., Bouwmeester, H.J., Ruyter-Spira, C., 2018. The interaction of strigolactones with abscisic acid during the drought response in rice. J. Exp. Bot. 69, 2403–2414. https://doi.org/10.1093/jxb/ery089

Hamann, T., Mayer, U., Jurgens, G., 1999. The auxin-insensitive bodenlos mutation affects primary root formation and apical-basal patterning in the Arabidopsis embryo. Development 126, 1387–1395. https://doi.org/10.1242/dev.126.7.1387

Hayama, R., Sarid-Krebs, L., Richter, R., Fernández, V., Jang, S., Coupland, G., 2017. PSEUDO RESPONSE REGULATORs stabilize CONSTANS protein to promote flowering in response to day length. EMBO J. 36, 904–918. https://doi.org/10.15252/embj.201693907

He, D., Singh, S.K., Peng, L., Kaushal, R., Vílchez, J.I., Shao, C., Wu, X., Zheng, S., Morcillo, R.J.L., Paré, P.W., Zhang, H., 2022. Flavonoid-attracted Aeromonas sp. from the Arabidopsis root microbiome enhances plant dehydration resistance. ISME J. 16, 2622–2632. https://doi.org/10.1038/s41396-022-01288-7

Heckmann, A.B., Lombardo, F., Miwa, H., Perry, J.A., Bunnewell, S., Parniske, M., Wang, T.L., Downie, J.A., 2006. *Lotus japonicus* nodulation

requires two GRAS domain regulators, one of which is functionally conserved in a non-legume. Plant Physiol. 142, 1739–1750. https://doi.org/10.1104/pp.106.089508

Heller, J., Tudzynski, P., 2011. Reactive oxygen species in phytopathogenic fungi: signaling, development, and disease. Annu. Rev. Phytopathol. 49, 369–390. https://doi.org/10.1146/annurev-phyto-072910-095355

Hiltenbrand, R., Thomas, J., McCarthy, H., Dykema, K.J., Spurr, A., Newhart, H., Winn, M.E., Mukherjee, A., 2016. A Developmental and Molecular View of Formation of Auxin-Induced Nodule-Like Structures in Land Plants. Front. Plant Sci. 7. https://doi.org/10.3389/fpls.2016.01692

Hirsch, S., Kim, J., Muñoz, A., Heckmann, A.B., Downie, J.A., Oldroyd, G.E.D., 2009. GRAS Proteins Form a DNA Binding Complex to Induce Gene Expression during Nodulation Signaling in *Medicago truncatula*. Plant Cell 21, 545–557. https://doi.org/10.1105/tpc.108.064501

Holbrook-Smith, D., Toh, S., Tsuchiya, Y., McCourt, P., 2016. Small-molecule antagonists of germination of the parasitic plant *Striga hermonthica*. Nat. Chem. Biol. 12, 724–729. https://doi.org/10.1038/nchembio.2129

Hou, J., Zheng, X., Ren, R., Shi, Q., Xiao, H., Chen, Z., Yue, M., Wu, Y., Hou, H., Li, L., 2022. The histone deacetylase 1/GSK3/SHAGGY-like kinase 2/BRASSINAZOLE-RESISTANT 1 module controls lateral root formation in rice. Plant Physiol. 189, 858–873. https://doi.org/10.1093/plphys/kiac015

Ioio, R.D., Linhares, F.S., Scacchi, E., Casamitjana-Martinez, E., Heidstra, R., Costantino, P., Sabatini, S., 2007. Cytokinins Determine Arabidopsis Root-Meristem Size by Controlling Cell Differentiation. Curr. Biol. 17, 678–682. https://doi.org/10.1016/j.cub.2007.02.047

Iqbal, N., Khan, N.A., Ferrante, A., Trivellini, A., Francini, A., Khan, M.I.R., 2017. Ethylene role in plant growth, development and senescence: interaction with other phytohormones. Front. Plant Sci. 8, 475. https://doi.org/10.3389/FPLS.2017.00475/BIBTEX

Jia, K.P., Luo, Q., He, S.B., Lu, X.D., Yang, H.Q., 2014. Strigolactone-Regulated Hypocotyl Elongation Is Dependent on Cryptochrome and Phytochrome Signaling Pathways in Arabidopsis. Mol. Plant 7, 528–540. https://doi.org/10.1093/mp/sst093

Jia, Z., Giehl, R.F.H., von Wirén, N., 2022. Nutrient–hormone relations: Driving root plasticity in plants. Mol. Plant 15, 86–103. https://doi.org/10.1016/j.molp.2021.12.004

Jia, Z., Giehl, R.F.H., von Wirén, N., 2020. The Root Foraging Response under Low Nitrogen Depends on DWARF1-Mediated Brassinosteroid

Biosynthesis. Plant Physiol. 183, 998–1010. https://doi.org/10.1104/pp.20.00440

Jiang, L., Matthys, C., Marquez-Garcia, B., De Cuyper, C., Smet, L., De Keyser, A., Boyer, F.D., Beeckman, T., Depuydt, S., Goormachtig, S., 2016. Strigolactones spatially influence lateral root development through the cytokinin signaling network. J. Exp. Bot. 67, 379–389. https://doi.org/10.1093/jxb/erv478

Jiang, W., Yin, Q., Wu, R., Zheng, G., Liu, J., Dixon, R.A., Pang, Y., 2015. Role of a chalcone isomerase-like protein in flavonoid biosynthesis in *Arabidopsis thaliana*. J. Exp. Bot. 66, 7165–7179. https://doi.org/10.1093/jxb/erv413

Jin, J., Tian, F., Yang, D.C., Meng, Y.Q., Kong, L., Luo, J., Gao, G., 2017. PlantTFDB 4.0: toward a central hub for transcription factors and regulatory interactions in plants. Nucleic Acids Res. 45, D1040–D1045. https://doi.org/10.1093/NAR/GKW982

Jung, J., McCouch, S., 2013. Getting to the roots of it: Genetic and hormonal control of root architecture. Front. Plant Sci. 4. https://doi.org/10.3389/fpls.2013.00186

Kaló, P., Gleason, C., Edwards, A., Marsh, J., Mitra, R.M., Hirsch, S., Jakab, J., Sims, S., Long, S.R., Rogers, J., Kiss, G.B., Downie, J.A., Oldroyd, G.E.D., 2005. Nodulation Signaling in Legumes Requires NSP2, a Member of the GRAS Family of Transcriptional Regulators. Science 308, 1786 LP – 1789. https://doi.org/10.1126/science.1110951

Kapulnik, Y., Delaux, P.M., Resnick, N., Mayzlish-Gati, E., Wininger, S., Bhattacharya, C., Séjalon-Delmas, N., Combier, J.P., Bécard, G., Belausov, E., Beeckman, T., Dor, E., Hershenhorn, J., Koltai, H., 2011a. Strigolactones affect lateral root formation and root-hair elongation in Arabidopsis. Planta 233, 209–216. https://doi.org/10.1007/s00425-010-1310-y

Kapulnik, Y., Resnick, N., Mayzlish-Gati, E., Kaplan, Y., Wininger, S., Hershenhorn, J., Koltai, H., 2011b. Strigolactones interact with ethylene and auxin in regulating root-hair elongation in Arabidopsis. J. Exp. Bot. 62, 2915–2924. https://doi.org/10.1093/jxb/erq464

Ke, M., Ma, Z., Wang, D., Sun, Y., Wen, C., Huang, D., Chen, Z., Yang, L., Tan, S., Li, R., Friml, J., Miao, Y., Chen, X., 2021. Salicylic acid regulates PIN2 auxin transporter hyperclustering and root gravitropic growth via Remorin-dependent lipid nanodomain organisation in *Arabidopsis thaliana*. New Phytol. 229, 963–978. https://doi.org/10.1111/nph.16915

Kim, J.Y., Park, Y.J., Lee, J.H., Park, C.M., 2022. SMAX1 Integrates Karrikin and Light Signals into GA-Mediated Hypocotyl Growth during Seedling Establishment. Plant Cell Physiol. 63, 932–943. https://doi.org/10.1093/pcp/pcac055

Kobae, Y., Kameoka, H., Sugimura, Y., Saito, K., Ohtomo, R., Fujiwara, T., Kyozuka, J., 2018. Strigolactone Biosynthesis Genes of Rice are Required for the Punctual Entry of Arbuscular Mycorrhizal Fungi into the Roots. Plant Cell Physiol. 59, 544–553. https://doi.org/10.1093/pcp/pcy001

Kohlen, W., Charnikhova, T., Liu, Q., Bours, R., Domagalska, M.A., Beguerie, S., Verstappen, F., Leyser, O., Bouwmeester, H., Ruyter-Spira, C., 2011. Strigolactones Are Transported through the Xylem and Play a Key Role in Shoot Architectural Response to Phosphate Deficiency in Nonarbuscular Mycorrhizal Host Arabidopsis. Plant Physiol. 155, 974–987. https://doi.org/10.1104/pp.110.164640

Korenblum, E., Dong, Y., Szymanski, J., Panda, S., Jozwiak, A., Massalha, H., Meir, S., Rogachev, I., Aharoni, A., 2020. Rhizosphere microbiome mediates systemic root metabolite exudation by root-to-root signaling. Proc. Natl. Acad. Sci. 117, 3874–3883. https://doi.org/10.1073/pnas.1912130117

Krouk, G., Lacombe, B., Bielach, A., Perrine-Walker, F., Malinska, K., Mounier, E., Hoyerova, K., Tillard, P., Leon, S., Ljung, K., Zazimalova, E., Benkova, E., Nacry, P., Gojon, A., 2010. Nitrate-Regulated Auxin Transport by NRT1.1 Defines a Mechanism for Nutrient Sensing in Plants. Dev. Cell 18, 927–937. https://doi.org/10.1016/j.devcel.2010.05.008

Kumari, S., Yadav, S., Patra, D., Singh, S., Sarkar, A.K., Panigrahi, K.C.S., 2019. Uncovering the molecular signature underlying the light intensity-dependent root development in *Arabidopsis thaliana*. BMC Genomics 20, 596. https://doi.org/10.1186/s12864-019-5933-5

Kusajima, M., Fujita, M., Soudthedlath, K., Nakamura, H., Yoneyama, K., Nomura, T., Akiyama, K., Maruyama-Nakashita, A., Asami, T., Nakashita, H., 2022. Strigolactones Modulate Salicylic Acid-Mediated Disease Resistance in *Arabidopsis thaliana*. Int. J. Mol. Sci. 23, 5246. https://doi.org/10.3390/ijms23095246

Laplaze, L., Benkova, E., Casimiro, I., Maes, L., Vanneste, S., Swarup, R., Weijers, D., Calvo, V., Parizot, B., Herrera-Rodriguez, M.B., Offringa, R., Graham, N., Doumas, P., Friml, J., Bogusz, D., Beeckman, T., Bennett, M., 2007. Cytokinins Act Directly on Lateral Root Founder

Cells to Inhibit Root Initiation. Plant Cell 19, 3889–3900. https://doi.org/10.1105/tpc.107.055863

Larose, G., Chênevert, R., Moutoglis, P., Gagné, S., Piché, Y., Vierheilig, H., 2002. Flavonoid levels in roots of *Medicago sativa* are modulated by the developmental stage of the symbiosis and the root colonizing arbuscular mycorrhizal fungus. J. Plant Physiol. 159, 1329–1339. https://doi.org/10.1078/0176-1617-00896

Lauressergues, D., André, O., Peng, J., Wen, J., Chen, R., Ratet, P., Tadege, M., Mysore, K.S., Rochange, S.F., 2015. Strigolactones contribute to shoot elongation and to the formation of leaf margin serrations in *Medicago truncatula* R108. J. Exp. Bot. 66, 1237–1244. https://doi.org/10.1093/jxb/eru471

Lazar, G., Goodman, H.M., 2006. MAX1, a regulator of the flavonoid pathway, controls vegetative axillary bud outgrowth in Arabidopsis. Proc. Natl. Acad. Sci. U. S. A. 103, 472–476. https://doi.org/10.1073/pnas.0509463102

Lee, H.J., Park, Y.J., Ha, J.H., Baldwin, I.T., Park, C.M., 2017. Multiple Routes of Light Signaling during Root Photomorphogenesis. Trends Plant Sci. 22, 803–812. https://doi.org/10.1016/j.tplants.2017.06.009

Lee, M.M., Schiefelbein, J., 2002. Cell Pattern in the Arabidopsis Root Epidermis Determined by Lateral Inhibition with Feedback. Plant Cell 14, 611–618. https://doi.org/10.1105/tpc.010434

Lee, M.M., Schiefelbein, J., 1999. WEREWOLF, a MYB-related protein in Arabidopsis, is a position-dependent regulator of epidermal cell patterning. Cell 99, 473–483. https://doi.org/10.1016/s0092-8674(00)81536-6

Lee, S.B., Jung, S.J., Go, Y.S., Kim, H.U., Kim, J.K., Cho, H.J., Park, O.K., Suh, M.C., 2009. Two Arabidopsis 3-ketoacyl CoA synthase genes, KCS20 and KCS2/DAISY, are functionally redundant in cuticular wax and root suberin biosynthesis, but differentially controlled by osmotic stress. Plant J. 60, 462–475. https://doi.org/10.1111/J.1365-313X.2009.03973.X

Legris, M., Ince, Y.Ç., Fankhauser, C., 2019. Molecular mechanisms underlying phytochrome-controlled morphogenesis in plants. Nat. Commun. 10, 5219. https://doi.org/10.1038/s41467-019-13045-0

Lewis, D.R., Olex, A.L., Lundy, S.R., Turkett, W.H., Fetrow, J.S., Muday, G.K., 2013. A Kinetic Analysis of the Auxin Transcriptome Reveals Cell Wall Remodeling Proteins That Modulate Lateral Root Development in

Arabidopsis. Plant Cell 25, 3329–3346. https://doi.org/10.1105/tpc.113.114868

Li, C., Lu, S., 2014. Genome-wide characterization and comparative analysis of R2R3-MYB transcription factors shows the complexity of MYB-associated regulatory networks in *Salvia miltiorrhiza*. BMC Genomics 15, 277. https://doi.org/10.1186/1471-2164-15-277

Li, C., Yu, W., Xu, J., Lu, X., Liu, Y., 2022a. Anthocyanin Biosynthesis Induced by MYB Transcription Factors in Plants. Int. J. Mol. Sci. 23, 11701. https://doi.org/10.3390/ijms231911701

Li, P., Dong, Q., Ge, S., He, X., Verdier, J., Li, D., Zhao, J., 2016a. Metabolic engineering of proanthocyanidin production by repressing the isoflavone pathways and redirecting anthocyanidin precursor flux in legume. Plant Biotechnol. J. 14, 1604–1618. https://doi.org/10.1111/pbi.12524

Li, Q., Martín-Fontecha, E.S., Khosla, A., White, A.R.F., Chang, S., Cubas, P., Nelson, D.C., 2022b. The strigolactone receptor D14 targets SMAX1 for degradation in response to GR24 treatment and osmotic stress. Plant Commun. 3, 100303. https://doi.org/10.1016/j.xplc.2022.100303

Li, S., Chen, L., Li, Y., Yao, R., Wang, F., Yang, M., Gu, M., Nan, F., Xie, D., Yan, J., 2016b. Effect of GR24 Stereoisomers on Plant Development in Arabidopsis. Mol. Plant 9, 1432–1435. https://doi.org/10.1016/j.molp.2016.06.012

Li, W., Gupta, A., Tian, H., Nguyen, K.H., Tran, C.D., Watanabe, Y., Tian, C., Li, K., Yang, Y., Guo, J., Luo, Y., Miao, Y., Phan Tran, L.S., 2020a. Different strategies of strigolactone and karrikin signals in regulating the resistance of *Arabidopsis thaliana* to water-deficit stress. Plant Signal. Behav. 15, 1789321. https://doi.org/10.1080/15592324.2020.1789321

Li, W., Nguyen, K.H., Chu, H.D., Ha, C.V., Watanabe, Y., Osakabe, Y., Leyva-González, M.A., Sato, M., Toyooka, K., Voges, L., Tanaka, M., Mostofa, M.G., Seki, M., Seo, M., Yamaguchi, S., Nelson, D.C., Tian, C., Herrera-Estrella, L., Tran, L.S.P., 2017a. The karrikin receptor KAI2 promotes drought resistance in *Arabidopsis thaliana*. PLOS Genet. 13, e1007076. https://doi.org/10.1371/JOURNAL.PGEN.1007076

Li, W., Nguyen, K.H., Chu, H.D., Watanabe, Y., Osakabe, Y., Sato, M., Toyooka, K., Seo, M., Tian, L., Tian, C., Yamaguchi, S., Tanaka, M., Seki, M., Tran, L.S.P., 2020b. Comparative functional analyses of DWARF14 and KARRIKIN INSENSITIVE 2 in drought adaptation of *Arabidopsis thaliana*. Plant J. 103, 111–127. https://doi.org/10.1111/tpj.14712

Li, W., Nguyen, K.H., Tran, C.D., Watanabe, Y., Tian, C., Yin, X., Li, K., Yang, Y., Guo, J., Miao, Y., Yamaguchi, S., Tran, L.S.P., 2020c. Negative Roles of Strigolactone-Related SMXL6, 7 and 8 Proteins in Drought Resistance in Arabidopsis. Biomolecules 10, 607. https://doi.org/10.3390/biom10040607

Li, X., Chen, L., Forde, B.G., Davies, W.J., 2017b. The Biphasic Root Growth Response to Abscisic Acid in Arabidopsis Involves Interaction with Ethylene and Auxin Signalling Pathways. Front. Plant Sci. 8, 1493. https://doi.org/10.3389/fpls.2017.01493

Li, X.R., Sun, J., Albinsky, D., Zarrabian, D., Hull, R., Lee, T., Jarratt-Barnham, E., Chiu, C.H., Jacobsen, A., Soumpourou, E., Albanese, A., Kohlen, W., Luginbuehl, L.H., Guillotin, B., Lawrensen, T., Lin, H., Murray, J., Wallington, E., Harwood, W., Choi, J., Paszkowski, U., Oldroyd, G.E.D., 2022c. Nutrient regulation of lipochitooligosaccharide recognition in plants via NSP1 and NSP2. Nat. Commun. 13, 6421. https://doi.org/10.1038/s41467-022-33908-3

Li, Y., Tian, B., Wang, Y., Wang, J., Zhang, Hongbo, Wang, L., Sun, G., Yu, Y., Zhang, Huihui, 2022d. The Transcription Factor MYB37 Positively Regulates Photosynthetic Inhibition and Oxidative Damage in Arabidopsis Leaves Under Salt Stress. Front. Plant Sci. 13. https://doi.org/10.3389/fpls.2022.943153

Liang, T., Shi, C., Peng, Y., Tan, H., Xin, P., Yang, Y., Wang, F., Li, X., Chu, J., Huang, J., Yin, Y., Liu, H., 2020. Brassinosteroid-activated BRI1-EMS-SUPPRESSOR 1 inhibits flavonoid biosynthesis and coordinates growth and UV-B stress responses in plants. Plant Cell 32, 3224–3239. https://doi.org/10.1105/tpc.20.00048

Lin, Q., Ohashi, Y., Kato, M., Tsuge, T., Gu, H., Qu, L.J., Aoyama, T., 2015. GLABRA2 Directly Suppresses Basic Helix-Loop-Helix Transcription Factor Genes with Diverse Functions in Root Hair Development. Plant Cell 27, 2894–2906. https://doi.org/10.1105/tpc.15.00607

Liu, B., Wu, J., Yang, S., Schiefelbein, J., Gan, Y., 2020a. Nitrate regulation of lateral root and root hair development in plants. J. Exp. Bot. 71, 4405–4414. https://doi.org/10.1093/jxb/erz536

Liu, F., Rice, J.H., Lopes, V., Grewal, P., Lebeis, S.L., Hewezi, T., Staton, M.E., 2020b. Overexpression of Strigolactone-Associated Genes Exerts Fine-Tuning Selection on Soybean Rhizosphere Bacterial and Fungal Microbiome. Phytobiomes J. 4, 239–251. https://doi.org/10.1094/PBIOMES-01-20-0003-R

Liu, J., Moore, S., Chen, C., Lindsey, K., 2017. Crosstalk Complexities between Auxin, Cytokinin, and Ethylene in Arabidopsis Root

Development: From Experiments to Systems Modeling, and Back Again. Mol. Plant 10, 1480–1496. https://doi.org/10.1016/j.molp.2017.11.002

Liu, J., Novero, M., Charnikhova, T., Ferrandino, A., Schubert, A., Ruyter-Spira, C., Bonfante, P., Lovisolo, C., Bouwmeester, H.J., Cardinale, F., 2013. Carotenoid cleavage dioxygenase 7 modulates plant growth, reproduction, senescence, and determinate nodulation in the model legume *Lotus japonicus*. J. Exp. Bot. 64, 1967–1981. https://doi.org/10.1093/jxb/ert056

Liu, W., Kohlen, W., Lillo, A., Op den Camp, R., Ivanov, S., Hartog, M., Limpens, E., Jamil, M., Smaczniak, C., Kaufmann, K., Yang, W.C., Hooiveld, G.J.E.J., Charnikhova, T., Bouwmeester, H.J., Bisseling, T., Geurts, R., 2011. Strigolactone biosynthesis in *Medicago truncatula* and rice requires the symbiotic GRAS-type transcription factors NSP1 and NSP2. Plant Cell 23, 3853–3865. https://doi.org/10.1105/tpc.111.089771

Lohar, D.P., Schaff, J.E., Laskey, J.G., Kieber, J.J., Bilyeu, K.D., Bird, D.M., 2004. Cytokinins play opposite roles in lateral root formation, and nematode and Rhizobial symbioses. Plant J. Cell Mol. Biol. 38, 203–214. https://doi.org/10.1111/j.1365-313X.2004.02038.x

López-Ráez, J.A., Charnikhova, T., Gómez-Roldán, V., Matusova, R., Kohlen, W., De Vos, R., Verstappen, F., Puech-Pages, V., Bécard, G., Mulder, P., Bouwmeester, H., 2008. Tomato strigolactones are derived from carotenoids and their biosynthesis is promoted by phosphate starvation. New Phytol. 178, 863–874. https://doi.org/10.1111/j.1469-8137.2008.02406.x

Love, M.I., Huber, W., Anders, S., 2014. Moderated estimation of fold change and dispersion for RNA-seq data with DESeq2. Genome Biol. 15, 550. https://doi.org/10.1186/s13059-014-0550-8

Lu, Y., Chen, Q., Bu, Y., Luo, R., Hao, S., Zhang, J., Tian, J., Yao, Y., 2017. Flavonoid Accumulation Plays an Important Role in the Rust Resistance of Malus Plant Leaves. Front. Plant Sci. 8. https://doi.org/10.3389/fpls.2017.01286

Lyu, G., Li, D., Li, S., Hu, H., 2019. STO and GA negatively regulate UV-B-induced Arabidopsis root growth inhibition. Plant Signal. Behav. 14, 1675471. https://doi.org/10.1080/15592324.2019.1675471

Ma, N., Hu, C., Wan, L., Hu, Q., Xiong, J., Zhang, C., 2017. Strigolactones Improve Plant Growth, Photosynthesis, and Alleviate Oxidative Stress under Salinity in Rapeseed (*Brassica napus L.*) by Regulating Gene Expression. Front. Plant Sci. 8. https://doi.org/10.3389/fpls.2017.01671

Mähönen, A.P., ten Tusscher, K., Siligato, R., Smetana, O., Díaz-Triviño, S., Salojärvi, J., Wachsman, G., Prasad, K., Heidstra, R., Scheres, B., 2014. PLETHORA gradient formation mechanism separates auxin responses. Nature 515, 125–129. https://doi.org/10.1038/nature13663

Mangano, S., Juárez, S.P.D., Estevez, J.M., 2016. ROS Regulation of Polar Growth in Plant Cells. Plant Physiol. 171, 1593–1605. https://doi.org/10.1104/pp.16.00191

Marchant, A., Bhalerao, R., Casimiro, I., Eklöf, J., Casero, P.J., Bennett, M., Sandberg, G., 2002. AUX1 promotes lateral root formation by facilitating indole-3-acetic acid distribution between sink and source tissues in the Arabidopsis seedling. Plant Cell 14, 589–597. https://doi.org/10.1105/tpc.010354

Martin, R.E., Marzol, E., Estevez, J.M., Muday, G.K., 2022. Ethylene signaling increases reactive oxygen species accumulation to drive root hair initiation in Arabidopsis. Development 149, dev200487. https://doi.org/10.1242/dev.200487

Mase, K., Tsukagoshi, H., 2021. Reactive Oxygen Species Link Gene Regulatory Networks During Arabidopsis Root Development. Front. Plant Sci. 12. https://doi.org/10.3389/fpls.2021.660274

Mashiguchi, K., Sasaki, E., Shimada, Y., Nagae, M., Ueno, K., Nakano, T., Yoneyama, K., Suzuki, Y., Asami, T., 2009. Feedback-Regulation of Strigolactone Biosynthetic Genes and Strigolactone-Regulated Genes in Arabidopsis. Biosci. Biotechnol. Biochem. 73, 2460–2465. https://doi.org/10.1271/bbb.90443

Masucci, J.D., Rerie, W.G., Foreman, D.R., Zhang, M., Galway, M.E., Marks, M.D., Schiefelbein, J.W., 1996. The homeobox gene GLABRA2 is required for position-dependent cell differentiation in the root epidermis of *Arabidopsis thaliana*. Dev. Camb. Engl. 122, 1253–1260. https://doi.org/10.1242/dev.122.4.1253

Mayzlish-Gati, E., De-Cuyper, C., Goormachtig, S., Beeckman, T., Vuylsteke, M., Brewer, P.B., Beveridge, C.A., Yermiyahu, U., Kaplan, Y., Enzer, Y., Wininger, S., Resnick, N., Cohen, M., Kapulnik, Y., Koltai, H., 2012. Strigolactones Are Involved in Root Response to Low Phosphate Conditions in Arabidopsis. Plant Physiol. 160, 1329 LP – 1341. https://doi.org/10.1104/pp.112.202358

Mayzlish-Gati, E., LekKala, S.P., Resnick, N., Wininger, S., Bhattacharya, C., Lemcoff, J.H., Kapulnik, Y., Koltai, H., 2010. Strigolactones are positive regulators of light-harvesting genes in tomato. J. Exp. Bot. 61, 3129–3136. https://doi.org/10.1093/jxb/erq138

McAdam, E.L., Hugill, C., Fort, S., Samain, E., Cottaz, S., Davies, N.W., Reid, J.B., Foo, E., 2017. Determining the Site of Action of Strigolactones during Nodulation. Plant Physiol. 175, 529–542. https://doi.org/10.1104/pp.17.00741

Meng, Y., Shuai, H., Luo, X., Chen, F., Zhou, W., Yang, W., Shu, K., 2017. Karrikins: Regulators Involved in Phytohormone Signaling Networks during Seed Germination and Seedling Development. Front. Plant Sci. 7. https://doi.org/10.3389/fpls.2016.02021

Meng, Y., Varshney, K., Incze, N., Badics, E., Kamran, M., Davies, S.F., Oppermann, L.M.F., Magne, K., Dalmais, M., Bendahmane, A., Sibout, R., Vogel, J., Laudencia-Chingcuanco, D., Bond, C.S., Soós, V., Gutjahr, C., Waters, M.T., 2022. KARRIKIN INSENSITIVE2 regulates leaf development, root system architecture and arbuscular-mycorrhizal symbiosis in *Brachypodium distachyon*. Plant J. Cell Mol. Biol. 109, 1559–1574. https://doi.org/10.1111/tpj.15651

Meng, Z., Ruberti, C., Gong, Z., Brandizzi, F., 2017. CPR5 modulates salicylic acid and the unfolded protein response to manage tradeoffs between plant growth and stress responses. Plant J. Cell Mol. Biol. 89, 486–501. https://doi.org/10.1111/tpj.13397

Mockler, T.C., Michael, T.P., Priest, H.D., Shen, R., Sullivan, C.M., Givan, S.A., McEntee, C., Kay, S.A., Chory, J., 2007. The DIURNAL project: DIURNAL and circadian expression profiling, model-based pattern matching, and promoter analysis. Cold Spring Harb. Symp. Quant. Biol. 72, 353–363. https://doi.org/10.1101/sqb.2007.72.006

Mortier, V., Wasson, A., Jaworek, P., De Keyser, A., Decroos, M., Holsters, M., Tarkowski, P., Mathesius, U., Goormachtig, S., 2014. Role of LONELY GUY genes in indeterminate nodulation on *Medicago truncatula*. New Phytol. 202, 582–593. https://doi.org/10.1111/nph.12681

Mravec, J., Skůpa, P., Bailly, A., Hoyerová, K., Křeček, P., Bielach, A., Petrášek, J., Zhang, J., Gaykova, V., Stierhof, Y.D., Dobrev, P.I., Schwarzerová, K., Rolčík, J., Seifertová, D., Luschnig, C., Benková, E., Zažímalová, E., Geisler, M., Friml, J., 2009. Subcellular homeostasis of phytohormone auxin is mediated by the ER-localized PIN5 transporter. Nature 459, 1136–1140. https://doi.org/10.1038/nature08066

Muday, G.K., Rahman, A., Binder, B.M., 2012. Auxin and ethylene: collaborators or competitors? Trends Plant Sci. 17, 181–195. https://doi.org/10.1016/j.tplants.2012.02.001

Nakabayashi, R., Mori, T., Saito, K., 2014. Alternation of flavonoid accumulation under drought stress in *Arabidopsis thaliana*. Plant Signal. Behav. 9, e29518. https://doi.org/10.4161/psb.29518

Nakamichi, N., Kiba, T., Henriques, R., Mizuno, T., Chua, N.H., Sakakibara, H., 2010. PSEUDO-RESPONSE REGULATORS 9, 7, and 5 Are Transcriptional Repressors in the Arabidopsis Circadian Clock. Plant Cell 22, 594–605. https://doi.org/10.1105/tpc.109.072892

Nascimento, F.X., Brígido, C., Glick, B.R., Rossi, M.J., 2016. The Role of Rhizobial ACC Deaminase in the Nodulation Process of Leguminous Plants. Int. J. Agron. 2016, e1369472. https://doi.org/10.1155/2016/1369472

Nasir, F., Shi, S., Tian, L., Chang, C., Ma, L., Li, X., Gao, Y., Tian, C., 2019. Strigolactones shape the rhizomicrobiome in rice (*Oryza sativa*). Plant Sci. Int. J. Exp. Plant Biol. 286, 118–133. https://doi.org/10.1016/j.plantsci.2019.05.016

Naulin, P.A., Armijo, G.I., Vega, A.S., Tamayo, K.P., Gras, D.E., de la Cruz, J., Gutiérrez, R.A., 2020. Nitrate Induction of Primary Root Growth Requires Cytokinin Signaling in *Arabidopsis thaliana*. Plant Cell Physiol. 61, 342–352. https://doi.org/10.1093/pcp/pcz199

Nelson, D.C., Riseborough, J.A., Flematti, G.R., Stevens, J., Ghisalberti, E.L., Dixon, K.W., Smith, S.M., 2009. Karrikins Discovered in Smoke Trigger Arabidopsis Seed Germination by a Mechanism Requiring Gibberellic Acid Synthesis and Light. Plant Physiol. 149, 863–873. https://doi.org/10.1104/pp.108.131516

Oláh, D., Feigl, G., Molnár, Á., Ördög, A., Kolbert, Z., 2020. Strigolactones Interact With Nitric Oxide in Regulating Root System Architecture of *Arabidopsis thaliana*. Front. Plant Sci. 11. https://doi.org/10.3389/fpls.2020.01019

Oláh, D., Molnár, Á., Soós, V., Kolbert, Z., 2021. Nitric oxide is associated with strigolactone and karrikin signal transduction in Arabidopsis roots. Plant Signal. Behav. 16, 1868148. https://doi.org/10.1080/15592324.2020.1868148

Oldroyd, G.E.D., Long, S.R., 2003. Identification and Characterization of Nodulation-Signaling Pathway 2, a Gene of *Medicago truncatula* Involved in Nod Factor Signaling. Plant Physiol. 131, 1027–1032. https://doi.org/10.1104/pp.102.010710

Omae, N., Tsuda, K., 2022. Plant-Microbiota Interactions in Abiotic Stress Environments. Mol. Plant-Microbe Interactions 35, 511–526. https://doi.org/10.1094/MPMI-11-21-0281-FI

Ortega-Martínez, O., Pernas, M., Carol, R.J., Dolan, L., 2007. Ethylene modulates stem cell division in the *Arabidopsis thaliana* root. Science 317, 507–510. https://doi.org/10.1126/science.1143409

Pan, X., Cao, P., Su, X., Liu, Z., Li, M., 2020. Structural analysis and comparison of light-harvesting complexes I and II. Biochim. Biophys. Acta BBA - Bioenerg., Light harvesting 1861, 148038. https://doi.org/10.1016/j.bbabio.2019.06.010

Park, D.H., Lim, P.O., Kim, J.S., Cho, D.S., Hong, S.H., Nam, H.G., 2003. The Arabidopsis COG1 gene encodes a Dof domain transcription factor and negatively regulates phytochrome signaling. Plant J. 34, 161–171. https://doi.org/10.1046/j.1365-313X.2003.01710.x

Pasternak, T., Groot, E.P., Kazantsev, F.V., Teale, W., Omelyanchuk, N., Kovrizhnykh, V., Palme, K., Mironova, V.V., 2019. Salicylic Acid Affects Root Meristem Patterning via Auxin Distribution in a Concentration-Dependent Manner. Plant Physiol. 180, 1725–1739. https://doi.org/10.1104/pp.19.00130

Petricka, J.J., Winter, C.M., Benfey, P.N., 2012. Control of Arabidopsis Root Development. Annu. Rev. Plant Biol. 63, 563–590. https://doi.org/10.1146/annurev-arplant-042811-105501

Planas-Riverola, A., Gupta, A., Betegón-Putze, I., Bosch, N., Ibañes, M., Caño-Delgado, A.I., 2019. Brassinosteroid signaling in plant development and adaptation to stress. Dev. Camb. Engl. 146, dev151894. https://doi.org/10.1242/dev.151894

Postiglione, A.E., Muday, G.K., 2020. The Role of ROS Homeostasis in ABA-Induced Guard Cell Signaling. Front. Plant Sci. 11, 968. https://doi.org/10.3389/fpls.2020.00968

Promchuea, S., Zhu, Y., Chen, Z., Zhang, J., Gong, Z., 2017. ARF2 coordinates with PLETHORAs and PINs to orchestrate ABA-mediated root meristem activity in Arabidopsis. J. Integr. Plant Biol. 59, 30–43. https://doi.org/10.1111/jipb.12506

Qin, Y.M., Hu, C.Y., Pang, Y., Kastaniotis, A.J., Hiltunen, J.K., Zhu, Y.X., 2007. Saturated Very-Long-Chain Fatty Acids Promote Cotton Fiber and Arabidopsis Cell Elongation by Activating Ethylene Biosynthesis. Plant Cell 19, 3692–3704. https://doi.org/10.1105/TPC.107.054437

Rahman, A., Hosokawa, S., Oono, Y., Amakawa, T., Goto, N., Tsurumi, S., 2002. Auxin and Ethylene Response Interactions during Arabidopsis Root Hair Development Dissected by Auxin Influx Modulators. Plant Physiol. 130, 1908–1917. https://doi.org/10.1104/pp.010546

Rasmussen, A., Mason, M.G., De Cuyper, C., Brewer, P.B., Herold, S., Agusti, J., Geelen, D., Greb, T., Goormachtig, S., Beeckman, T., Beveridge, C.A., 2012. Strigolactones Suppress Adventitious Rooting in Arabidopsis and Pea. Plant Physiol. 158, 1976–1987. https://doi.org/10.1104/pp.111.187104

Rehman, N., Ali, M., Ahmad, M.Z., Liang, G., Zhao, J., 2018. Strigolactones promote rhizobia interaction and increase nodulation in soybean (*Glycine max*). Microb. Pathog. 114, 420–430. https://doi.org/10.1016/j.micpath.2017.11.049

Reid, D., Liu, H., Kelly, S., Kawaharada, Y., Mun, T., Andersen, S.U., Desbrosses, G., Stougaard, J., 2018. Dynamics of Ethylene Production in Response to Compatible Nod Factor. Plant Physiol. 176, 1764–1772. https://doi.org/10.1104/pp.17.01371

Reid, D.E., Heckmann, A.B., Novák, O., Kelly, S., Stougaard, J., 2016. CYTOKININ OXIDASE/DEHYDROGENASE3 Maintains Cytokinin Homeostasis during Root and Nodule Development in *Lotus japonicus*. Plant Physiol. 170, 1060–1074. https://doi.org/10.1104/pp.15.00650

Renard, J., Martínez-Almonacid, I., Sonntag, A., Molina, I., Moya-Cuevas, J., Bissoli, G., Muñoz-Bertomeu, J., Faus, I., Niñoles, R., Shigeto, J., Tsutsumi, Y., Gadea, J., Serrano, R., Bueso, E., 2020. PRX2 and PRX25, peroxidases regulated by COG1, are involved in seed longevity in Arabidopsis. Plant Cell Environ. 43, 315–326. https://doi.org/10.1111/pce.13656

Richmond, B.L., Coelho, C.L., Wilkinson, H., McKenna, J., Ratchinski, P., Schwarze, M., Frost, M., Lagunas, B., Gifford, M.L., 2022. Elucidating connections between the strigolactone biosynthesis pathway, flavonoid production and root system architecture in *Arabidopsis thaliana*. Physiol. Plant. 174, e13681. https://doi.org/10.1111/ppl.13681

Rightmyer, A.P., Long, S.R., 2011. Pseudonodule Formation by Wild-Type and Symbiotic Mutant *Medicago truncatula* in Response to Auxin Transport Inhibitors. Mol. Plant-Microbe Interactions 24, 1372–1384. https://doi.org/10.1094/MPMI-04-11-0103

Roy, S., Liu, W., Nandety, R.S., Crook, A., Mysore, K.S., Pislariu, C.I., Frugoli, J., Dickstein, R., Udvardi, M.K., 2020. Celebrating 20 Years of Genetic Discoveries in Legume Nodulation and Symbiotic Nitrogen Fixation. Plant Cell 32, 15–41. https://doi.org/10.1105/tpc.19.00279

Roy, S., Robson, F., Lilley, J., Liu, C.W., Cheng, X., Wen, J., Walker, S., Sun, J., Cousins, D., Bone, C., Bennett, M.J., Downie, J.A., Swarup, R., Oldroyd, G., Murray, J.D., 2017. MtLAX2, a Functional Homologue of the Arabidopsis Auxin Influx Transporter AUX1, Is Required for Nodule

Organogenesis. Plant Physiol. 174, 326–338. https://doi.org/10.1104/pp.16.01473

Ruegger, M., Dewey, E., Hobbie, L., Brown, D., Bernasconi, P., Turner, J., Muday, G., Estelle, M., 1997. Reduced naphthylphthalamic acid binding in the tir3 mutant of Arabidopsis is associated with a reduction in polar auxin transport and diverse morphological defects. Plant Cell 9, 745–757. https://doi.org/10.1105/tpc.9.5.745

Ruyter-Spira, C., Kohlen, W., Charnikhova, T., van Zeijl, A., van Bezouwen, L., de Ruijter, N., Cardoso, C., Lopez-Raez, J.A., Matusova, R., Bours, R., Verstappen, F., Bouwmeester, H., 2011. Physiological Effects of the Synthetic Strigolactone Analog GR24 on Root System Architecture in Arabidopsis: Another Belowground Role for Strigolactones? Plant Physiol. 155, 721 LP – 734. https://doi.org/10.1104/pp.110.166645

Ryan, K.G., Swinny, E.E., Winefield, C., Markham, K.R., 2001. Flavonoids and UV photoprotection in Arabidopsis mutants. Z. Naturforschung C J. Biosci. 56, 745–754. https://doi.org/10.1515/znc-2001-9-1013

Rymen, B., Kawamura, A., Schäfer, S., Breuer, C., Iwase, A., Shibata, M., Ikeda, M., Mitsuda, N., Koncz, C., Ohme-Takagi, M., Matsui, M., Sugimoto, K., 2017. ABA Suppresses Root Hair Growth via the OBP4 Transcriptional Regulator. Plant Physiol. 173, 1750–1762. https://doi.org/10.1104/pp.16.01945

Sang, D., Chen, D., Liu, G., Liang, Y., Huang, L., Meng, X., Chu, J., Sun, X., Dong, G., Yuan, Y., Qian, Q., Li, J., Wang, Y., 2014. Strigolactones regulate rice tiller angle by attenuating shoot gravitropism through inhibiting auxin biosynthesis. Proc. Natl. Acad. Sci. 111, 11199–11204. https://doi.org/10.1073/pnas.1411859111

Sanz, L., Fernández-Marcos, M., Modrego, A., Lewis, D.R., Muday, G.K., Pollmann, S., Dueñas, M., Santos-Buelga, C., Lorenzo, O., 2014. Nitric Oxide Plays a Role in Stem Cell Niche Homeostasis through Its Interaction with Auxin. Plant Physiol. 166, 1972–1984. https://doi.org/10.1104/pp.114.247445

Scaffidi, A., Waters, M.T., Ghisalberti, E.L., Dixon, K.W., Flematti, G.R., Smith, S.M., 2013. Carlactone-independent seedling morphogenesis in Arabidopsis. Plant J. 76, 1–9. https://doi.org/10.1111/tpj.12265

Scaffidi, A., Waters, M.T., Sun, Y.K., Skelton, B.W., Dixon, K.W., Ghisalberti, E.L., Flematti, G.R., Smith, S.M., 2014. Strigolactone Hormones and Their Stereoisomers Signal through Two Related Receptor Proteins to Induce Different Physiological Responses in Arabidopsis. Plant Physiol. 165, 1221–1232. https://doi.org/10.1104/PP.114.240036

Scervino, J.M., Ponce, M.A., Erra-Bassells, R., Vierheilig, H., Ocampo, J.A., Godeas, A., 2005. Flavonoids exclusively present in mycorrhizal roots of white clover exhibit a different effect on arbuscular mycorrhizal fungi than flavonoids exclusively present in non-mycorrhizal roots of white clover. J. Plant Interact. 1, 15–22. https://doi.org/10.1080/17429140500192597

Schiessl, K., Lilley, J.L.S., Lee, T., Tamvakis, I., Kohlen, W., Bailey, P.C., Thomas, A., Luptak, J., Ramakrishnan, K., Carpenter, M.D., Mysore, K.S., Wen, J., Ahnert, S., Grieneisen, V.A., Oldroyd, G.E.D., 2019. NODULE INCEPTION Recruits the Lateral Root Developmental Program for Symbiotic Nodule Organogenesis in *Medicago truncatula*. Curr. Biol. CB 29, 3657-3668.e5. https://doi.org/10.1016/j.cub.2019.09.005

Schindelin, J., Arganda-Carreras, I., Frise, E., Kaynig, V., Longair, M., Pietzsch, T., Preibisch, S., Rueden, C., Saalfeld, S., Schmid, B., Tinevez, J.Y., White, D.J., Hartenstein, V., Eliceiri, K., Tomancak, P., Cardona, A., 2012. Fiji: an open-source platform for biological-image analysis. Nat. Methods 2012 97 9, 676–682. https://doi.org/10.1038/nmeth.2019

Schliemann, W., Ammer, C., Strack, D., 2008. Metabolite profiling of mycorrhizal roots of *Medicago truncatula*. Phytochemistry 69, 112–146. https://doi.org/10.1016/j.phytochem.2007.06.032

Schmittgen, T.D., Livak, K.J., 2008. Analyzing real-time PCR data by the comparative C(T) method. Nat. Protoc. 3, 1101–1108. https://doi.org/10.1038/nprot.2008.73

Sedaghat, M., Emam, Y., Mokhtassi-Bidgoli, A., Hazrati, S., Lovisolo, C., Visentin, I., Cardinale, F., Tahmasebi-Sarvestani, Z., 2021. The Potential of the Synthetic Strigolactone Analogue GR24 for the Maintenance of Photosynthesis and Yield in Winter Wheat under Drought: Investigations on the Mechanisms of Action and Delivery Modes. Plants 10, 1223. https://doi.org/10.3390/plants10061223

Shani, E., Weinstain, R., Zhang, Y., Castillejo, C., Kaiserli, E., Chory, J., Tsien, R.Y., Estelle, M., 2013. Gibberellins accumulate in the elongating endodermal cells of Arabidopsis root. Proc. Natl. Acad. Sci. 110, 4834–4839. https://doi.org/10.1073/pnas.1300436110

Sheehan, H., Moser, M., Klahre, U., Esfeld, K., Dell'Olivo, A., Mandel, T., Metzger, S., Vandenbussche, M., Freitas, L., Kuhlemeier, C., 2016. MYB-FL controls gain and loss of floral UV absorbance, a key trait affecting pollinator preference and reproductive isolation. Nat. Genet. 48, 159–166. https://doi.org/10.1038/ng.3462

Sheerin, D.J., Menon, C., zur Oven-Krockhaus, S., Enderle, B., Zhu, L., Johnen, P., Schleifenbaum, F., Stierhof, Y.D., Huq, E., Hiltbrunner, A., 2015. Light-Activated Phytochrome A and B Interact with Members of the SPA Family to Promote Photomorphogenesis in Arabidopsis by Reorganizing the COP1/SPA Complex. Plant Cell 27, 189–201. https://doi.org/10.1105/tpc.114.134775

Shen, H., Zhu, L., Bu, Q.Y., Huq, E., 2012. MAX2 Affects Multiple Hormones to Promote Photomorphogenesis. Mol. Plant 5, 750–762. https://doi.org/10.1093/mp/sss029

Shigeto, J., Itoh, Y., Hirao, S., Ohira, K., Fujita, K., Tsutsumi, Y., 2015. Simultaneously disrupting AtPrx2, AtPrx25 and AtPrx71 alters lignin content and structure in Arabidopsis stem. J. Integr. Plant Biol. 57, 349–356. https://doi.org/10.1111/jipb.12334

Shtin, M., Dello Ioio, R., Del Bianco, M., 2022. It's Time for a Change: The Role of Gibberellin in Root Meristem Development. Front. Plant Sci. 13. https://doi.org/10.3389/fpls.2022.882517

Silva-Navas, J., Moreno-Risueno, M.A., Manzano, C., Téllez-Robledo, B., Navarro-Neila, S., Carrasco, V., Pollmann, S., Gallego, F.J., Pozo, J.C. del, 2016. Flavonols Mediate Root Phototropism and Growth through Regulation of Proliferation-to-Differentiation Transition. Plant Cell 28, 1372. https://doi.org/10.1105/tpc.15.00857

Singh, A., Sharma, A., Singh, N., Nandi, A.K., 2022. MTO1-RESPONDING DOWN 1 (MRD1) is a transcriptional target of OZF1 for promoting salicylic acid-mediated defense in Arabidopsis. Plant Cell Rep. 41, 1319–1328. https://doi.org/10.1007/s00299-022-02861-2

Singh, S., Yadav, S., Singh, Alka, Mahima, M., Singh, Archita, Gautam, V., Sarkar, A.K., 2020. Auxin signaling modulates LATERAL ROOT PRIMORDIUM1 (LRP1) expression during lateral root development in Arabidopsis. Plant J. 101, 87–100. https://doi.org/10.1111/tpj.14520

Sorefan, K., Booker, J., Haurogné, K., Goussot, M., Bainbridge, K., Foo, E., Chatfield, S., Ward, S., Beveridge, C., Rameau, C., Leyser, O., 2003. MAX4 and RMS1 are ortholosgous dioxygenase-like genes that regulate shoot branching in Arabidopsis and pea. Genes Dev. 17, 1469–1474. https://doi.org/10.1101/gad.256603

Soto, M.J., Fernández-Aparicio, M., Castellanos-Morales, V., García-Garrido, J.M., Ocampo, J.A., Delgado, M.J., Vierheilig, H., 2010. First indications for the involvement of strigolactones on nodule formation in alfalfa (*Medicago sativa*). Soil Biol. Biochem. 42, 383–385. https://doi.org/10.1016/j.soilbio.2009.11.007

Soundappan, I., Bennett, T., Morffy, N., Liang, Y., Stanga, J.P., Abbas, A., Leyser, O., Nelsona, D.C., 2015. SMAX1-LIKE/D53 family members enable distinct MAX2-dependent responses to strigolactones and karrikins in Arabidopsis. Plant Cell 27, 3143–3159. https://doi.org/10.1105/tpc.15.00562

Stanga, J.P., Morffy, N., Nelson, D.C., 2016. Functional redundancy in the control of seedling growth by the karrikin signaling pathway. Planta 243, 1397–1406. https://doi.org/10.1007/s00425-015-2458-2

Stanga, J.P., Smith, S.M., Briggs, W.R., Nelson, D.C., 2013. SUPPRESSOR OF MORE AXILLARY GROWTH2 1 Controls Seed Germination and Seedling Development in Arabidopsis. Plant Physiol. 163, 318–330. https://doi.org/10.1104/pp.113.221259

Stirnberg, P., Furner, I.J., Leyser, H.M.O.L., 2007. MAX2 participates in an SCF complex which acts locally at the node to suppress shoot branching. Plant J. 50, 80–94. https://doi.org/10.1111/J.1365-313X.2007.03032.X

Stirnberg, P., van de Sande, K., Leyser, H.M.O., 2002. MAX1 and MAX2 control shoot lateral branching in Arabidopsis. Development 129, 1131–1141. https://doi.org/10.1242/dev.129.5.1131

Strader, L.C., Chen, G.L., Bartel, B., 2010. Ethylene directs auxin to control root cell expansion. Plant J. Cell Mol. Biol. 64, 874–884. https://doi.org/10.1111/j.1365-313X.2010.04373.x

Street, I.H., Aman, S., Zubo, Y., Ramzan, A., Wang, X., Shakeel, S.N., Kieber, J.J., Schaller, G.E., 2015. Ethylene Inhibits Cell Proliferation of the Arabidopsis Root Meristem. Plant Physiol. 169, 338–350. https://doi.org/10.1104/pp.15.00415

Struk, S., Braem, L., Matthys, C., Walton, A., Vangheluwe, N., Van Praet, S., Jiang, L., Baster, P., De Cuyper, C., Boyer, F.D., Stes, E., Beeckman, T., Friml, J., Gevaert, K., Goormachtig, S., 2022. Transcriptional Analysis in the Arabidopsis Roots Reveals New Regulators that Link *rac*-GR24 Treatment with Changes in Flavonol Accumulation, Root Hair Elongation and Lateral Root Density. Plant Cell Physiol. 63, 104–119. https://doi.org/10.1093/pcp/pcab149

Subramanian, S., Stacey, G., Yu, O., 2006. Endogenous isoflavones are essential for the establishment of symbiosis between soybean and Bradyrhizobium japonicum. Plant J. 48, 261–273. https://doi.org/10.1111/j.1365-313X.2006.02874.x

Sun, H., Tao, J., Liu, S., Huang, S., Chen, S., Xie, X., Yoneyama, K., Zhang, Y., Xu, G., 2014. Strigolactones are involved in phosphate- and nitrate-

deficiency-induced root development and auxin transport in rice. J. Exp. Bot. 65, 6735–6746. https://doi.org/10.1093/jxb/eru029

Sun, L.R., Wang, Y.B., He, S.B., Hao, F.S., 2018. Mechanisms for Abscisic Acid Inhibition of Primary Root Growth. Plant Signal. Behav. 13, e1500069. https://doi.org/10.1080/15592324.2018.1500069

Sun, X., Li, Y., He, W., Ji, C., Xia, P., Wang, Y., Du, S., Li, H., Raikhel, N., Xiao, J., Guo, H., 2017. Pyrazinamide and derivatives block ethylene biosynthesis by inhibiting ACC oxidase. Nat. Commun. 8, 15758. https://doi.org/10.1038/ncomms15758

Swarup, R., Perry, P., Hagenbeek, D., Van Der Straeten, D., Beemster, G.T.S., Sandberg, G., Bhalerao, R., Ljung, K., Bennett, M.J., 2007. Ethylene Upregulates Auxin Biosynthesis in Arabidopsis Seedlings to Enhance Inhibition of Root Cell Elongation. Plant Cell 19, 2186–2196. https://doi.org/10.1105/tpc.107.052100

Takei, K., Ueda, N., Aoki, K., Kuromori, T., Hirayama, T., Shinozaki, K., Yamaya, T., Sakakibara, H., 2004. AtIPT3 is a key determinant of nitrate-dependent cytokinin biosynthesis in Arabidopsis. Plant Cell Physiol. 45, 1053–1062. https://doi.org/10.1093/pcp/pch119

Teale, W.D., Pasternak, T., Dal Bosco, C., Dovzhenko, A., Kratzat, K., Bildl, W., Schwörer, M., Falk, T., Ruperti, B., V Schaefer, J., Shahriari, M., Pilgermayer, L., Li, X., Lübben, F., Plückthun, A., Schulte, U., Palme, K., 2021. Flavonol-mediated stabilization of PIN efflux complexes regulates polar auxin transport. EMBO J. 40, e104416. https://doi.org/10.15252/embj.2020104416

Tenhaken, R., 2015. Cell wall remodeling under abiotic stress. Front. Plant Sci. 5. https://doi.org/10.3389/fpls.2014.00771

Thula, S., Moturu, T.R., Salava, H., Balakhonova, V., Berka, M., Kerchev, P., Mishra, K.B., Nodzynski, T., Simon, S., 2022. Strigolactones Stimulate High Light Stress Adaptation by Modulating Photosynthesis Rate in Arabidopsis. J. Plant Growth Regul. https://doi.org/10.1007/s00344-022-10764-5

Thussagunpanit, J., Nagai, Y., Nagae, M., Mashiguchi, K., Mitsuda, N., Ohme-Takagi, M., Nakano, T., Nakamura, H., Asami, T., 2017. Involvement of STH7 in light-adapted development in *Arabidopsis thaliana* promoted by both strigolactone and karrikin. Biosci. Biotechnol. Biochem. 81, 292–301. https://doi.org/10.1080/09168451.2016.1254536

Tian, F., Yang, D.C., Meng, Y.Q., Jin, J., Gao, G., 2020. PlantRegMap: charting functional regulatory maps in plants. Nucleic Acids Res. 48, D1104–D1113. https://doi.org/10.1093/NAR/GKZ1020

Toh, S., McCourt, P., Tsuchiya, Y., 2012. HY5 is involved in strigolactone-dependent seed germination in Arabidopsis. Plant Signal. Behav. 7, 556–558. https://doi.org/10.4161/psb.19839

Tohge, T., Kusano, M., Fukushima, A., Saito, K., Fernie, A.R., 2011. Transcriptional and metabolic programs following exposure of plants to UV-B irradiation. Plant Signal. Behav. 6, 1987–1992. https://doi.org/10.4161/psb.6.12.18240

Torres-Martínez, H.H., Rodríguez-Alonso, G., Shishkova, S., Dubrovsky, J.G., 2019. Lateral Root Primordium Morphogenesis in Angiosperms. Front. Plant Sci. 10. https://doi.org/10.3389/fpls.2019.00206

Tsuchiya, Y., Vidaurre, D., Toh, S., Hanada, A., Nambara, E., Kamiya, Y., Yamaguchi, S., McCourt, P., 2010. A small-molecule screen identifies new functions for the plant hormone strigolactone. Nat. Chem. Biol. 6, 741–749. https://doi.org/10.1038/nchembio.435

Tsurumoto, T., Fujikawa, Y., Onoda, Y., Ochi, Y., Ohta, D., Okazawa, A., 2022. Transcriptome and metabolome analyses revealed that narrowband 280 and 310 nm UV-B induce distinctive responses in Arabidopsis. Sci. Rep. 12, 4319. https://doi.org/10.1038/s41598-022-08331-9

Tyburski, J., Dunajska-Ordak, K., Skorupa, M., Tretyn, A., 2012. Role of Ascorbate in the Regulation of the *Arabidopsis thaliana* Root Growth by Phosphate Availability. J. Bot. 2012, e580342. https://doi.org/10.1155/2012/580342

Ubeda-Tomás, S., Swarup, R., Coates, J., Swarup, K., Laplaze, L., Beemster, G.T.S., Hedden, P., Bhalerao, R., Bennett, M.J., 2008. Root growth in Arabidopsis requires gibberellin/DELLA signalling in the endodermis. Nat. Cell Biol. 10, 625–628. https://doi.org/10.1038/ncb1726

Ueda, H., Kusaba, M., 2015. Strigolactone Regulates Leaf Senescence in Concert with Ethylene in Arabidopsis. Plant Physiol. 169, 138–147. https://doi.org/10.1104/PP.15.00325

Umehara, M., Hanada, A., Yoshida, S., Akiyama, K., Arite, T., Takeda-Kamiya, N., Magome, H., Kamiya, Y., Shirasu, K., Yoneyama, K., Kyozuka, J., Yamaguchi, S., 2008. Inhibition of shoot branching by new terpenoid plant hormones. Nat. 2008 4557210 455, 195–200. https://doi.org/10.1038/nature07272

Varma Penmetsa, R., Uribe, P., Anderson, J., Lichtenzveig, J., Gish, J.C., Nam, Y.W., Engstrom, E., Xu, K., Sckisel, G., Pereira, M., Baek, J.M., Lopez-Meyer, M., Long, S.R., Harrison, M.J., Singh, K.B., Kiss, G.B., Cook, D.R., 2008. The *Medicago truncatula* ortholog of Arabidopsis EIN2, sickle, is a negative regulator of symbiotic and pathogenic

microbial associations. Plant J. 55, 580–595. https://doi.org/10.1111/j.1365-313X.2008.03531.x

Vega, A., O'Brien, J.A., Gutiérrez, R.A., 2019. Nitrate and hormonal signaling crosstalk for plant growth and development. Curr. Opin. Plant Biol., Cell biology 52, 155–163. https://doi.org/10.1016/j.pbi.2019.10.001

Vieten, A., Vanneste, S., Wiśniewska, J., Benková, E., Benjamins, R., Beeckman, T., Luschnig, C., Friml, J., 2005. Functional redundancy of PIN proteins is accompanied by auxin-dependent cross-regulation of PIN expression. Development 132, 4521–4531. https://doi.org/10.1242/dev.02027

Villaécija-Aguilar, J.A., Hamon-Josse, M., Carbonnel, S., Kretschmar, A., Schmidt, C., Dawid, C., Bennett, T., Gutjahr, C., 2019. SMAX1/SMXL2 regulate root and root hair development downstream of KAI2-mediated signalling in Arabidopsis. PLOS Genet. 15, e1008327. https://doi.org/10.1371/journal.pgen.1008327

Villaécija-Aguilar, J.A., Körösy, C., Maisch, L., Hamon-Josse, M., Petrich, A., Magosch, S., Chapman, P., Bennett, T., Gutjahr, C., 2022. KAI2 promotes Arabidopsis root hair elongation at low external phosphate by controlling local accumulation of AUX1 and PIN2. Curr. Biol. 32, 228-236.e3. https://doi.org/10.1016/j.cub.2021.10.044

Vogel, J.T., Walter, M.H., Giavalisco, P., Lytovchenko, A., Kohlen, W., Charnikhova, T., Simkin, A.J., Goulet, C., Strack, D., Bouwmeester, H.J., Fernie, A.R., Klee, H.J., 2010. SlCCD7 controls strigolactone biosynthesis, shoot branching and mycorrhiza-induced apocarotenoid formation in tomato. Plant J. Cell Mol. Biol. 61, 300–311. https://doi.org/10.1111/j.1365-313X.2009.04056.x

Vragović, K., Sela, A., Friedlander-Shani, L., Fridman, Y., Hacham, Y., Holland, N., Bartom, E., Mockler, T.C., Savaldi-Goldstein, S., 2015. Translatome analyses capture of opposing tissue-specific brassinosteroid signals orchestrating root meristem differentiation. Proc. Natl. Acad. Sci. U. S. A. 112, 923–928. https://doi.org/10.1073/pnas.1417947112

Vukašinović, N., Wang, Y., Vanhoutte, I., Fendrych, M., Guo, B., Kvasnica, M., Jiroutová, P., Oklestkova, J., Strnad, M., Russinova, E., 2021. Local brassinosteroid biosynthesis enables optimal root growth. Nat. Plants 7, 619–632. https://doi.org/10.1038/s41477-021-00917-x

Waidmann, S., Ruiz Rosquete, M., Schöller, M., Sarkel, E., Lindner, H., LaRue, T., Petřík, I., Dünser, K., Martopawiro, S., Sasidharan, R., Novak, O., Wabnik, K., Dinneny, J.R., Kleine-Vehn, J., 2019. Cytokinin

functions as an asymmetric and anti-gravitropic signal in lateral roots. Nat. Commun. 10, 3540. https://doi.org/10.1038/s41467-019-11483-4

Waidmann, S., Sarkel, E., Kleine-Vehn, J., 2020. Same same, but different: growth responses of primary and lateral roots. J. Exp. Bot. 71, 2397–2411. https://doi.org/10.1093/jxb/eraa027

Walton, A., Stes, E., Goeminne, G., Braem, L., Vuylsteke, M., Matthys, C., De Cuyper, C., Staes, A., Vandenbussche, J., Boyer, F.D., Vanholme, R., Fromentin, J., Boerjan, W., Gevaert, K., Goormachtig, S., 2016. The response of the root proteome to the synthetic strigolactone GR24 in Arabidopsis. Mol. Cell. Proteomics 15, 2744–2755. https://doi.org/10.1074/mcp.M115.050062

Wang, D., Pajerowska-Mukhtar, K., Culler, A.H., Dong, X., 2007. Salicylic acid inhibits pathogen growth in plants through repression of the auxin signaling pathway. Curr. Biol. CB 17, 1784–1790. https://doi.org/10.1016/j.cub.2007.09.025

Wang, F., Han, T., Song, Q., Ye, W., Song, X., Chu, J., Li, J., Chen, Z.J., 2020a. The Rice Circadian Clock Regulates Tiller Growth and Panicle Development Through Strigolactone Signaling and Sugar Sensing. Plant Cell 32, 3124–3138. https://doi.org/10.1105/TPC.20.00289

Wang, L., Wang, B., Jiang, L., Liu, X., Li, X., Lu, Z., Meng, X., Wang, Y., Smith, S.M., Lia, J., 2015a. Strigolactone signaling in Arabidopsis regulates shoot development by targeting D53-like SMXL repressor proteins for ubiquitination and degradation. Plant Cell 27, 3128–3142. https://doi.org/10.1105/tpc.15.00605

Wang, L., Wang, B., Yu, H., Guo, H., Lin, T., Kou, L., Wang, A., Shao, N., Ma, H., Xiong, G., Li, X., Yang, J., Chu, J., Li, J., 2020b. Transcriptional regulation of strigolactone signalling in Arabidopsis. Nature 583, 277–281. https://doi.org/10.1038/s41586-020-2382-x

Wang, L., Waters, M.T., Smith, S.M., 2018. Karrikin-KAI2 signalling provides Arabidopsis seeds with tolerance to abiotic stress and inhibits germination under conditions unfavourable to seedling establishment. New Phytol. 219, 605–618. https://doi.org/10.1111/nph.15192

Wang, L., Xu, Q., Yu, H., Ma, H., Li, X., Yang, J., Chu, J., Xie, Q., Wang, Y., Smith, S.M., Li, J., Xiong, G., Wang, B., 2020c. Strigolactone and Karrikin Signaling Pathways Elicit Ubiquitination and Proteolysis of SMXL2 to Regulate Hypocotyl Elongation in Arabidopsis. Plant Cell 32, 2251–2270. https://doi.org/10.1105/tpc.20.00140

Wang, R., Liu, X., Liang, S., Ge, Q., Li, Y., Shao, J., Qi, Y., An, L., Yu, F., 2015b. A subgroup of MATE transporter genes regulates hypocotyl cell

elongation in Arabidopsis. J. Exp. Bot. 66, 6327–6343. https://doi.org/10.1093/jxb/erv344

Wang, Y., Sun, S., Zhu, W., Jia, K., Yang, H., Wang, X., 2013. Strigolactone/MAX2-Induced Degradation of Brassinosteroid Transcriptional Effector BES1 Regulates Shoot Branching. Dev. Cell 27, 681–688. https://doi.org/10.1016/J.DEVCEL.2013.11.010

Wasson, A.P., Pellerone, F.I., Mathesius, U., 2006. Silencing the Flavonoid Pathway in *Medicago truncatula* Inhibits Root Nodule Formation and Prevents Auxin Transport Regulation by Rhizobia. Plant Cell 18, 1617–1629. https://doi.org/10.1105/tpc.105.038232

Waters, M.T., Nelson, D.C., Scaffidi, A., Flematti, G.R., Sun, Y.K., Dixon, K.W., Smith, S.M., 2012. Specialisation within the DWARF14 protein family confers distinct responses to karrikins and strigolactones in Arabidopsis. Development 139, 1285–1295. https://doi.org/10.1242/DEV.074567

Waters, M.T., Scaffidi, A., Moulin, S.L.Y., Sun, Y.K., Flematti, G.R., Smith, S.M., 2015. A *Selaginella moellendorffii* Ortholog of KARRIKIN INSENSITIVE2 Functions in Arabidopsis Development but Cannot Mediate Responses to Karrikins or Strigolactones. Plant Cell 27, 1925–1944. https://doi.org/10.1105/tpc.15.00146

Wei, C.Q., Chien, C.W., Ai, L.F., Zhao, J., Zhang, Z., Li, K.H., Burlingame, A.L., Sun, Y., Wang, Z.Y., 2016. The Arabidopsis B-box protein BZS1/BBX20 interacts with HY5 and mediates strigolactone regulation of photomorphogenesis. J. Genet. Genomics 43, 555–563. https://doi.org/10.1016/j.jgg.2016.05.007

Weidenbach, D., Jansen, M., Bodewein, T., Nagel, K.A., Schaffrath, U., 2015. Shoot and root phenotyping of the barley mutant *kcs6* (*3-ketoacyl-CoA synthase6*) depleted in epicuticular waxes under water limitation. https://doi.org/10.1080/15592324.2014.1003752

Wendrich, J.R., Yang, B., Vandamme, N., Verstaen, K., Smet, W., Van de Velde, C., Minne, M., Wybouw, B., Mor, E., Arents, H.E., Nolf, J., Van Duyse, J., Van Isterdael, G., Maere, S., Saeys, Y., De Rybel, B., 2020. Vascular transcription factors guide plant epidermal responses to limiting phosphate conditions. Science 370. https://doi.org/10.1126/science.aay4970

Werner, T., Motyka, V., Laucou, V., Smets, R., Van Onckelen, H., Schmülling, T., 2003. Cytokinin-Deficient Transgenic Arabidopsis Plants Show Multiple Developmental Alterations Indicating Opposite Functions of Cytokinins in the Regulation of Shoot and Root Meristem Activity. Plant Cell 15, 2532–2550. https://doi.org/10.1105/tpc.014928

Westhoek, A., Clark, L.J., Culbert, M., Dalchau, N., Griffiths, M., Jorrin, B., Karunakaran, R., Ledermann, R., Tkacz, A., Webb, I., James, E.K., Poole, P.S., Turnbull, L.A., 2021. Conditional sanctioning in a legume–Rhizobium mutualism. Proc. Natl. Acad. Sci. 118, e2025760118. https://doi.org/10.1073/pnas.2025760118

Wilkinson, H., Coppock, A., Richmond, B. L., Lagunas, B., & Gifford, M. L. 2023. Plant–Environment Response Pathway Regulation Uncovered by Investigating Non-Typical Legume Symbiosis and Nodulation. *Plants*, *12*(10), Article 10. https://doi.org/10.3390/plants12101964

Wu, T., Hu, E., Xu, S., Chen, M., Guo, P., Dai, Z., Feng, T., Zhou, L., Tang, W., Zhan, L., Fu, X., Liu, S., Bo, X., Yu, G., 2021. clusterProfiler 4.0: A universal enrichment tool for interpreting omics data. Innovation 2, 100141. https://doi.org/10.1016/j.xinn.2021.100141

Xiao, Y., Chu, L., Zhang, Y., Bian, Y., Xiao, J., Xu, D., 2022. HY5: A Pivotal Regulator of Light-Dependent Development in Higher Plants. Front. Plant Sci. 12. https://doi.org/10.3389/fpls.2021.800989

Xie, Y., Liu, Y., Ma, M., Zhou, Q., Zhao, Y., Zhao, B., Wang, B., Wei, H., Wang, H., 2020. Arabidopsis FHY3 and FAR1 integrate light and strigolactone signaling to regulate branching. Nat. Commun. 11, 1955. https://doi.org/10.1038/s41467-020-15893-7

Xu, L., Zhao, H., Ruan, W., Deng, M., Wang, F., Peng, J., Luo, J., Chen, Z., Yi, K., 2017. ABNORMAL INFLORESCENCE MERISTEM1 Functions in Salicylic Acid Biosynthesis to Maintain Proper Reactive Oxygen Species Levels for Root Meristem Activity in Rice. Plant Cell 29, 560–574. https://doi.org/10.1105/tpc.16.00665

Yang, X., Bai, Y., Shang, J., Xin, R., Tang, W., 2016. The antagonistic regulation of abscisic acid-inhibited root growth by brassinosteroids is partially mediated via direct suppression of ABSCISIC ACID INSENSITIVE 5 expression by BRASSINAZOLE RESISTANT 1. Plant Cell Environ. 39, 1994–2003. https://doi.org/10.1111/pce.12763

Yi, K., Menand, B., Bell, E., Dolan, L., 2010. A basic helix-loop-helix transcription factor controls cell growth and size in root hairs. Nat. Genet. 42, 264–267. https://doi.org/10.1038/ng.529

Yokawa, K., Kagenishi, T., Baluška, F., 2013. Root photomorphogenesis in laboratory-maintained Arabidopsis seedlings. Trends Plant Sci. 18, 117–119. https://doi.org/10.1016/j.tplants.2013.01.002

Yu, C., Sun, C., Shen, C., Wang, S., Liu, F., Liu, Y., Chen, Y., Li, C., Qian, Q., Aryal, B., Geisler, M., Jiang, D.A., Qi, Y., 2015. The auxin transporter, OsAUX1, is involved in primary root and root hair elongation and in Cd

stress responses in rice (*Oryza sativa L.*). Plant J. Cell Mol. Biol. 83, 818–830. https://doi.org/10.1111/tpj.12929

Yu, X., Li, L., Zola, J., Aluru, M., Ye, H., Foudree, A., Guo, H., Anderson, S., Aluru, S., Liu, P., Rodermel, S., Yin, Y., 2011. A brassinosteroid transcriptional network revealed by genome-wide identification of BESI target genes in *Arabidopsis thaliana*. Plant J. 65, 634–646. https://doi.org/10.1111/J.1365-313X.2010.04449.X

Yu, Y.T., Wu, Z., Lu, K., Bi, C., Liang, S., Wang, X.F., Zhang, D.P., 2016. Overexpression of the MYB37 transcription factor enhances abscisic acid sensitivity, and improves both drought tolerance and seed productivity in *Arabidopsis thaliana*. Plant Mol. Biol. 90, 267–279. https://doi.org/10.1007/s11103-015-0411-1

Zhang, H., Han, W., De Smet, I., Talboys, P., Loya, R., Hassan, A., Rong, H., Jürgens, G., Paul Knox, J., Wang, M.H., 2010. ABA promotes quiescence of the quiescent centre and suppresses stem cell differentiation in the Arabidopsis primary root meristem. Plant J. 64, 764–774. https://doi.org/10.1111/j.1365-313X.2010.04367.x

Zhang, H., Zhang, L., Wu, S., Chen, Y., Yu, D., Chen, L., 2020. AtWRKY75 positively regulates age-triggered leaf senescence through gibberellin pathway. Plant Divers. 43, 331–340. https://doi.org/10.1016/j.pld.2020.10.002

Zhang, J., Mazur, E., Balla, J., Gallei, M., Kalousek, P., Medveďová, Z., Li, Y., Wang, Y., Prát, T., Vasileva, M., Reinöhl, V., Procházka, S., Halouzka, R., Tarkowski, P., Luschnig, C., Brewer, P.B., Friml, J., 2020a. Strigolactones inhibit auxin feedback on PIN-dependent auxin transport canalization. Nat. Commun. 11, 3508. https://doi.org/10.1038/s41467-020-17252-y

Zhang, J., Mazur, E., Balla, J., Gallei, M., Kalousek, P., Medveďová, Z., Li, Y., Wang, Y., Prát, T., Vasileva, M., Reinöhl, V., Procházka, S., Halouzka, R., Tarkowski, P., Luschnig, C., Brewer, P.B., Friml, J., 2020b. Strigolactones inhibit auxin feedback on PIN-dependent auxin transport canalization. Nat. Commun. 11, 3508. https://doi.org/10.1038/s41467-020-17252-y

Zhang, S., Huang, L., Yan, A., Liu, Y., Liu, B., Yu, C., Zhang, A., Schiefelbein, J., Gan, Y., 2016. Multiple phytohormones promote root hair elongation by regulating a similar set of genes in the root epidermis in Arabidopsis. J. Exp. Bot. 67, 6363–6372. https://doi.org/10.1093/jxb/erw400

Zhang, Y., Butelli, E., De Stefano, R., Schoonbeek, H., Magusin, A., Pagliarani, C., Wellner, N., Hill, L., Orzaez, D., Granell, A., Jones, J.D.G., Martin, C., 2013. Anthocyanins Double the Shelf Life of

Tomatoes by Delaying Overripening and Reducing Susceptibility to Gray Mold. Curr. Biol. 23, 1094–1100. https://doi.org/10.1016/j.cub.2013.04.072

Zhang, Y., Li, C., Zhang, J., Wang, J., Yang, J., Lv, Y., Yang, N., Liu, J., Wang, X., Palfalvi, G., Wang, G., Zheng, L., 2017. Dissection of HY5/HYH expression in Arabidopsis reveals a root-autonomous HY5-mediated photomorphogenic pathway. PLoS ONE 12, e0180449. https://doi.org/10.1371/journal.pone.0180449

Zhang, Y., Wang, C., Xu, H., Shi, X., Zhen, W., Hu, Z., Huang, J., Zheng, Y., Huang, P., Zhang, K.X., Xiao, X., Hao, X., Wang, X., Zhou, C., Wang, G., Li, C., Zheng, L., 2019. HY5 Contributes to Light-Regulated Root System Architecture Under a Root-Covered Culture System. Front. Plant Sci. 10. https://doi.org/10.3389/fpls.2019.01490

Zheng, J., Hong, K., Zeng, L., Wang, L., Kang, S., Qu, M., Dai, J., Zou, L., Zhu, L., Tang, Z., Meng, X., Wang, B., Hu, J., Zeng, D., Zhao, Y., Cui, P., Wang, Q., Qian, Q., Wang, Y., Li, J., Xiong, G., 2020. Karrikin Signaling Acts Parallel to and Additively with Strigolactone Signaling to Regulate Rice Mesocotyl Elongation in Darkness. Plant Cell 32, 2780–2805. https://doi.org/10.1105/tpc.20.00123

Zheng, X., Yang, X., Chen, Z., Xie, W., Yue, X., Zhu, H., Chen, S., Sun, X., 2021. Arabidopsis SMAX1 overaccumulation suppresses rosette shoot branching and promotes leaf and petiole elongation. Biochem. Biophys. Res. Commun. 553, 44–50. https://doi.org/10.1016/j.bbrc.2021.03.00